Alma Mater Studiorum - Università di Bologna

SCUOLA DI SCIENZE

Dipartimento di Chimica Industriale "Toso Montanari"

Corso di Laurea Magistrale in

Chimica Industriale

Classe LM-71 - Scienze e Tecnologie della Chimica Industriale

Synthesis and analysis of benzisoxazoles as substrates for the Kemp elimination in presence of hemoproteins

Tesi di laurea sperimentale

CANDIDATO

Telese Dario

RELATORE

Prof.ssa Carla Boga

CORRELATORE

Prof. Marcello Forconi

Dott. Gabriele Micheletti

Anno Accademico 2016-2017

Abstract

This elaborate focuses on the synthesis and kinetic analysis of substituted benzisoxazoles as substrates for the Kemp reaction, in presence of three hemoproteins, i.e. cytochrome c, myoglobin and hemoglobin. Formylation of a phenol derivative, nucleophilic addition of hydroxylamine and a final ciclization are the three step keys which afforded the desired fused isoxazole rings. The base-catalyzed decomposition of synthesized substrates was monitored through UV/Vis spectrophotometry, in order to study the catalytic effect of different enzymes under examination, using a common spectrophotometer UV/Vis. Finally the kinetic isotope effect of a deuterated substrate was analyzed to evidence the nature of the rate-limiting step of Kemp elimination.

Index:

1. Introduction

1.1. Enzyme catalysis

Enzymes are macromolecules specialized in catalysis of biological reactions. Whereas some enzymes are made of nucleic acid (RNA), most of the known ezymes are proteins. Enzymes represent one of the most important classes of biomolecules known for their highly specificity and their catalytic activity. More than 2000 different types of enzymes are known of today[1], many of them have been isolated in homogeneous form, and almost 200 of them have been crystallized: their structure has been elucidated through X-rays diffraction analysis. Although most of enzymes involved in principal metabolic processes of cells, have been identified, many problems remain to be resolved such as the genetic control of the synthesis of enzymes, the molecular mechanism that regulates enzymatic activity and the role of multiple forms of some enzymes. The activity of some enzymes depends only on their protein structure, while other enzymes require one or two non-proteic components, called cofactors. Cofactors can be metallic ions or organic molecules called coenzymes. Cofactors are usually thermostable, while most enzymes lose their activity after heating. The catalytic active complex enzyme-cofactor is called holoenzyme. The enzymes that require metallic ions are called metalloenzymes. In some metalloenzymes, the metal component alone is already characterized by a primitive catalytic activity, that is highly increased by protein scaffold. For example, the enzyme called catalase, containing a iron-porphyrin, catalyzes a quickly decomposition of hydrogen peroxide to water and oxygen, while some iron salts catalyze the same reaction albeit much more slowly. Coenzymes are usually intermediate transporters of functional group, atoms or electrons that can be transferred to the enzymatic reaction. When the coenzyme is tightly bound to the enzyme molecule, it is usually called prosthetic group: hemoglobin, myoglobin and cytochromes (which will be object of my internship) are characterized by a heme group, that is prosthetic group, containing an iron atom, that represents the non-protein part of enzyme (more details will be discussed in the third paragraph).

The general principles of kinetic of chemical reactions can be applied to reactions catalyzed by enzymes, but these reactions show also a particular characteristic that isn't usually observed in non-enzyme reactions: the saturation phenomenon from the substrate. As shown in **Figure 1**, at concentrations of substrate << K_M the initial velocity of the reaction increases linearly with respect to the concentration of substrate, so that the reaction is approximately first-order relative to the substrate.

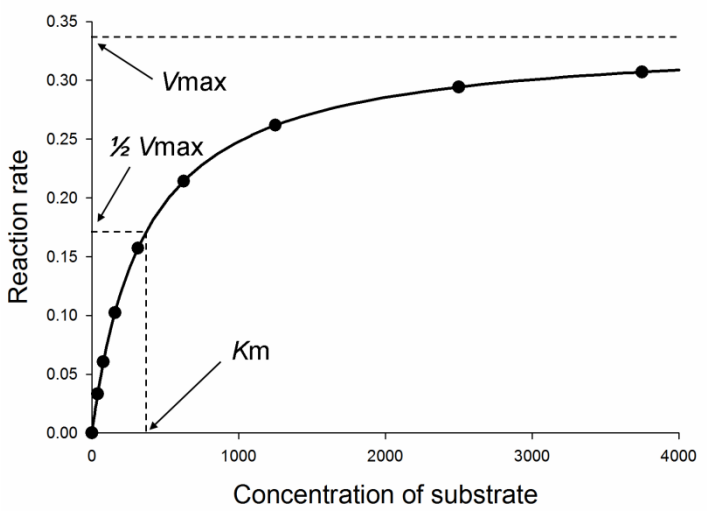

Figure 1. Concentration effect of substrate on the velocity of a catalyzed reaction by an enzyme.

However, as the concentration of substrate increases, the initial velocity of the reaction reaches a plateau, so that it does not depend on the substrate concentration anymore. Further increasing the concentration of the substrate does not significantly changes the initial velocity of the reaction, which approaches asymptotically to a costant rate (V_{max}). In this zone the reaction is zero-order with respect to the substrate, so the enzyme is saturated with its substrate. Each enzyme shows a saturation effect, but the concentration of the substrate required to achieve it changes greatly from one enzyme to the other. This saturation effect brought the first researchers to hypothesize that the enzyme and the substrate interact with each other reversibly, creating a complex that represents the intermediate phase in the catalyzed reaction. In 1913 a general kinetic theory has been developed by L. Michaelis and M. L. Menten: this theory applies to the simple case of a reaction in which there is only one substrate, as well as more complex ones with multiple

substrates involved. The Michaelis-Menten's theory assumes that the enzyme **E** combines with the substrate **S** forming the enzyme-substrate complex **ES**; this last one reacts, forming the free enzyme and the product **P** (**Scheme 1**).

$$E + S \underset{k_{-1}}{\overset{k_{+1}}{\rightleftharpoons}} ES \underset{k_{-2}}{\overset{k_{+2}}{\rightleftharpoons}} E + P$$

Scheme 1. Michaelis-Menten's theory: basic equation.

To express the correlation between the initial velocity (v_0), the maximum rate (V_{max}) and the initial concentration of substrate, we must look at the relationship between the rate of formation and the rate of cleavage of the enzyme-substrate **ES** complex. The initial velocity is equal to the rate of cleavage of the enzyme-substrate complex **ES**:

$$v_0 = k_{+2}[ES]$$

where [ES] is the concentration of enzyme-substrate complex. However, as neither k_{+2} nor [ES] can be easily determined by direct measurements, we must find an alternative correlation for v_0. Thus, the rate of formation of **ES** from **E** and **S** becomes:

$$\frac{d[ES]}{dt} = k_{+1}\,([E_T] - [ES])[S]$$

where $[E_T]$ is the total concentration of enzyme (the sum of the free form and the bound one). Although **ES** can be formed also from **E** and **P**, the rate of this inverse reaction can be neglected because initial velocities are defined when [S] is very high and [P] is close to zero. So the rate of cleavage of **ES** is equal to:

$$-\frac{d[ES]}{dt} = k_{-1}[ES] + k_{+2}[ES]$$

When the rates of formation and cleavage of **ES** are equal, it is said that the system has reached steady state:

$$k_{+1}([E_T] - [ES])[S] = k_{-1}[ES] + k_{+2}[ES]$$

This equation can be rearranged to find:

$$\frac{([E_T] - [ES])[S]}{[ES]} = \frac{k_{-1} + k_{+2}}{k_{+1}} = K_M$$

where the K_M value is called the Michaelis's costant. So from the last equivalence it can be obtained the concentration of **ES** on balance:

$$[ES] = \frac{[E_T][S]}{K_M + [S]}$$

Because $v_0 = k_{+2}[ES]$, substituting:

$$v_0 = k_{+2} \frac{[E_T][S]}{K_M + [S]}$$

When the enzyme is saturated, you get to the maximum starting rate V_{max}:

$$V_{max} = k_{+2}[E_T]$$

Substituting:

$$\boxed{v_0 = \frac{V_{max}[S]}{K_M + [S]}}$$

This is the Michaelis-Menten equation, which links the rate of an enzymatic reaction to the initial concentration of one substrate. Obviously, K_M value isn't a fixed value, but it may change with the structure of substrate, with pH and the temperature. When the initial velocity of the reaction is half of the maximum rate:

$$\frac{V_{max}}{2} = \frac{V_{max}[S]}{K_M + [S]}$$

Dividing by V_{max} then gives:

$$K_M = [S]$$

Thus, K_M is equal to the concentration of the substrate when the initial velocity is half of maximum rate, indipendently from the concentration of enzyme.
Instead the catalyst rate constant (k_{cat}), or turnover number, is represented by k of the limiting reaction, that is sometimes correlated to the rate of cleavage (k_{+2}) of the enzyme-substrate complex **ES**.
In the Michelis-Menten's model, it is defined as:

$$V_{max} = k_{+2}[E_T] = k_{cat}[E_T]$$
$$k_{cat} = \frac{V_{max}}{[E_T]}$$

Thus, the k_{cat} is defined as the maximum number of substrate molecule converted into a product in the unit of time by enzyme. If $V_{max}=k_{cat}[E_T]$, v_0 is equal to:

$$v_0 = \frac{k_{cat}[E_T][S]}{K_M + [S]}$$

When $[S]<<K_M$, [S] becomes a negligible value, so:

$$v_0 = \frac{k_{cat}}{K_M}\,[E_T][S]$$

The ratio k_{cat}/K_M , called also specificity costant, is a measure of how efficiently an enzyme converts substrates into products, and it can be expressed as $M^{-1}\,s^{-1}$. k_{cat}/K_M is an apparent second-order rate constant, and represents a measure of how fast an enzyme reacts when the substrate concentration is low, which is often the case in biological systems. The upper limit for k_{cat}/K_M is the diffusion limit.

Many enzymes display a characteristic pH at which their activity is maximum. Although the activity-pH trends of most enzymes shows a bell-shaped trend, as in case of trypsin and pepsin, in some cases their trend changes: for example, in case of cholinesterase, the activity increases as the pH increases up to a costant value, and in case of papain the activity is constant, regardless of pH[1] (**Figure 2**).

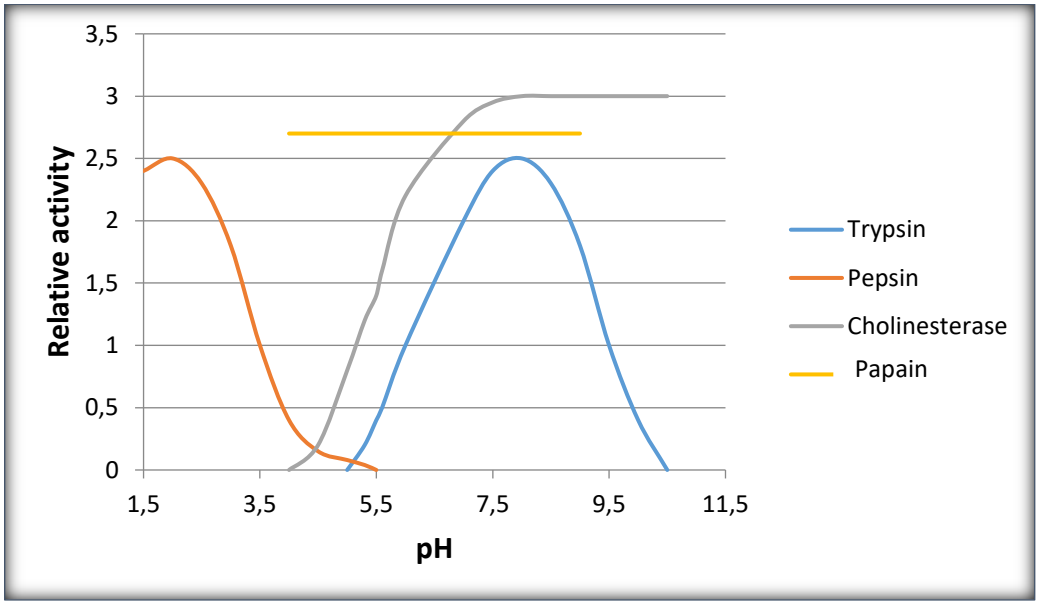

Figure 2. The activity-pH trends of some enzymes.

The relationship between enzymatic activity and pH of each enzyme depends on the acid-base behavior of enzyme and substrate, as well as many other factors that are difficult to analyze quantitatively. In general, the trend in pH when the enzyme is saturated reflects ionizations that occur in the bounds enzyme and bound susbtrate, while the trend in pH in subsaturating sub-strate conditions reflect the ionizations present in the enzyme and in the free substrate.

When it is possible, enzymes are dosed in systems where the pH is optimal and the concentration of substrate is over the saturation level, so the initial velocity of the reaction is zero-order with respect to the substrate. In these conditions, the initial velocity is dependent on the concentration of enzyme only.

How can we measure the efficiency of enzymes as catalysts? How much do they increase the rate of the reaction? An example explains that hydrolysis of urea, catalyzed by urease (as shown in **Scheme 2**), is characterized by a k_{cat} value of $3x10^4$ s^{-1} (pH=8 and T=20°C)[1]. Instead, the same reaction proceeds with a first-order rate constant of $3x10^{-10}$ s^{-1}, under the same conditions[1].

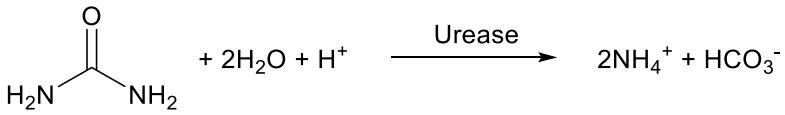

Scheme 2. Hydrolysis of urea.

Thus, the enzyme urease catalyzes the reaction by a factor of 10^{14}: only a few synthetic catalysts approach such rate accelerations, while most of them are less efficient.

Four main factors are important for the acceleration on the rate of reaction produced by enzymes. Not all enzymes use these four catalytic strategies.

The first one is the precise orientation of the substrate and the catalytic group with respect to each other, so that the orbitals are pre-aligned in the correct geometry conducive to the transition state.

The second factor that may contribute to catalysis is the stabilization of a highly reactive covalent intermediate between the enzyme and the substrate, so that the intermediate can sample multiple different environments. For example, when chymotrypsin is added to an equimolar amount of *p*-nitrophenyl ester acetate, a relatively "slow"substrate, p-nitrophenol is released with a higher rate than acetate[1]. So this reaction is divided into two steps, as shown in **Scheme 3**:

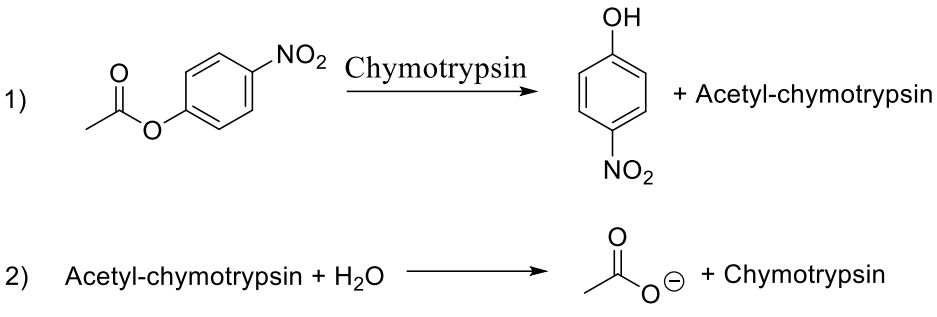

Scheme 3. Hydrolysis of *p*-nitrophenyl acetate.

The first reaction is relatively faster than second one where there is release of free acetate from the covalent intermediate acetyl-chymotrypsin.

The third one strategy relies on the presence of functional groups able to donate or accept proton, so the enzyme can catalyze an acid-base reaction. There are two types of acid-base catalysis: specific and general acid-base catalysis. Specific acid/base catalysis is defined as the increased rate of reaction due to the concentration of H^+ and OH^-, but this catalysis type is relatively limited into enzymatic reactions. The most common class of acid/base catalysis is called general acid/base catalysis: it is defined as the increase of the rate of the reaction due to the concentration of Brønsted-Lowry acids and bases. Two factors influence the rate of reactions catalyzed by a general acid or base: the strength of general acid or base, that is represented by the dissociation constant of its acidic form, and the rate with which an acid or a base can donate or accept a proton. An example is the imidazole group of histidine, that is both an acceptor and a donor of proton. Furthermore it has a rate of protonation and deprotonation very fast, even at neutral pH.

The fourth one is characterized by conformational changes of the enzyme, induced by the substrate, which can increase the reaction rate: when the substrate binds to enzyme, the binding interactions that are established between the enzyme and its substrater induce a conformational change that positions the catalytic groups and the substrate in the optimal position for the reaction (induced fit model).

Often, none of these factors is responsible for the entire catalytic activity of enzymes: it is more likely that for each enzyme there is a specific combination of factors responsible for the total acceleration of the rate of reaction.

1.2. Kemp elimination

The base-catalyzed decomposition of benzisoxazole to yield 2-cyanophenol is called Kemp elimination, a well-studied benchmark for catalysts design and a model for enzymatic C-H bond abstraction[2,3]. This reaction involves a N-O bond cleavage on the benzisoxazole ring, through a concerted E2 mechanism, thanks to deprotonation of CH bond, adjacent to nitrogen atom, by a base[4,5] (**Scheme 4**).

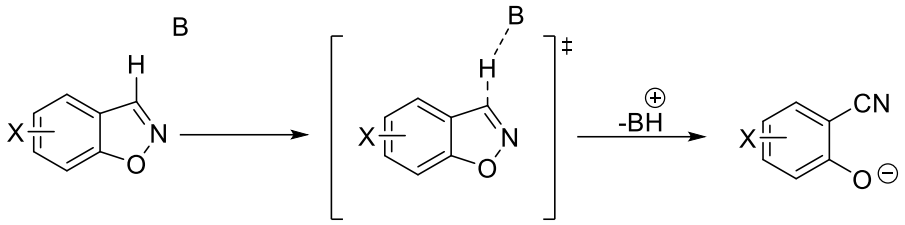

Scheme 4. Kemp elimination

Its popularity, besides for their use for computational design, is due also by the easy preparation of benzisoxazoles from salicylaldehydes[6,7,8,9] and by the fact that it is possibile to measure kinetic rates with a spectrophotometer. In fact, the substituted salicylnitriles formed from benzisoxazole decomposition under basic conditions show intense ultraviolet absorption maxima in the range of 310-400 nm. In particular I was focused, during my internship, on 5-NO_2-, 5-Br-, 6-OMe- and unsubstitued – benzisoxazoles whose products show λ_{max}=380, 337, 317, 323 nm, respectively[10].

Furthermore, the role of substituents on to benzisoxazole ring affects the rates of Kemp elimination: the reaction is strongly accelerated by electron-withdrawing groups because of facilitated delocalization of the negative charge developed during the transition state[8]. In addition this effect corresponds to a decrease of pKa of products: the values of p*Ka* for 5-NO_2, 5-Br, 6-OMe and unsubstituted benzisoxazole are 4.1, 5.9, 6.6, 6.9 respectively[6]. Moreover the solvent influences the delocalization of charge, since in less polar solvents the developed charge is destabilized and a substituent that attracts the negative charge will effectively spread the charge on the ring system and reduce the destabilization, with the result of speeding up the reaction. Indeed, it has been seen that the acetate-catalyzed

reaction of benzisoxazole in acetone (aprotic solvent), where acetate was used as the base, was about seven order of magnitude larger than that estimated in water ($k_{acetone}$=33 M^{-1} s^{-1}; k_{H2O}=2.7x10^{-6} M^{-1} s^{-1})[11]. This results can be understood as an anticatalytic role for the strong interactions between the negative charge of acetate and protic solvent, while in aprotic solvent these interactions don't exist, and the rate significantly increases.

Another catalyst for this reaction is given by host-guest system characterized by xylene-bridged hosts that catalyze the Kemp reaction. This reaction between host and benzisoxazole is characterized by a fast pre-equilibrium, followed by a slow intercavity reaction, product release, and subsequent sequestration of the host as the product complex. These compounds catalyze the decomposition of benzisoxazole to cyanophenol with large rate accelerations in $CDCl_3$, acting as the base. For the host-guest system **1**, shown in **Figure 3**, the *k* value is 6.1x10^{-2} M^{-1} s^{-1}, while the same reaction with pyridine **2**, without host-guest system, has the k value equal to 1.9x10^{-4} M^{-1} s^{-1} [12].

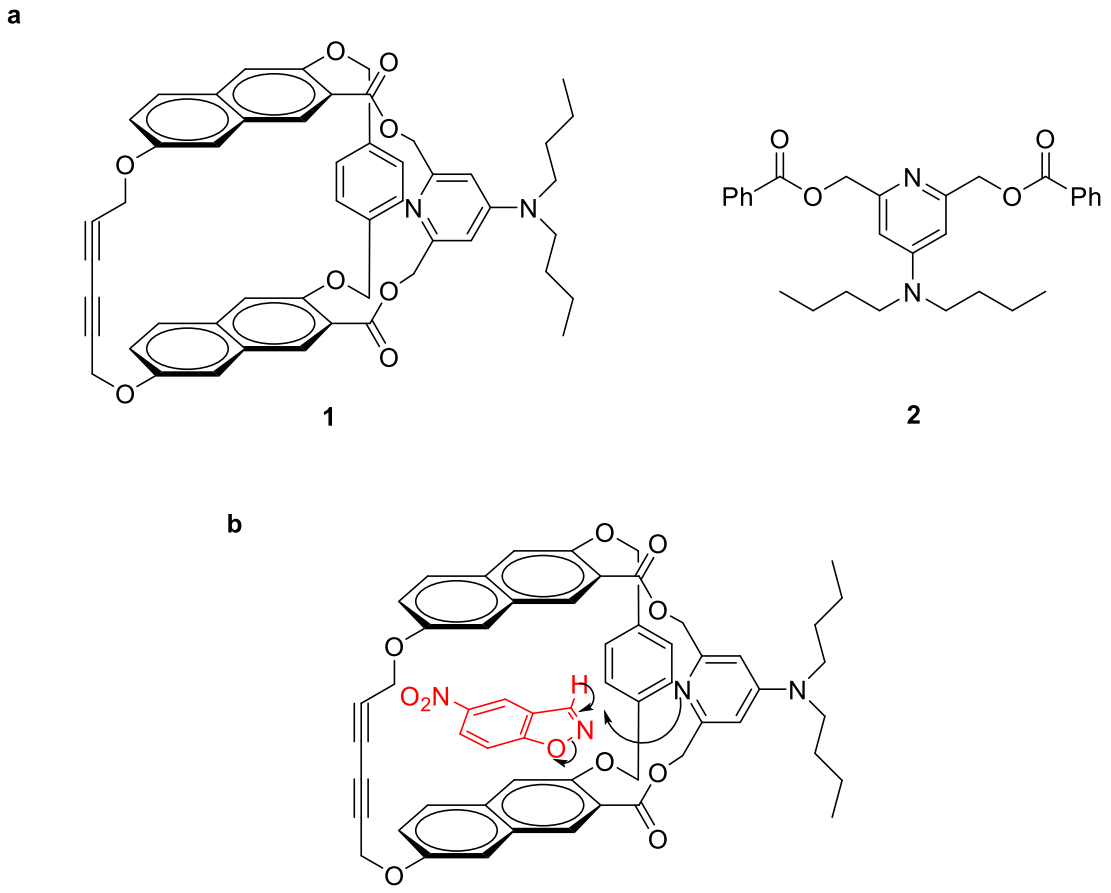

Figure 3. a: Possible bases; **b:** Proposed mechanism.

Another parameter useful to evaluate the reaction rate is the base strenght since bases with elevated pKa extract the proton in 3-position more easily than bases with low pKa. Thus, the speeding up of the reaction can be evaluated through kinetic isotope effect (KIE) between unsubstituted benzisoxazole and 3-D-benzisoxazoles with different bases: the ratio between the kinetic costant k_H refers to unsubstituted benzisoxazole that reacts with the base, and the kinetic costant k_D refers to 3-D-benzisoxazole that reacts with the same base, providing a value that can be compared to estimate the ease in extracting the proton/deuterium by each base. From the **Table 1** it can be marked the behavior of k_H/k_D for each base with benzisoxazole: increasing the strenght of the base increases the isotopic effect, so accelerating the abstraction of proton[6].

Table 1. Screening of Kinetic Deuterium Isotope Effect for Kemp reaction with bases.

Base	pKa	k_H/k_D for benzisoxazole
Hydroxide	15	4.59
Trimethylamine	9.8	4.16
N-Methylmorpholine	7.4	3.85

Scaffolds similar to benzisoxazoles, that undergo a N-O bond cleavage, present pharmacological properties such as leflunomide (**Scheme 5**), characterized by isoxazole core[13]. This compound is knewn as an orally active disease-modifying anti-inflammatory agent for the tratment of advanced rheumatoid arthritis. The pathway for metabolic process involves an N-O bond cleavage on its isoxazole ring, leading to the formation of butyramide A771726 (**Scheme 5**), metabolite that resides in same oxidation state as the parent drug. The N-O bond cleavage can occur through two different pathways: one involves the reduction of leflunomide followed by its cytochrome-P450-catalyzed dehydratation to A771726 (**Scheme 5**, **a**); the second instead involves a enzymatic or non-enzymatic deprotonation of the C3-H on the isoxazole ring followed by N-O bond cleavage to metabolite (**Scheme 5**, **b**). Two factors very important in each pathway are the presence of molecular oxygen and NADPH as a reducer: the isoxazole ring opening is also catalyzed by Fe(II) active form of cytochrome P450 thanks to NADPH that reduces Fe(III) to Fe(II); instead the oxygen inhibits the formation of A771726 because of great cytochrome's affinity for oxygen that take place at the active site of enzyme.

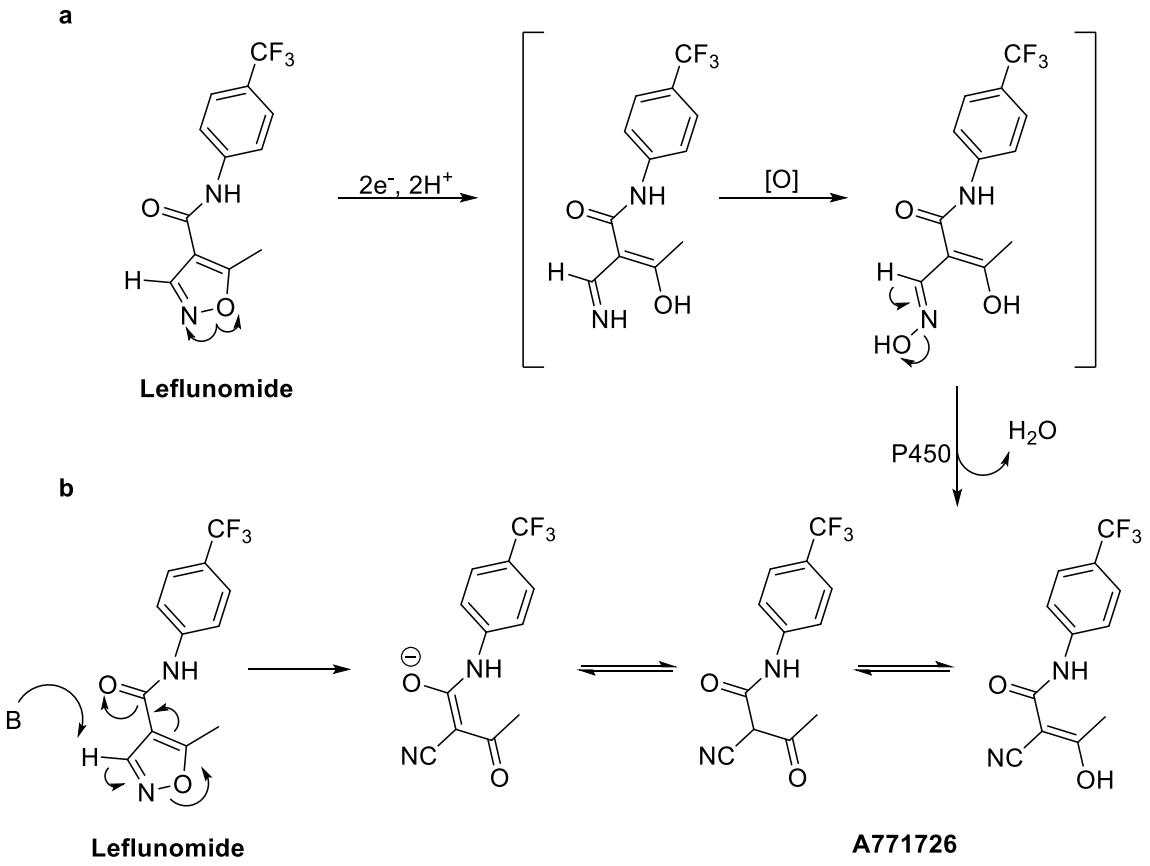

Scheme 5. Mechanisms for the metabolic isoxazole ring opening in the anti-flammatory agent Leflunomide. **a:** Redox pathway; **b:** Base-catalyzed pathway.

Other examples of compounds containing a benzisoxazole core with pharmacological properties are zonisamide and risperidone (**Figure 4**). The former is an anticonvulsant agent, whereas the latter is an antipsychotic agent[14]. However, these compounds have a substituent in the 3-C position other than hydrogen. Each one can be subjected to reductive ring scission leading to the respective active metabolite, thanks to cytochrome-P450, but in this case a mechanism that involves proton transfer would be impossibile because the 3-C position is occupied by a substituent other than hydrogen. Thus, the reaction undergoes a redox pathway.

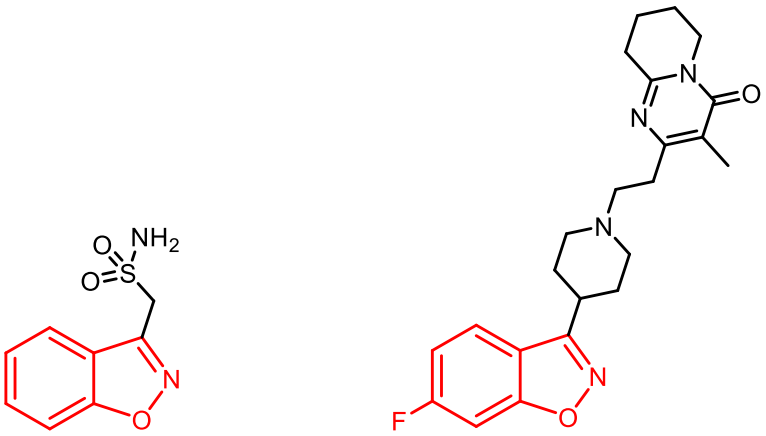

Zonisamide **Risperidone**

Figure 4. Benzisoxazoles with pharmacological properites.

1.3. Natural systems with Kemp eliminase activity

In contrast to other proton transfer reactions, the negative charge that forms at transition state is delocalized throughout the aromatic system, making the Kemp elimination a relatively easy reaction to catalyse. Indeed, many systems have been used to accelerate the Kemp reaction: cationic micelles, cavitands, serum albumins and catalytic antibodies[14].
In the case of micelles, the Kemp reaction takes place at the interface between water and hydrophilic head, a region also called the Stern layer, with characteristics more similar to water than to the highly hydrophobic core of the micelle. The abstraction of the proton from the substrate is accelerated by four orders of magnitude thanks to a electrostatic interaction between negatively charged long-chain base, such as sodium laurate ($C11_{COO^-}$), associated with positivitely charged micelles, such as cetrylmethylammonium chloride (CTAC). The anionic base intercalates within the micelle with the long hydrophobic chain and leaves the negatively charged head to interact with the positively charged head of the micelle, with the substrate present in the Stern layer rather than embedded in the micelle. The simple micellar system, with its value of k_{cat}/K_M=0.98 M^{-1} s^{-1}, is less efficient than more complex systems that use a carboxylate base, such as KE59 (k_{cat}/K_M= 160 M^{-1} s^{-1}) and HG3 (k_{cat}/K_M=1300 M^{-1} s^{-1})[15]. However, the 10^4 - rate acceleration measured in the micellar system is only two-three orders of magnitude smaller than the rate acceleration provided by the computationally designed enzymes (106 for KE59 and 107 for HG3). Synthetic cavitands and protein cavities have been widely studied as models for ligand recognition and more recently cavity sites in protein themselves have been studied as model systems in enzymatic catalysis[15]. These protein cavities are characterized by burial from bulk water and the dominance of a single type of ligand-protein interaction. Such dominating interactions can be nonpolar complementarity, as in the engineered core cavity in T4 lysozyme L99A. In contrast to the cavitands, model proteins have the advantages of ready solubility in water, easy introduction of functionality by site-directed mutation and of being readily over-expressed. The substrate of the Kemp elimination, whose reactivity is enhanced by a polar and aprotic environment, made it well-suited to such a cavity. Among the simplest of these cavities is the fully apolar site in T4 lysozyme, created by the

core substitution Leu99→Ala. The L99A construct was characterized by minimal Kemp eliminase activity (k_{cat}/K_M=0.017 M^{-1} s^{-1} and ΔΔG=-5.2 kcal/mol), but a few mutations, in or around the native lysozyme active site, were made to overcome this problem. However these substitutions increased activity but also reduced stability, and often required restabilization of the protein at distal sites. Using molecular docking, the Met102→His substitution (His102 acts as the catalytic base) and the Leu118→Gln substitution (Gln118 likely stabilizes the negative charge that develops during the reaction) into the cavity led to an increase of activity (k_{cat}/K_M=1.8 M^{-1} s^{-1}) and a decrease of stability (ΔΔG=-2 kcal/mol)[16].

The family of serum albumins (the globular proteins from plasma, produced by hepatic cells, that regulates the oncotic pressure) from different species shows catalytic properties towards the Kemp reaction, with k_{cat} values that run between 0,47 min^{-1} and 360 min^{-1} [16]. All of the serum albumins accelerate the Kemp elimination, but those with the higher catalytic activity are bovine (BSA) and human (HSA) serum albumin, with k_{cat}/K_M values equal to 347 M^{-1} s^{-1} and 157 M^{-1} s^{-1} respectively[17]. These proteins are proposed to use a lysine side-chain amino group as the catalytic general base: the active involvement of lysine residues is consistent with the observed inhibition of catalytic activity by side-chain-specific covalent modification. Indeed pyridoxal phosphate (**Figure 5**), which forms a covalent complex with BSA, where the aldehyde group reacts with one or two adjacent lysine side chains to form a Schiff base or a *gem*-diamino group leds to up to 80% of activity loss[17].

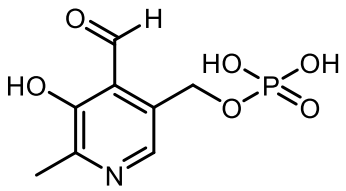

Figure 5. Pyridoxal phosphate.

With HSA, pyridoxal phosphate reacts less favourably (up to 40% of activity lost) and the catalytic activity of HSA is correspondingly less sensitive to added pyridoxal phosphate. Catalysis is also inhibited by a series of anionic ligands, including octanoate and drugs such as ibuprofen, warfarin and diazepam (**Figure 6**), which bind specifically to HSA. As shown in **Figure 6**, these different compounds can inhibit catalysis more or less completely, dependig on preferences for one of the two catalytic sites (IIA or IIIA) of serum albumin.

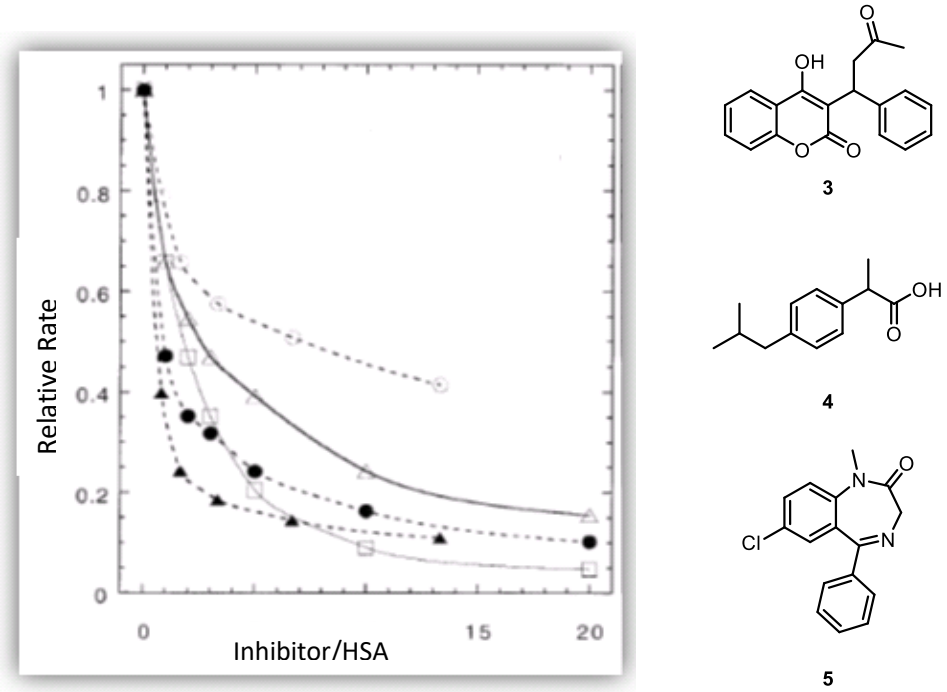

Figure 6. Inhibition of HSA catalysis by drugs.
Activities are plotted against the ratio [inhibitor]/[HSA].
Inhibitors used: Warfarin 3 (close circles); Ibuprofen 4 (open squares); Diazepam 5 (open circles); octanoate (open triangles) and triiodobenzoate (close triangles).

For BSA the catalysis occurs predominantly at the IIA binding site where Lys222 acts as active residue, while the well-defined IIIA binding pocket appears to be less important. Instead for HSA, where Lys199 acts as active residue, the IIIA site appears to make a more significant contribution of up to some 30% of the overall activity[17].

In addition to protein systems described above, in the last few years it has been studied the potential of naturally occuring enzymes to catalyze the Kemp elimination. One of these enzymes is ketosteroid isomerase (KSI), which catalyzes the Kemp elimination through an acid/base mechanism, and aldoxime dehydratases and cytochrome P450-BM3, which are possibly characterized by redox mechanism involving the heme group.
Ketosteroid isomerase from *Comamonas testosteroni* (tKSI) is an enzyme used in the synthesis of steroids and catalyzes migration of a proton from C4 to C6 of 3-oxo-Δ ketosteroide using aspartate Asp38 as active site (**Scheme 6**)[10].

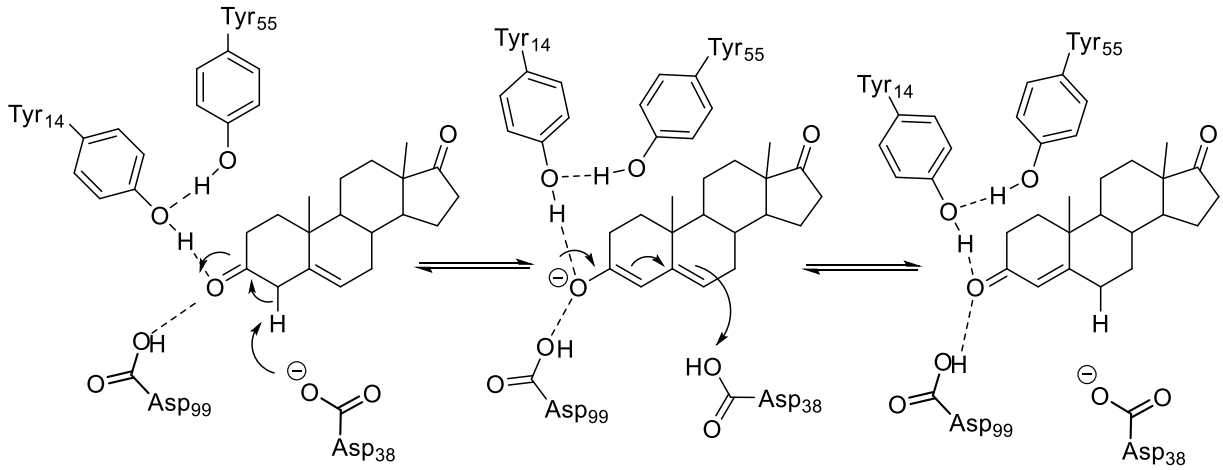

Scheme 6. Reaction pathway for the KSI-catalyzed reaction.

Although the active site of this enzyme is hydrophobic, it contains hydrophilic residues which confer to the enzyme the catalytic property: in particular the residue Asp99 forms a hydrogen bond with 3-carbonyl and an oxyanion hole, thus producing a catalytic environment for the isomerization of ketosteroid. Although an unstable enol intermediate is formed, the reaction is shifted to the right by removing the proton in the beta position from C4. Asp99 and Tyr14 serve to stabilize the reaction intermediate. In the Kemp reaction with 5-nitrobenzisoxazole as substrate, the best active variant of tKSI is the D38N mutant, which displays a k_{cat}/K_M of 1.7×10^4 M^{-1} s^{-1} (7000-fold better than wild-type tKSI, that presents a k_{cat}/K_M equal to 2.5 M^{-1} s^{-1})[10]. This enzyme likely uses Asp99 as the general base to promote the Kemp elimination.

Proteins as aldoxime dehydratases, cytochromes, myoglobin and hemoglobin complex iron through the aid of a prosthetic heme group, a planar (or nearly planar) four-coordinate porphyrin ligands known as protoporphyrin IX[17], shown in **Figure 7**. This heme group is classified as a heme b, the same porphyrin ligand system that ligates iron in cytochrome P450.

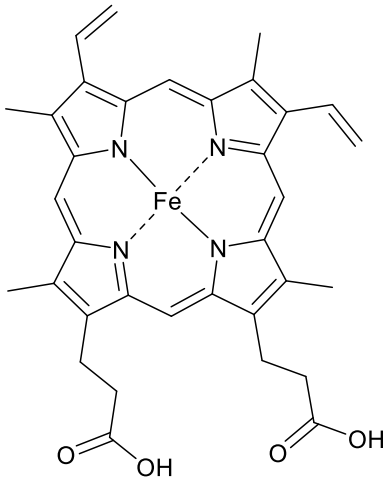

Figure 7. Protoporphyrin IX.

Iron is the most abundant of transition metal found in biological systems with a percentage by weight in the human body, for instance $5x10^{-3}$ % [20]. Therefore iron-containing proteins and enzymes are found in a large number and varieties of many biological species. Iron-containing species are divided in two categories: those containing a porphyrin ligand system with an iron-bearing heme moiety (on which I concentrated during my internship) and those not containing porphyrin ligands with non-heme iron-containing proteins.

In general, the heme group is characterized by pentacoordinate iron(II), in which the metal ion lies slightly out of the plane of the porphyrin's four pyrrole-nitrogen donor ligands, and a vacant distal coordinate site. In fact the protoporphyrin cofactor is held in place in the protein principally by non covalent hydrophobic interaction of some 80 or so residues, principally leucine, isoleucine, valine and other residues, and one covalent linkage that takes up the fifth position of heme group. In cytochrome c, the heme group is covalently bound to the protein; in the case of hemoglobin and myoglobin the fifth position is occupied by proximal histidine residue (**Figure 8**); indeed for cytochrome P450,

the heme group is held in the catalytic pocket through a covalent bond between the iron and a cysteine amino acid side chain from the protein[20] (**Figure 8**).

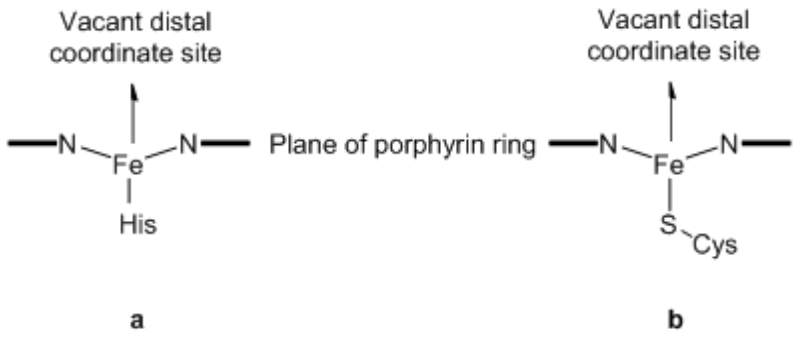

Figure 8. Heme group for **a.** Hemoglobin and Myoglobin and **b.** Cytochrome P450.

The naturally occuring aldoxime dehydratase (Oxd) also catalyzes the Kemp reaction. The heme group containing enzyme is part of the aldoxime-nitrile pathway in various micro-organisms (**Scheme 7**), where it catalyzes the dehydration of an aliphatic or aryl-aldoxime to the corresponding nitrile[18].

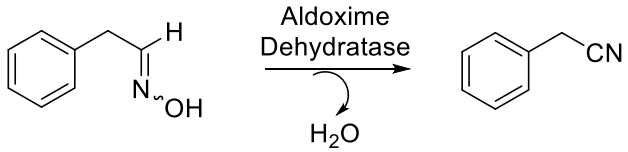

Scheme 7. Aldoxime dehydratase-catalyzed dehydration of aldoxime.

Oxd-catalyzed dehydration of aldoxime begins with the heme iron in its ferrous state (+2) and involves the direct approach of substrate to the heme iron and deprotonation of β-hydrogen of aldoxime using a histidine as a general base. The same has been proposed to apply to benzisoxazoles that binds to the heme iron of Oxd in a similar manner to that of the natural substrate during catalysis. Furthermore it can be highlighted a close relationship between oxidation state and catalytic efficiency: in the ferric state (+3), it can be observed a decrease of catalytic efficiency (k_{cat}/K_M = 143 M^{-1} s^{-1}) with respect to ferrous

state (+2) (k_{cat}/K_M= 6.6x10^4 M^{-1} s^{-1})[21]. Reduction was achieved using $Na_2S_2O_4$ (sodium dithionite) as the reducing agent. So it has been proposed that the ferrous state of heme iron increases the base-catalyzed Kemp elimination, as opposed to ferric state that disadvantages the bond cleavage of benzisoxazole.

Finally, human cytochrome enzymes play an important role in the metabolism of therapeutic drugs, including the degradation of isoxazole-based pharmaceuticals, such as leflunomide above described. In comparison with other protein scaffolds that involve an acid/base mechanism for Kemp reaction, the enzyme cytochrome P450 monooxygenase from *Bacillus megaterium* (P450-BM3) is proposed to use a redox process. This mechanism was proposed on the basis of molecular dynamics (MD) and molecular mechanics (MM) calculations coupled with mechanistic and mutational studies, as shown in **Scheme 8**, Fe^{II} is oxidized to Fe^{III} by electron-flow to the electron-deficient benzisoxazole, followed by proton transfer and formation of cyanophenol[19] (**Scheme 8**).

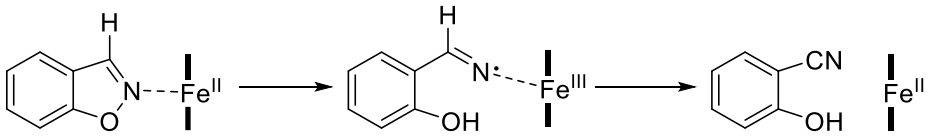

Scheme 8. Possible redox-mediated process.

This redox process needed a reducing agent (NADPH) in such a way as to keep the heme cofactor reduced, otherwise no reaction occurred; furthermore, the addition of oxygen or carbon monoxide led to 10-fold loss of activity, because of competition with the substrate in coordinating to ferrous heme. Simulations suggest that the π-π interaction, between the phenyl group of phenyalanine (F87) and the substrate, sterically prevents tight binding of benzisoxazole with Fe^{II} necessary for optimal redox reaction. In agreement with this proposal, the A82F mutant led to a significant improvement in catalytic efficency (k_{cat}/K_M =31000 M^{-1} s^{-1}, versus 240 M^{-1} s^{-1} of wild-type P450)[22]. This value is higher than in any of the previously designed Kemp eliminases (except for HG3.17 which has a k_{cat}/K_M=230000 M^{-1} s^{-1})[26]. However, the rate of the redox-mediated Kemp elimination in

the absence of the heme protein is unknown, and thus the acceleration rate cannot be quantified.

1.4. Computational enzyme design

The design of stable enzymes with new catalytic activities is of great pratical interest, with potential applications in biotechnology, biomedicine and industrial processes[20]. Furthermore, the computational design of new enzymes for reactions not catalysed by naturally occuring biocatalysts is a challenge for protein engineering and is a critical test of understanding of enzyme catalysis. To boost the results from protein engineering, directed evolution is often used in conjunction with the design process. Directed evolution is a powerful and commonly used approach to enzyme engineering that relies on interative cycles of mutagenesis and selection. Example of its application include improved themostability, tolerance to organic solvents, strengthened protein-protein interaction, enhanced enzymatic activity and inversion of enantioselectivity[20].

Other protein engineering approaches are catalytic antibodies, that have been produced for a wide range of chemical transformations. It seems that enzymes provide an environment complementary in structure and electronic distribution to that of the rate-limiting transition state[20]. For example, when challenged with a hapten (minute molecule that elicit an immune response when bounded to a large carrier such as a protein) that resembles the key transition state characteristics for a given reaction, antibodies are produced that can bind the hapten and thus also the transition state it mimics. The production of catalytic antibodies takes advantage of the rapid rates of mutation and selection against a specific antigen that is a key characteristics of adaptive immune responses. The resulting binding interactions are specific and can be harnessed to catalyze non-natural reactions and also to promote the conversion of non-natural substrates. One relatively simple strategy to create functionalized binding pockets exploits charge complementarity between antibody and antigen. This approach is exemplified by efforts to create bifunctional catalysts for the Kemp elimination of benzisoxazoles **6** to give the corresponding opening product **7** using the cationic benzimidazolium derivative **8** as a hapten[21] (**Figure 9**).

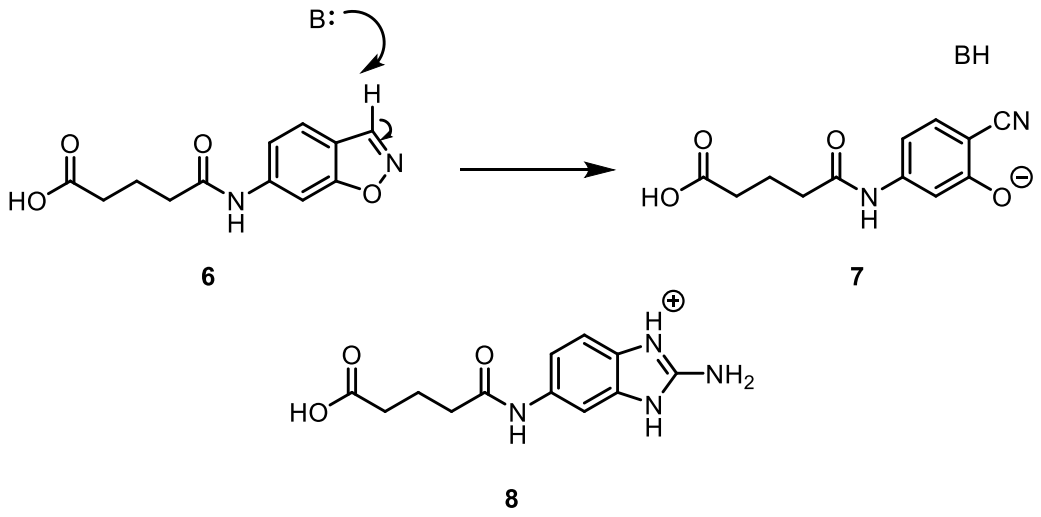

Figure 9. The base-catalyzed Kemp Elimination of **6** and hapten **8** to generate antibody 13G5.

The guanidinium group of **8** was expected to induce a base and an acid, to initiate proton transfer and stabilize developing negative charge at the phenoxide leaving group. Consistent with this design, antibody 13G5, which binds **8** with low affinity, promotes the selective cleavage of 6-glutaramidebenzisoxazoles, an unreactive substrate, with multiple turnover and rate acceleration >10^5 over background[21]. Furthermore the antibody 13G5 contains three polar residues, but only one doesn't abolishes or reduces catalytic efficiency: $Glu^{L34}Ala$ promotes the proton abstraction at 13G5 active site with a k_{cat}/K_M value equal to 270 M^{-1} s^{-1} [21].

The failure of antibodies to attain the levels of efficiency of natural enzymes also stems from a combination of factors: transition state analogues are at best poor mimics of true transition state and many reactions involve more than one transition state that requires stabilization. Through the use of haptenic charge it is possibile to overcome these problems[22]: a careful hapten design and an efficient screening of the immune response, to identify antibodies with optimally positioned catalytic residues, are the key factors for this catalysis. Using hybridoma technology, a method for producing of identical anti-bodies (called also monoclonal antibodies) that react with other cells to produce a cell line with hybride ability (called hybridoma) that when react with an antigen provokes a immune response, it has been possible to increase the efficiency. For example, monoclonal antibodies generated against a thyroglobulin (a large, water soluble glycoprotein that is

a major component of the thyroid follicular colloid, with the principal role of synthesis of thyroid hormones) conjugate of **9** (**Figure 10**) catalyses the Kemp elimination[23].

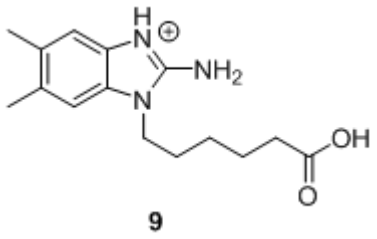

9

Figure 10. Positively charged hapten

The corrisponding hybridoma 34E4, catalyzes the abstraction of proton using carboxylate, as the general base mechanism in apolar environment, with a k_{cat}/K_M value equal to 5.5x103 M^{-1} s^{-1} thanks to the relative positioning of the catalytic residue and the substrate. For comparison with 13G5, that utilizes three polar residue, the hybridoma 34E4 utilizes a single carboxylate residue (Glu^{H50}) that is located near the mouth of an apolar pocket of deprotonated activated bensizoxoles[21].

The increasing interest for catalytic antibodies is involved into therapeutic applications, such as neutralizing HIV-1, antibody-directed enzyme prodrug therapy and the inactivation of addictive substances through the antibody-mediated break-down of drug molecules[23]. But catalytic antibodies often suffer from product inhibition and can generally not be programmed for elaborate arrays of catalytic functionality. For example by using transition state analogues to elicit antibodies with catalytic activities, has generally failed to deliver true enzymatic rates.

The advent of computational design approaches, combined with directed evolution, has provided an opportunity to revisit this problem. Indeed a general method for computational design of enzymes that can efficiently catalyze arbitrary chemical reactions would allow the benefits of enzymatic catalysis to be applied to chemical transformations of interest that are currently inaccessibile via natural enzymes[24].

In the last years, much effort has been put towards developing a computational enzyme design methodology to create new enzyme catalysts for a reaction for which no naturally

occuring enzyme exists: the Kemp elimination (**Scheme 4**). This reaction, used as a benchmark for the success of computational enzyme design, was popular in the past as an activated model system for understanding the catalysis of proton abstraction from carbon[2,3].

The method for designing new enzymes involves the choice of a catalytic mechanism and then the use of quantum mechanical transition state calculation to create an idealized active site with protein functional groups positioned in manner to maximize the transition state stabilization[24]. Transition state geometries were computed for idealized active sites containing a carboxylate as general base for deprotonation of a carbon-hydrogen bond. Aromatic side chains were placed above and below the transition state using π-stacking geometries to stabilize the transition state. Residues surrounding the catalytic side chains and transition state were repacked and redesigned to optimize steric, coulombic and hydrogen-bonding interactions with the transition state. Furthermore the best suite for the base-catalysed Kemp elimination is a non-polar environment because it increases the hydrophobic character of active site to facilitate the binding of hydrophobic substrate and also elevate the pK_a of the base[24] (**Figure 11**).

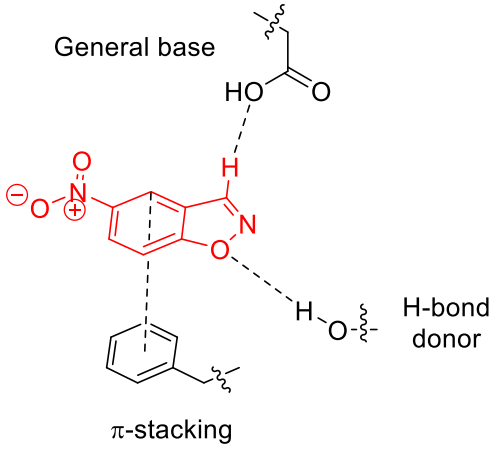

Figure 11. KE idealized active site.

For example in the KE59 design, Glu231 is the catalytic base and Trp110 facilitates charge delocalization by π-stacking to the transition state; Leu108, Ile133, Ile178, Val159 and Ala210 create a tightly packed hydrophobic pocket that envelops the substrate and the polar residue Ser211 provides hydrogen-bonding interactions with nitro group of the transition state (**Figure 12**[25]). This computational design resulted in a moderately active enzyme, with a k_{cat}/K_M of 163 M^{-1} s^{-1}. By comparison, k_{cat}/K_M for residue of acetate in water (the analog of Glu) is $5.98x10^{-5}$ M^{-1} s^{-1}, and thus the rate acceleration of KE59 design is 10^7-fold[25].

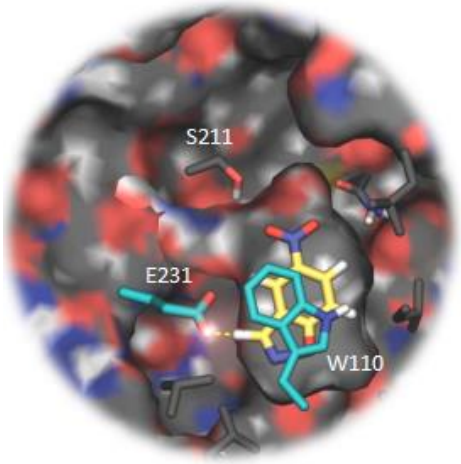

Figure 12. Computational design model of KE59.

Often, quantum mechanical transition state calculations are assisted by molecular dynamics (MD) simulation and X-ray analysis to investigate the activity of computational enzymes and to improve the catalytic turnover. Furthermore MD simulation and structural analysis of active and inactive designs, through an iterative approach, led a more complete understanding of the underlying principles of enzymatic catalysis and further progress toward reliably producing active enzymes. For example, investigating the inactivity of HG-1, a computational enzyme, using MD simulation and X-ray crystallography, it was possible to identificate causes of inactivity. The active site was overly exposed to solvent and critical active site residues showed a high degree of flexibility and orientations inconsistent with the design objectives, so showing his inactivity in KE reaction[26].

Iterating on the protein design process, have been corrected these problems in subsequent rounds of computational design using the same protein scaffold, leading to HG-3 with the highest activity with a k_{cat}/K_M of 430 M^{-1} s^{-1} [26].

To bridge the efficiency gap between natural and artificial enzymes, it has been proposed to place appropriate groups in the right active site environment through directed evolution: this evolution of catalytic function involved into optimization of computational enzyme includes both global and local mutagenesis, with an improvement of the sought-after property (stability, substrate specificity, activity, etc.). Typically the improvements in each round are small, and the process repated many times. For example, optimization of HG-3 after 17 rounds of mutagenesis and screening produced an enzyme (HG3.17) which cleaves 5-nitrobenzisoxazole with a k_{cat} of 700 s^{-1} and k_{cat}/K_M of 230000 M^{-1} s^{-1} [26]. In comparison, the k_{cat} and k_{cat}/K_M values for triosephosphate isomerase (TIM), that accelerates the conversion of dihydroxyacetone phosphate to R-glyceraldehyde-3-phosphate in glycolysis, are 430 s^{-1} and 440000 $M^{-1}s^{-1}$ respectively[26]. Comparison of HG-3.17 with the starting HG-3 enzyme suggests that three factors were decisive in the evolution of high activity: first, the evolved active site exhibits high shape complementarity to the substrate increasing catalytic efficiency (**Figure 13.a**); second, there is a efficient proton transfer thanks to interactions between the catalytic base Asp127 and the bound substrate because the energy penalty of using the wrong lone pair for proton abstraction may be small if the base and substrate are aligned (**Figure 13.b**); third, a new catalytic group, Gln50, capable of stabilizing developing negative charge in the transition state emerged over the course of evolution[26] (**Figure 13.c**). But the hydrogen bond between the side chain of Gln50 and the oxygen bearing the negative charge in the product, would result in more acceleration for non-activated benzisoxazoles, proposal perdiction that was not explicitly tested in the paper. Nevertheless, the steep slope in the LFER (linear free-energy relationships) that relates the enzymatic activity to the nature of the substituent on the benzisoxazole ring does not support this proposal, and suggests that rhe contribution of acid catalysis to the reaction is at most minimal.

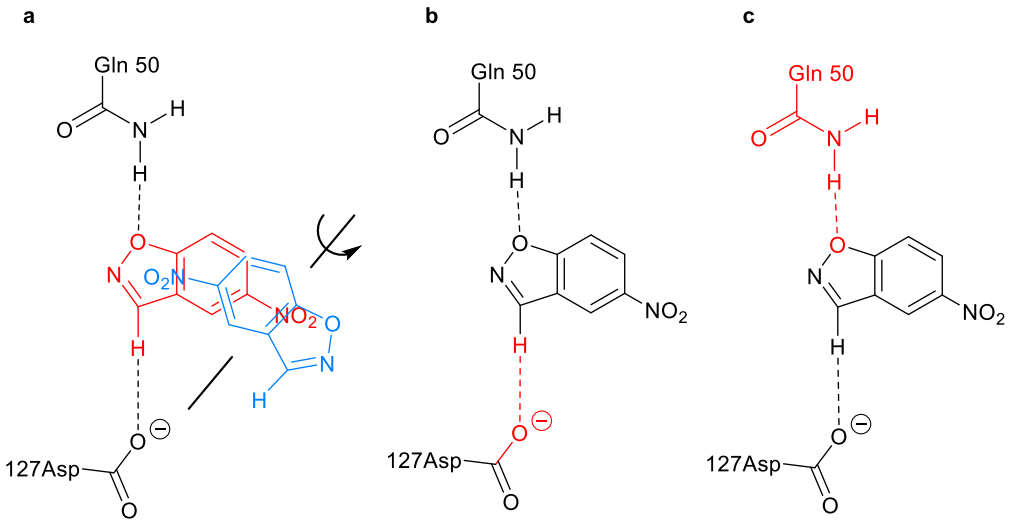

Figure 13. Catalytic improvement of HG-3**. a:** High shape complementarity between substrate (red molecule) and active site eliminated unproductive binding modes (blue molecule). **b:** Efficient proton transfer. **c:** Introduction of an oxyanion binder contributed to transition state stabilization.

Residues Asp127 and Gln50 are nevertheless important for activity in the Kemp reaction: in fact Asp127 is $4x10^9$-fold more effective than a simple carboxylate base such as acetate in aqueous solution and replacement of Asp127 with alanine or asparagine leads to a $>10^5$ –fold reduction in activity[26]. Replacement of Gln50 with alanine reduces the k_{cat}/K_M by 50-fold in the Kemp reaction[26]: this residue is well placed to position the substrate for proton abstraction and simultaneously facilitate charge transfer from the buried carboxylate to the phenolic oxygen. These results demonstrate that a bottom-up approach combining computational design with directed evolution can yield artificial biocatalysts capable of accelerating proton transfer with true enzymatic efficiency.

2. *Aim of the research*

The main subject of this project has been the study and kinetic analysis of Kemp elimination through the use of the UV/Vis spectrophotometric technique, using substituted benzisoxazoles as substrates in the presence of hemoproteins.

The first phase of the research has been the synthesis of benzisoxazoles bearing different substituents; particular attention was devoted to the reaction conditions optimization in order to optimize every synthetic step. The synthetic strategy involved three key steps, *i.e.* a formylation of a phenol derivative, followed by nucleophilic addition of hydroxylamine and by final cyclization to give a fused isoxazole ring (**Scheme 9**).

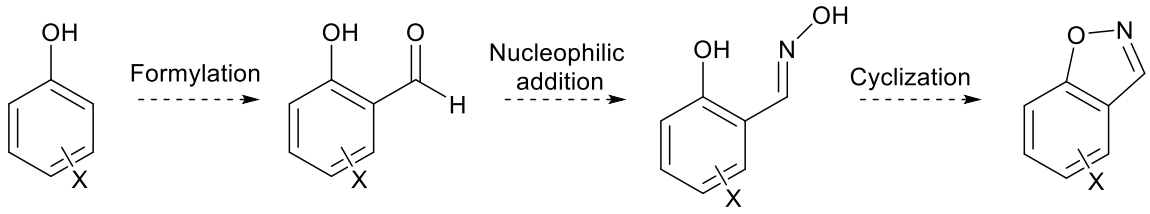

Scheme 9. Synthetic sequence to obtain substituted benzisoxazoles.

Afterwards, the base-catalyzed decomposition of the synthesized substrates, in the presence of Cytochrome c, hemoglobin and myoglobin was studied under different conditions.

Finally, the kinetic isotope effect, using a deuterated substrate, was studied to gain information on the nature of the rate-limiting step of the Kemp elimination.

3. Results and discussion

3.1. Synthesis of benzisoxazoles as substrates for the Kemp elimination

The mechanism of the Kemp reaction was investigated through UV/Vis spectrophotometry using 1,2-benzisoxazole derivatives as substrates. In particular, benzisoxazoles **15a-e** (**Figure 14**) were considered, and the deuterated compound **15c** was prepared with the aim to investigate on the isotope effect.

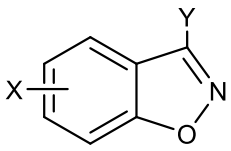

15a-e

15a. X=H; Y=H
15b. X=5-Br; Y=H
15c. X=5-Br; Y=D
15d. X=6-OMe; Y=H
15e. X=5-NO_2; Y=H

Figure 14. Benzisoxazole derivatives as substrates for Kemp elimination.

Among the synthetic pathways available for the obtainment of the above compounds we selected that described in **Scheme 10** for the preparation of **15a-d** while **15e** was obtained by nitration of commercial benzisoxazole (see below).

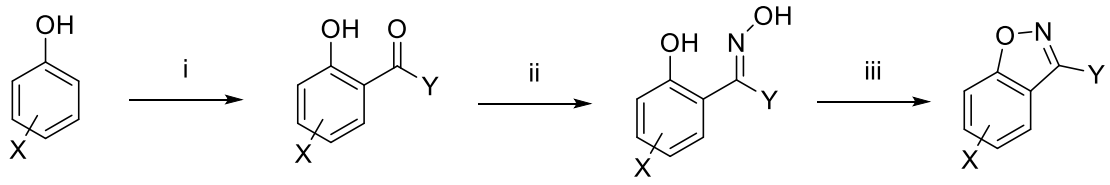

X=H, Br, OMe, NO_2
Y=H, D

i: $CHCl_3$, NaOH 10N, reflux, 90min (X=5-Br, Y=H) or $CDCl_3$, NaOD 10N, Ar, reflux, 120min (X=5-Br, Y=D);
ii: $NH_2OH \cdot HCl$, EtOH, 65°C, overnight (X=5-Br, Y=H,D) or $NH_2OH \cdot HCl$, NaOH 50%, EtOH:H_2O (1:2), 0°C→RT, 60min (X=4-OMe, Y=H);
iii: PPh_3/DDQ, DCM, Ar, RT, 5min (X=5-Br; 6-OMe; 5-NO_2; Y=H; D).

Scheme 10. Experimental reaction conditions to obtain substituted benzisoxazoles.

In particular, compounds **15a–c** were obtained subjecting the corresponding phenol precursor **10a** or **10b** through the complete synthetic sequence shown in **Scheme 10**. The first step is an *ortho*-formylation reaction, called Reimer-Tiemann reaction, between a phenol derivative and chloroform in alkaline solution to give the corresponding salicylaldehyde (**Scheme 11**). The reaction conditions used to obtain the salicylaldehydes **11a,b** and **11c** are shown in **Scheme 11**.

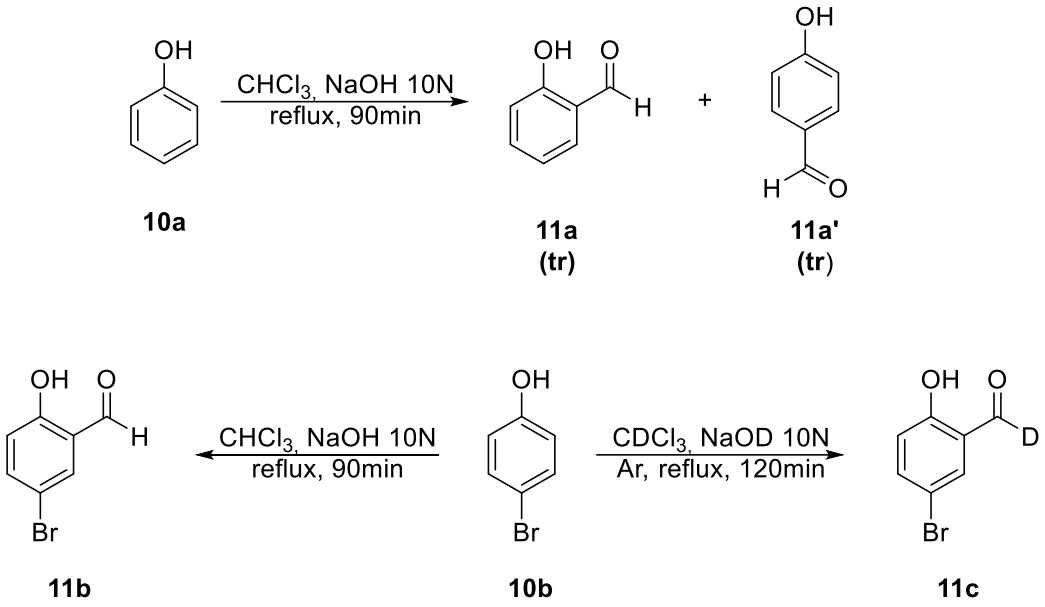

Scheme 11. Synthesis of deuterated salicylaldehyde and not.

This reaction involves an electrophilic substitution on the highly reactive phenate ring by dichlorocarbene, formed by action of a base on chloroform. A problem of this formylation reaction, when carried out on phenol (**10a**), is the regioselectivity because both *ortho*- and *para*- isomers can be produced, and the isolation of only one isomer requires a purification step; it has been reported[27,28] that the *ortho*-isomer can be separated by distillation. In **Table 2** are collected the conditions used for this reaction step. First, based on literature reports[29] the reaction between phenol and chloroform was carried out in the biphasic system 1,4-dioxane/40% aq. NaOH solution in the presence of benzyltrimethylammonium chloride (**BTMAC**), as emulsifying agent. After 2 hours at reflux and after the work-up of the reaction mixture (which ^{1}H NMR spectrum showed a large amount of

unreacted phenol and a great number of other signals), the isolation by flash cromatography of the product(s) was attempted but only traces of *ortho*- and *para*- isomers **11a** and **11a'** were isolated (**Table 2**, entry 1). Thus, to avoid regioselectivity problems, it has been decided to start from 4-bromophenol **10b** in such a way the attack in *para*-position might be avoided and only the formation of the ortho-isomer was expected. Also in this case, in the ^{1}H NMR spectrum of the crude from the reaction carried out under the same conditions of **10a**, appeared a very large number of signals belonging to unidentified compounds together with those of the starting 4-bromophenol (**Table 2**, entry 2). Since in the literature[30] it has been reported a very simple and fast procedure for the formylation of substituted phenols using aqueous alcoholic sodium hydroxide and chloroform under microwave irradiation, the reaction with **10b** and chloroform with 40% aq. NaOH was carried out both in a mixture H_2O:EtOH (9:1 v/v) and H_2O:EtOH (1:9 v/v) under microwave irradiation for 10 min (**Table 2**, entries 3 and 4, respectively). After acidification, in the first case, the ^{1}H-NMR spectrum of the reaction mixture showed signals of the aldehyde together with those of a large amount of unidentified by-products; whereas in the second case no aldehyde signals were detected. Thus, the reaction was carried out in a 10 M NaOH aqueous solution between **10b** and chloroform in a 1:2 molar ratio (**Table 2**, entry 5). After 1.5 hours at 65°C the reaction mixture was acidified with 10% aq. HCl; after work-up (see experimental section) and two consecutive chromatographic purifications on silica gel column, pure 5-bromosalicylaldehyde (**11b**) was isolated as yellow solid in 17% yield. The deuterated product **11c** was prepared from **10b** in the presence of a two fold equivalents of $CDCl_3$ and 40% NaOD in D_2O under inert atmosphere (Argon). In this case the desired product was obtained as white solid in 19% yield after two subsequent purifications by chromatography on silica gel. Although the yield of this step were low, we decided do not optimize them, but to focus our efforts on the subsequent steps to obtain the desired benzisoxazole.

Table 2. **Screening of the Riemer-Tiemann reaction conditions:**

Entry	Reagents	Solvent	Base	T	Time	Product (Yield)
1	**10a** + $CHCl_3$	1,4-dioxane	$NaOH_{(aq)}$ 40% BTMAC	70°C	90 min	**11a and 11a'**[a] (traces)
2	**10b** + $CHCl_3$	1,4-dioxane	$NaOH_{(aq)}$ 40% BTMAC	70°C	90 min	n.d.[b]
3	**10b** + $CHCl_3$	H_2O:EtOH(9:1)	$NaOH_{(aq)}$ 40%	100°C MW	10 min	**11b**[b] (traces)
4	**10b** + $CHCl_3$	H_2O:EtOH(1:9)	$NaOH_{(aq)}$ 40%	100°C MW	10 min	n.d.[c]
5	**10b** + $CHCl_3$	/	NaOH 10M	65°C	90 min	**11b**[d] (17%)
6	**10b** + $CDCl_3$	/	NaOD 40% in D_2O	65°C	120 min	**11c**[d] (19%)

[a] Presence of both *ortho*- and *para*-isomer togheter with starting reagent and many other by-products. [b] Presence of many by-products. [c] Aldehyde not detected. it hasn't formed any aldheyde. [d] 4-bromo-phenol/$CHCl_3$ (or $CDCl_3$) in a 1:2 molar ratio.

Once formed the salicyl aldehyde **11b** and the corresponding deuterated analogue **11c**, they were subjected to nucleophilic attack of hydroxylammine on the carbonyl group. In this manner, the corresponding oxime was formed, as shown in **Scheme 12**.

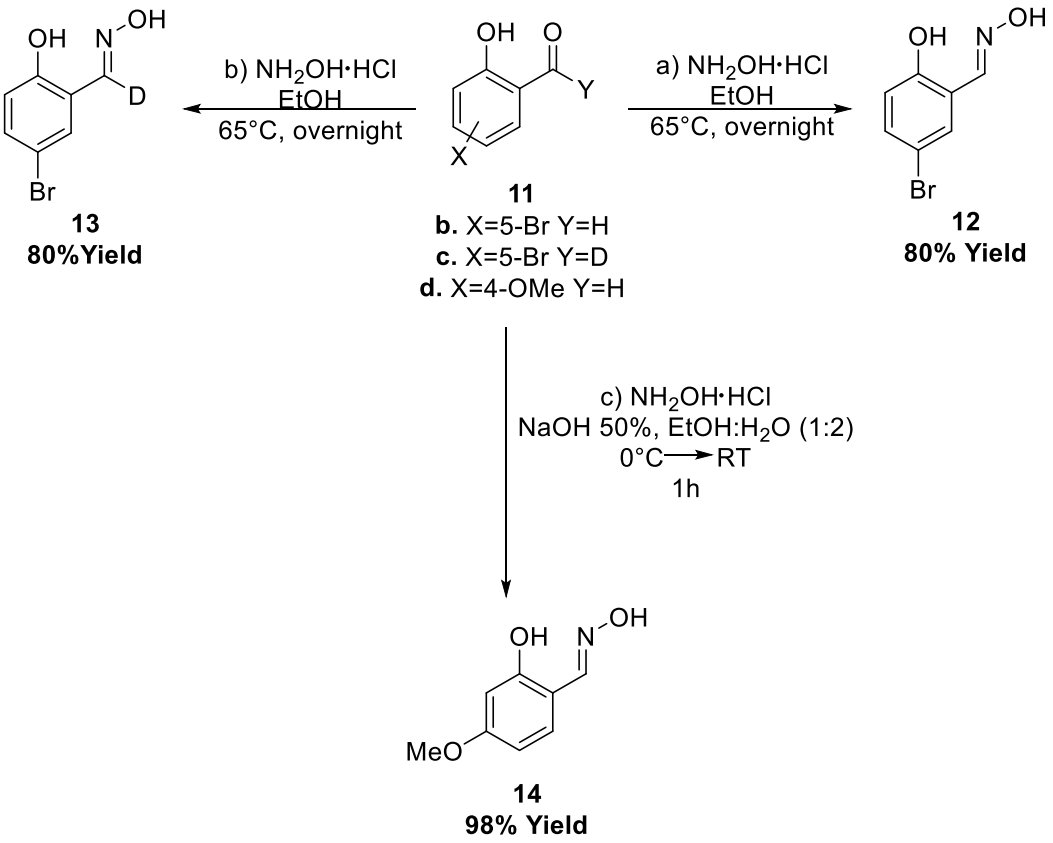

Scheme 12. Synthesis of different substituted oximes.

The oxime **12** has been obtained as white precipitate in 80% yield after addition of cold water to an ethanolic solution of **11b** and hydroxylamine hydrochloride stirred overnight at 65 °C. Under the same reaction conditions deuterated 5-bromosalicylaldehyde **11c** gave the corresponding deuterated oxime **13** in 80% yield. Applying the same conditions to the analogous reaction with 4-methoxysalicylaldehyde **11d** (commercially available), oxime **14** was obtained in 33% yield, also when an excess of hydroxylammine was used (yield reached 39%). Probably, the nucleophilic attack is unfavored in the case of 4-methoxysalicylaldehyde because of the presence of the methoxy group, an electron-donor group, in *para*-position to the carbonyl group and this makes the carbonyl carbon atom less electrophilic with respect to that of **11b** and **11c**. Thus, we treated hydroxylammine hydrochloride with NaOH in order to favor the nucleophilic attack to the 4-methoxysalicylaldheyde. The reaction was carried out in 1:2 EtOH:H_2O (v/v) starting from 0°C to room

temperature for 1 hour; after acidification of the final reaction mixture, the corresponding oxime **14** was obtained as a purple solid in 98% yield. The results are summarized in **Table 3.**

Table 3. **Screening of reaction of second step.**

Entry	Reagent	$NH_2OH{\cdot}HCl$	Base	Solvent	T	Time	Yield
1	**11b**	1.3eq	/	EtOH	65°C	over-night	80%
2	**11c**	1.3eq	/	EtOH	65°C	over-night	80%
3	**11d**	1.3eq	/	EtOH	65°C	over-night	33%
4[a]	**11d**	1.3+1.1eq	/	EtOH	65°C	55h	39%
5[b]	**11d**	1.2eq	$NaOH_{(aq)}$ 50%	EtOH:H_2O (1:2)	0°C to RT[c]	1h	98%

[a] After 48 hours there was starting reagent yet, also when a further amount (1.1eq) of NH_2OH/HCl was added and the reaction mixture stirred for 7 hours. [b] the final crude solution was acidified with HCl 1M until at pH=5. [c] The NaOH solution was added at 0°C dropwise.

The final step was the cyclization of the oximes **12-14**, in the presence to 2,3-dichloro-5,6-dicyano-1,4-benzoquinone (**DDQ**) and PPh_3 under anhydrous conditions (**Scheme 13**). This reaction occurred immediately: after 5 minutes the solution color changed from light green to mustard yellow. The benzisoxazole derivative was obtained after work-up and purification of the crude by flash chromatography that removed the excess of **DDQ** and PPh_3.

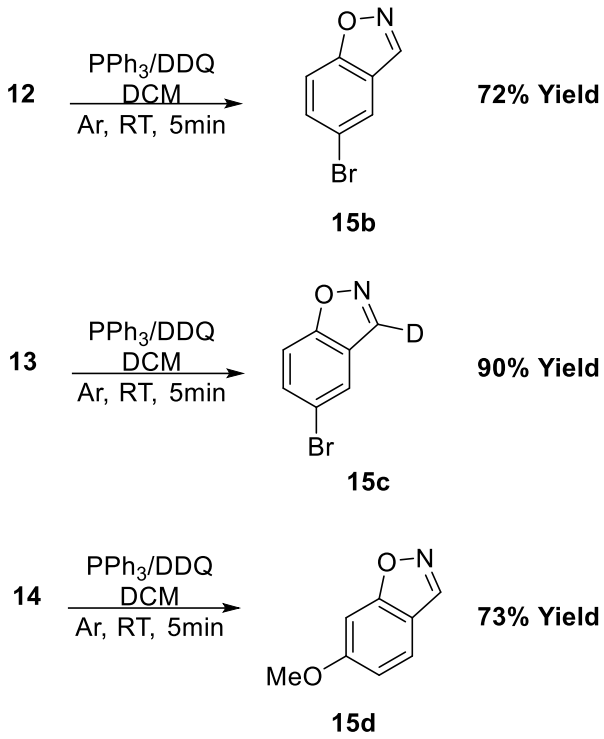

Scheme 13. Synthesis of deuterated (and not) substituted benzisoxazoles.

The 5-NO_2-benzisoxazole (**15e**) has been obtained by nitration of the commercially available unsubstituted benzisoxazole **15a**. The reaction, due to its exothermicity, was carried out by adding carefully at 0°C a mixture of H_2SO_4/HNO_3 (ratio about 1:3) to **15a** and stirring the reaction mixture for 30 minutes. After aqueous work-up and recrystallization from 95% EtOH, the product **15e** was recovered as white solid in 53% yield (**Scheme 14**).

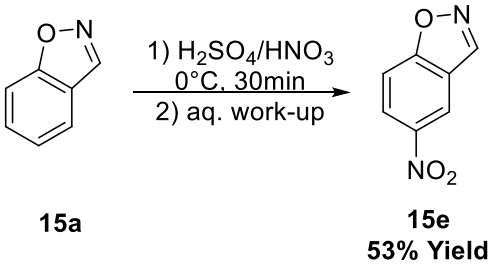

Scheme 14. Synthesis of 5-NO_2-benzisoxazole.

3.2. UV/Vis analysis of synthesized benzisoxazoles in the presence of hemoproteins

Once the substrates **15a-e** (hereafter also indicated as 5-BrBI; D-5-BrBI; 5-NO_2BI; 6-OMeBI) have been synthesized, kinetic studies on the Kemp reaction have been carried out under different conditions in aqueous solution, using three hemoproteins: Cytochrome c, myoglobin and hemoglobin. The reactions have been monitored through UV/Vis spectrophotometer at 20°C, exploiting the characteristic wavelengths of the opening products, already known in the literature[10], so as to detect the appearance of the opening product of the heterocyclic ring (**Scheme 15**).

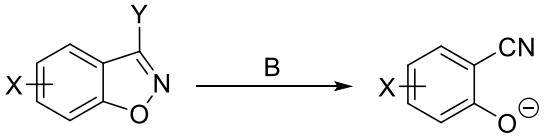

15a-e **$(15a-e)_a$**

15a. X=H; Y=H (BI)
15b. X=5-Br; Y=H (5-BrBI)
15c. X=5-Br; Y=D (5-D-BrBI)
15d. X=6-OMe; Y=H (6-OMeBI)
15e. X=5-NO_2; Y=H (5-NO_2BI)

15a. X=H; (BI_a)
15b. X=5-Br; (5-$BrBI_a$)
15d. X=6-OMe; (6-$OMeBI_a$)
15e. X=5-NO_2; (5-NO_2BI_a)

Scheme 15. Kemp reaction on synthesized benzisoxazoles.

3.2.1. Experiments with Cytochrome c

At first we tried to understand by what the Kemp reaction is catalyzed, doing various trials with different substrates (6-OMeBI, 5-BrBI and 5-NO_2BI) in presence of Cytochrome c. It has to be noted that some hemoproteins (e.g. Cytochrome P450[22] and aldoxime dehydratase[21]) require a reducing agent, for example L(+)-ascorbic acid, to catalyze the reaction, because of the possible active form of Fe(II) of heme group. So we tried to understand if other hemoproteins can catalyze the opening of the isoxazole ring of selected substrates and with which mechanism (redox or ionic) it occurs.

Four trials have been conducted for the substrate 6-OMeBI (results are shown in **Table 4**) and the reaction course was monitored by UV/Vis spectrophotometry, recording one scan every 5 min at λ_{max} = 317nm, which is the characteristic wavelength of the opening product of the heterocyclic ring of 6-OMeBI[10].

Table 4. Kemp reaction on 6-OMeBI. Trials with ±Cytc, ±asc.

Reagents	TRIALS			
	1	**2**	**3**	**4**
H_2O	470 µL	470 µL	470 µL	470 µL
Buffer 500 mM pH=8,25	25 µL	25 µL	25 µL	25 µL
6-OMeBI 74 mM	3 µL	3 µL	3 µL	3 µL
Cyt c 2,75 mM	5 µL	/	5 µL	/
Ascorbate 400 mM	5 µL	5 µL	/	/
Volume tot	508 µL	503 µL	503 µL	498 µL

It is known that the rate of an enzimatic reaction in subsaturating substate conditions can be described by the following general equation derived from the Michaelis-Menten treatment:

$$v = \frac{k_{cat}}{K_M}\,[E][S]$$

This equation requires that the substrate concentration is well below the K_M of the reaction. As we will see later, this condition was met for all the experiments. To found k_{cat}/K_M, the kinetic parameter that permits to compare different enzymatic reactions, it is necessary to know both the enzyme and substrate concentration and to know the effective rate of reaction. The effective concentration of enzyme and substrate can be easily obtained from the following relationships:

$$[E_{eff}] = \frac{[E]\cdot f}{V_{tot}} \qquad\qquad [S_{eff}] = \frac{[S]\cdot f}{V_{tot}}$$

Where f is a dilution factor and V_{tot} is the total volume of the solution in the cuvette. The total volume has been normalized to 500µL to facilitate the calculations: this influence negligibly (≈1-2%) the obtained results. The effective concentration of Cytochrome c in solution is equal to:

$$[CytC] = \frac{2{,}75\ mM \cdot 5}{500\ \mu L} = 2{,}75 \cdot 10^{-3} M$$

The effective concentration of the substrate is:

$$[6OMeBI] = \frac{74\ mM \cdot 3}{500\ \mu L} = 4{,}44 \cdot 10^{-4} M$$

The rate can be derivated by Lambert-Beer's law:

$$A = \varepsilon\, l\, C$$

Where A is absorbance (adimensional), ε is the molar extinction coefficient [M^{-1} cm^{-1}], C is the concentration of solution [M] and l is the optical path of the cuvette [cm].

Observing the reaction course as a function of time and plotting Abs vs time, a graphic indicating a direct proportionality is obtained. It is represented by a stright line where the angular coefficient represents a no-effective rate of reaction because it would be an absorbance (adimensional) on a time (minutes). So to convert this rate to the effective one, it is necessary to divide it by the molar extinction coefficient, obtaining a dimensionally correct rate [M/min].

Afterwards we can calculate the k_{cat}/K_M:

$$\frac{k_{cat}}{K_M} = \frac{v}{[E][S]}$$

The data obtained from the UV/Vis spectrophotometric technique of the four trials indicated in **Table 4** are the following:

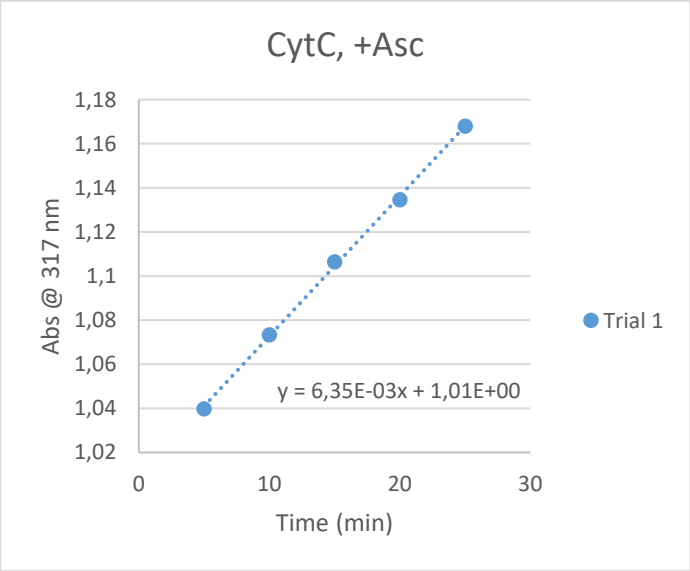

Figure 15. Trial 1 with Cytochrome c and ascorbate.

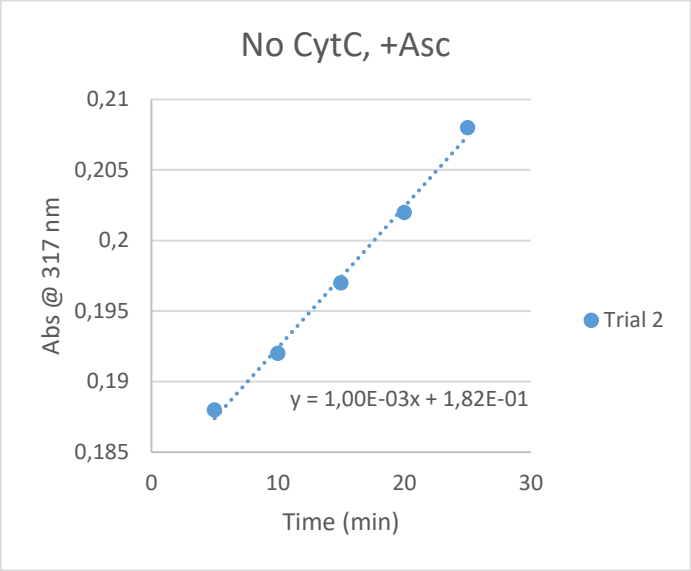

Figure 16. Trial 2 with ascorbate.

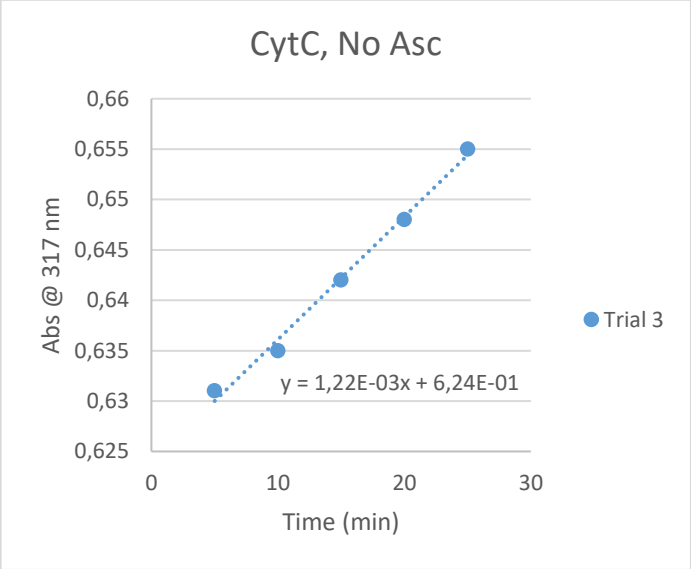

Figure 17. Trial 3 with Cytochrome c.

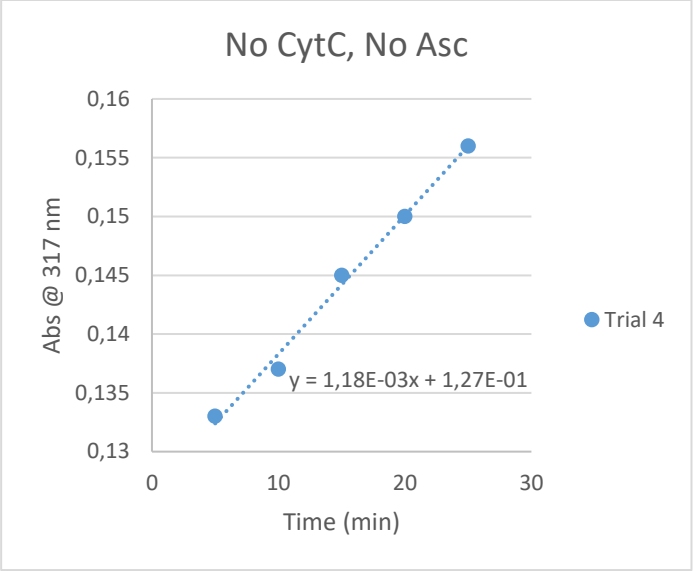

Figure 18. Trial 4 without Cytochrome c and ascorbate.

As can be shown from the four graphs obtained (**Figure 15-18**), the slopes of the four straight lines have the same order of magnitude. In order to made an easier comparison, it was established to normalize the 4 lines, obtaining the following graph (**Figure 19**):

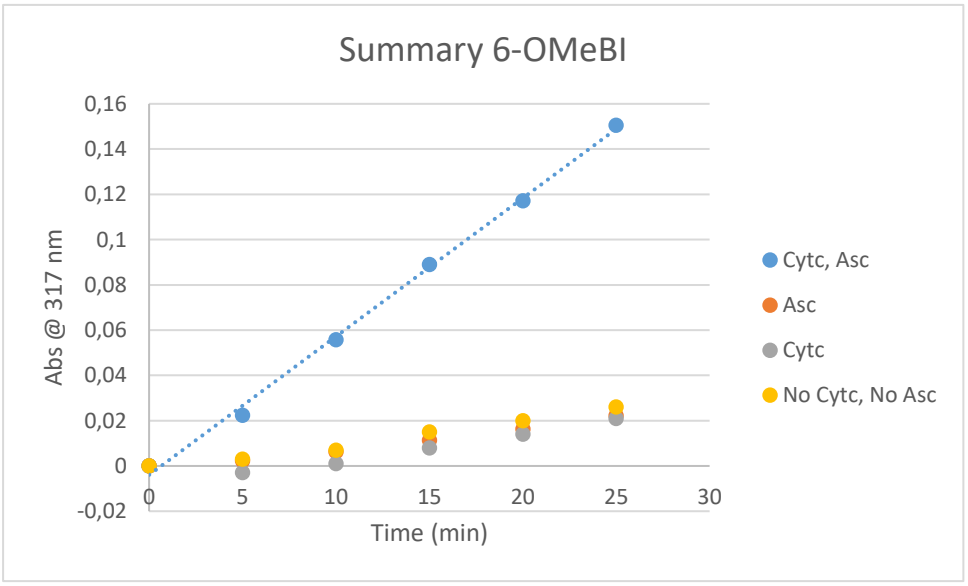

Figure 19. Summary of the data obtained with 6-OMeBI in the presence of Cytochrome c.

This graph shows that the slope of the line corresponding to trial 1, is greater than other ones: this suggests that the combined action of cytochrome c and ascorbate catalyzes in a more efficient manner the Kemp reaction on the substrate 6-OMeBI.
So it has been calculated k_{cat}/K_M referred to trial 1: to obtain the effective slope, given only by the action of Cytochrome c, it is necessary to subtract the slope of the straight line referred to trial 2 (it represents the reaction of background) to the slope of the straight line referred to trial 1 (that represents the background reaction + reaction due to Cytochrome c)

$$\frac{k_{cat}}{K_M} = \frac{m_1 - m_2}{\varepsilon_{6-OMeBI_a}[E][S]} = \frac{0{,}00635 - 0{,}001}{7500 \cdot 2{,}75 \cdot 10^{-3} \cdot 4{,}44 \cdot 10^{-4}} = 58{,}42\ M^{-1}min^{-1} = 0{,}964\ M^{-1}s^{-1}$$

Where $\varepsilon_{6-OMeBI_a}$ is the molar extinction coefficient of opening product of the heterocyclic ring[10].

In case of the substrate 5-BrBI, three trials have been conducted varying the concentrations of the enzyme (see **Table 5**) to ensure that the reaction on this substrate was dependent on the enzyme concentration, in other words, that we monitored an enzymatic reaction. The trials, shown in **Table 5**, have been monitored by UV/Vis spectrophotometry as a function of time (one scan every 5 min), using λ_{max}=337nm, the characteristic wavelength of the opening product of the heterocyclic ring of 5-BrBI[10].

Table 5. Kemp reaction on 5-BrBI. Trials varying [Cyt c].

Reagents	TRIALS		
	5	**6**	**7**
H_2O	470 µL	470 µL	470 µL
Buffer 500 mM pH=8,25	25 µL	25 µL	25 µL
5-BrBI 70 mM	3 µL	3 µL	3 µL
Cyt c 2,75 mM	3 µL	/	10 µL
Ascorbate 400 mM	5 µL	5 µL	5 µL
Volume tot	506 µL	503 µL	503 µL

The corresponding graphics (Abs vs. time) obtained are the following:

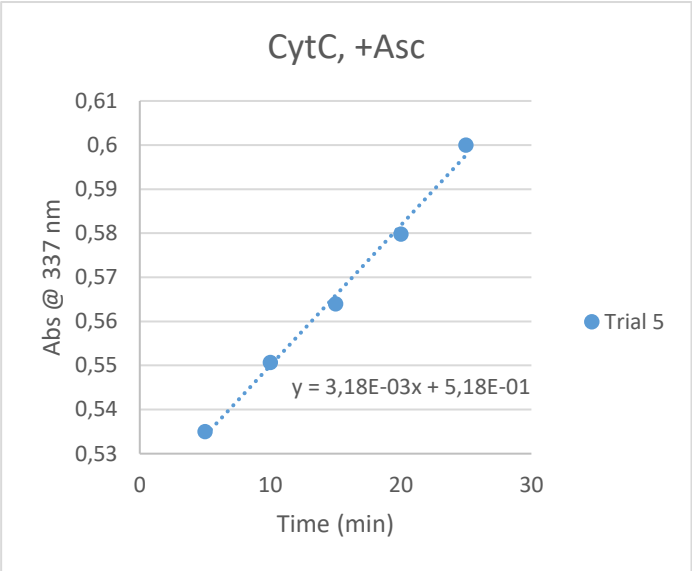

Figure 20. Trial 5 with Cytochrome c and ascorbate.

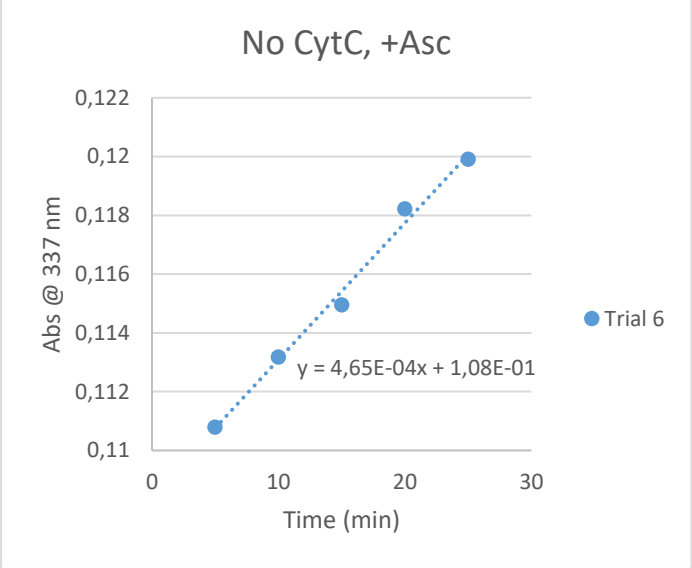

Figure 21. Trial 6 with ascorbate.

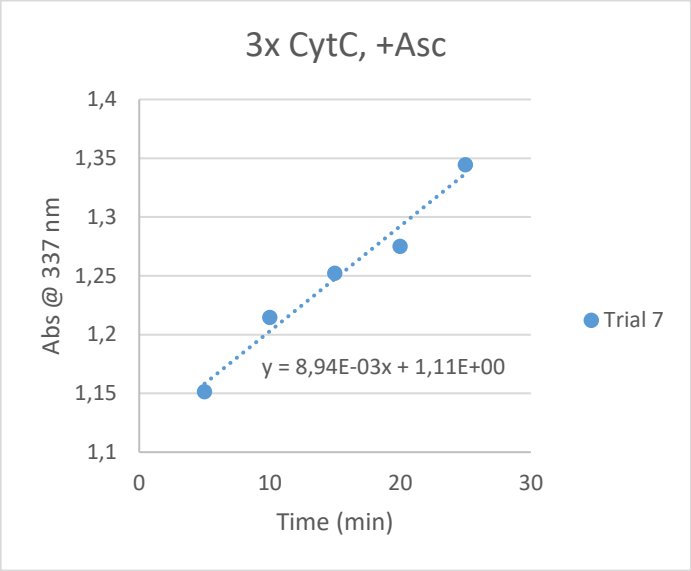

Figure 22. Trial 7 with Cytochrome c (x3) and ascorbate.

The concentrations of Cytochrome c in cases 5 and 7 are respectively:

$$[CytC]_5 = \frac{2{,}75\ mM \cdot 3}{500\ \mu L} = 1{,}65 \cdot 10^{-5} M$$

$$[CytC]_7 = \frac{2{,}75\ mM \cdot 10}{500\ \mu L} = 5{,}50 \cdot 10^{-5} M$$

The concentration of the substrate in all trials is:

$$[5BrBI] = \frac{70\ mM \cdot 3}{500\ \mu L} = 4{,}20 \cdot 10^{-4} M$$

On varying the concentrations of the enzyme, it is possible to see how the rate changes with the same substrate. For [E]= $1{,}65 \cdot 10^{-5} M$:

$$\frac{v}{[S]} = \frac{m_1 - m_2}{\varepsilon_{5-BrBI_a}[S]} = \frac{0{,}00318 - 0{,}000465}{6100\ \times 0{,}000420} = 0{,}00106\ min^{-1}$$

In the same way it is possible to calculate the rate for the other two points ([E]=0 M and [E]= $5{,}50 \cdot 10^{-5} M$). The data obtained are the following (**Table 6**):

Table 6. v/[S] values at different [E].

[E]	v/[S]
0	0,000181
0,0000165	0,00106
0,000055	0,003308

In **Figure 23** is shown the graphic obtained by plotting the above data:

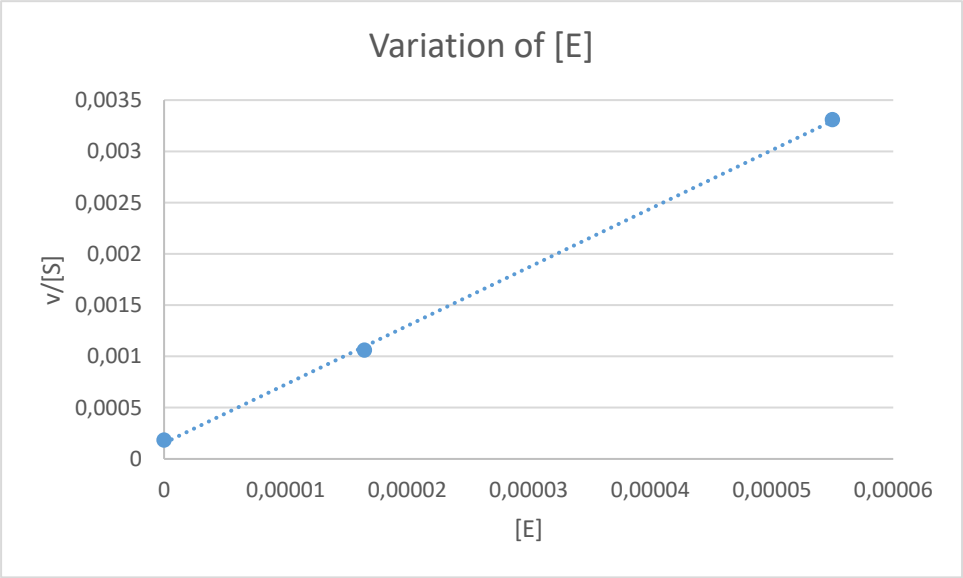

Figure 23. Plot of v/[S] vs [E].

This graph shows that at zero enzyme concentration, the rate is not zero: this can be considered as an indication of the occurrence of the background reaction that catalyzes the Kemp elimination by a hydroxide ion from the solvent.

To know the slope of this straight line, the k_{cat}/K_M is calculated with $\varepsilon_{5\text{-BrBI-a}}$=6100 $M^{-1}cm^{-1}$ for trials 5 and 7:

$$\frac{k_{cat}}{K_{M\ 5}} = \frac{0{,}00318 - 0{,}000465}{6100 \cdot 1{,}65 \cdot 10^{-5} \cdot 4{,}20 \cdot 10^{-4}} = 64{,}23\ M^{-1}min^{-1}$$

$$\frac{k_{cat}}{K_{M\ 7}} = \frac{0{,}00894 - 0{,}000465}{6100 \cdot 5{,}50 \cdot 10^{-5} \cdot 4{,}20 \cdot 10^{-4}} = 60{,}14\ M^{-1}min^{-1}$$

Since the values are almost equal, it can be established that the k_{cat}/K_M is constant for the two trials. The differences between the two values may be reasonably ascribed to the approximations made.

The results obtained from trials 5, 6 and 7, represented in previous graphs, after normalization, gave **Figure 24**:

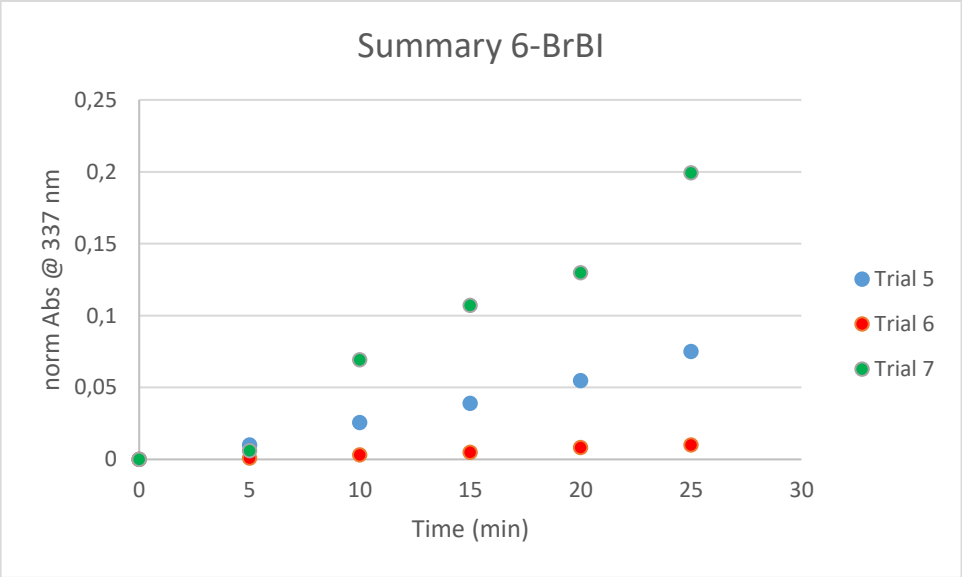

Figure 24. Summary of the data obtained with 5-BrBI in the presence of Cytochrome c.

As it can be shown from the above graph, the trial 7, with a higher concentration of cytochrome c respect to the trial 5, shows a slope greater than the other trials anyway. Furthermore, the conditions used in trial 6, where it is not present the protein but it is present only the ascorbate, are not sufficient to catalyze the Kemp reaction in a satisfactory manner. This may mean that: the cytochrome c catalyzes the Kemp reaction for the substrate 5-BrBI thanks to the possible combined action with ascorbate; the presence of ascorbate is necessary for its role in a possible reduction of Fe (III) into the heme group; finally, taking constant the concentration of the substrate, the rate of the reaction increases when the enzyme concentration increases.

Finally, we tried the Kemp reaction for the substrate 5-NO_2BI in the presence of Cytochrome c under different experimental conditions (see **Table 7**). Similarly to the previous

cases, the reaction course was monitored through UV/Vis spectrophotometry at λ_{max}=380nm, the characteristic wavelength of the opening product of the heterocyclic ring of 5-NO_2BI[10]. We tried to record the spectrum every 5 min and then every 3 min, but this is a too long time to monitor the reaction course: the data were affected by low reproducibiliy thus not guaranteeing a certain affidability. So we established to monitor the reaction every 20 seconds, in order to gain more accurate and reproducible data.

Table 7. Kemp reaction on 5-NO_2BI. Trials with ±CytC, ±asc.

Reagents	TRIALS		
	8	**9**	**10**
H_2O	470 µL	470 µL	470 µL
Buffer 500 mM pH=7,33	25 µL	25 µL	25 µL
5-NO_2BI 61 mM	3 µL	3 µL	3 µL
Cyt c 2,75 mM	3 µL	/	3 µL
Ascorbate 400 mM	5 µL	5 µL	/
Volume tot	506 µL	503 µL	501 µL

The data obtained through UV/Vis spectrophotometry, already normalized, are the following (**Figure 25**):

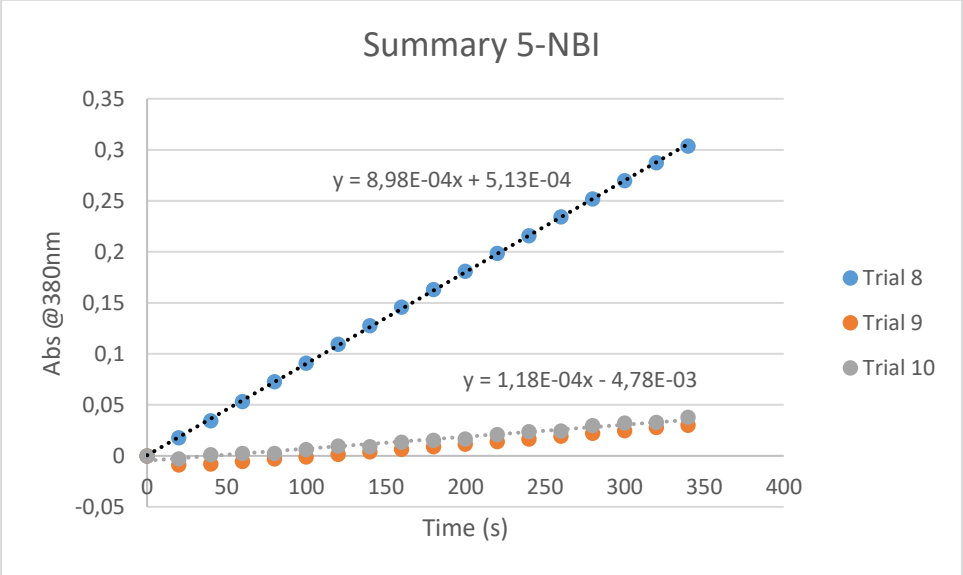

Figure 25. Summary of the data obtained with 5-NO_2BI in the presence of Cytochrome c.

The concentrations of enzyme and substrate are respectively:

$$[CytC] = \frac{2{,}75\ mM \cdot 3}{500\ \mu L} = 1{,}65 \cdot 10^{-5} M$$

$$[5NO_2BI] = \frac{61\ mM \cdot 3}{500\ \mu L} = 3{,}66 \cdot 10^{-4} M$$

The k_{cat}/K_M, value with $\varepsilon_{5\text{-}NO2BI\text{-}a}$=18400 $M^{-1}cm^{-1}$ [10], is:

$$\frac{k_{cat}}{K_M} = \frac{0{,}000898}{18400 \cdot 1{,}65 \cdot 10^{-5} \cdot 3{,}66 \cdot 10^{-4}} = 8{,}08\ M^{-1}s^{-1} = 484{,}89\ M^{-1}min^{-1}$$

As can be shown from the above graph, the slope of trial 8, obtained from the experiment carried out with both Cytochrome c and ascorbate, is greater than that of the other two trials: also in this case the combinated action of enzyme and reducing agent catalyzes more efficiently the Kemp reaction.

3.2.1.1. pH rate-profile using different substrates.

The heme group, characterized by two carboxy groups, has two p*Ka* values: 3,6 and 8,6[31]. It is known from the literature that other hemoproteins catalyze the opening of the benzisoxazolic ring just due to deprotonated carboxy groups. So we wanted to analyze the influence of pH on the rate of the ring-opening reaction on the different substrates herein considered. The reaction was carried out in the presence of Cytochrome c and ascorbate using buffers at the pH values: 6,88; 7,33; 7,64; 8,25; 8,70; 9,4.

In **Table 8** are collected the experimental conditions used in the case of 5-NO_2BI.

Table 8. Trials with 5-NO_2BI for pH-rate.

Reagents	TRIALS				
	11	**12**	**13**	**14**	**15**
H_2O	470 µL	470 µL	470 µL	470 µL	470 µL
Buffer 500 mM pH=9,40	25 µL	/	/	/	/
Buffer 500 mM pH=8,25	/	25 µL	/	/	/
Buffer 500 mM pH=7,64	/	/	25 µL	/	/
Buffer 500 mM pH=7,33	/	/	/	25 µL	/
Buffer 500 mM pH=6,88	/	/	/	/	25 µL
5-NO_2BI 61 mM	3 µL	3 µL	3 µL	3 µL	3 µL
Cyt c 2,75 mM	3 µL	3 µL	3 µL	3 µL	3 µL
Ascorbate 400 mM	5 µL	5 µL	5 µL	5 µL	5 µL
Volume tot	506 µL	506 µL	506 µL	506 µL	506 µL

A scan every 2 seconds was performed for the trials 11, 12 and 13; whereas a scan every 20 seconds was performed for the trials 14 and 15. The choice of these acquisition times was made in order to obtain more accurate data: actually, at lower pH values the reaction is slower, so it needs a longer acquisition time. The data obtained, already normalized, are reported in the graphics (**Figure 26-27**):

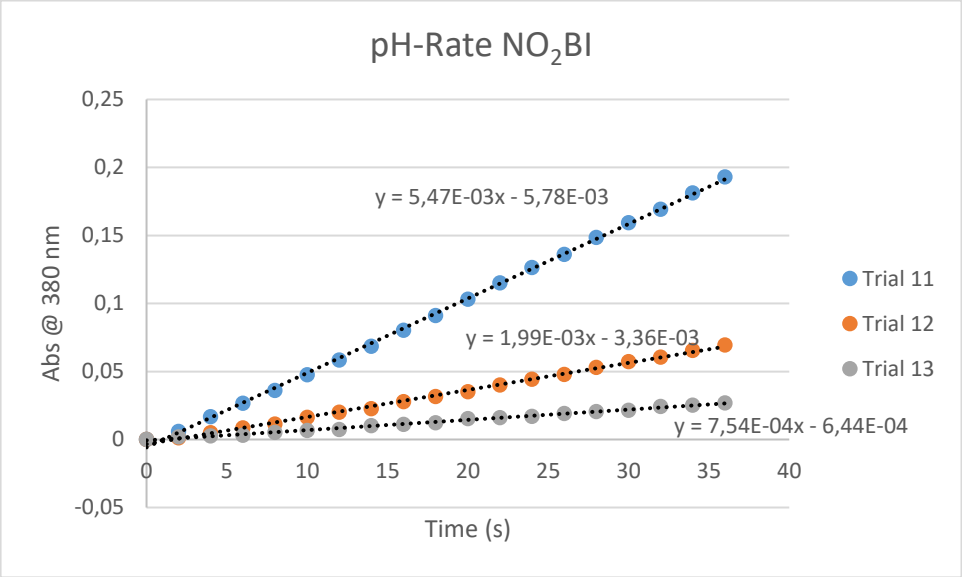

Figure 26. pH-rate of trials 11, 12 and 13.

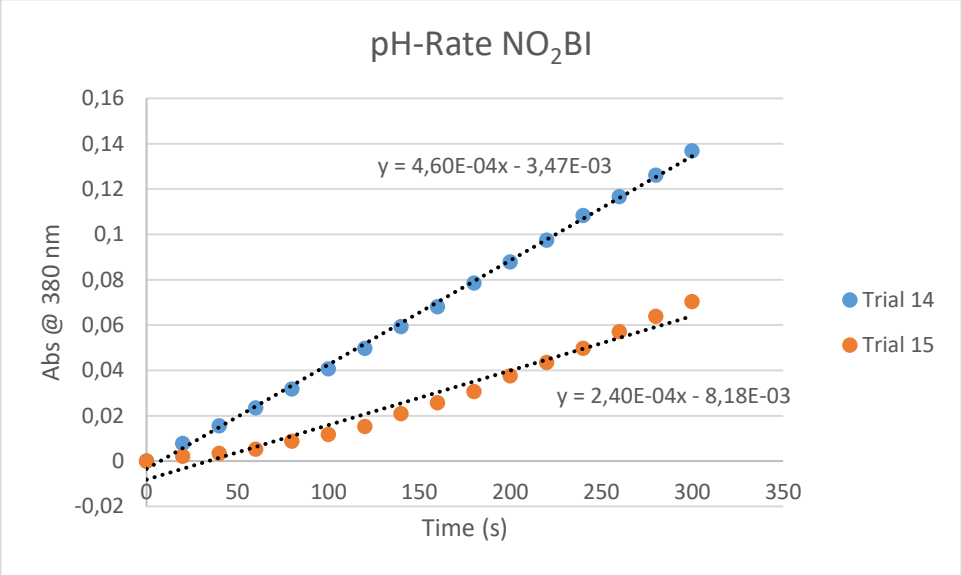

Figure 27. pH-rate of trials 14 and 15.

In a similiar way to the previous ones, the k_{cat}/K_M value was calculated for each pH and data obtained are shown in **Table 9**:

Table 9. pH-rate for 5-NO_2-BI.

pH	Abs (nm/s)	K_{cat}/K_M (M^{-1} s^{-1})	K_{cat}/K_M (M^{-1} min^{-1})
6,88	2,40E-4	2,14	128
7,33	4,60E-4	4,11	247
7,64	7,54E-4	6,75	405
8,25	1,99E-3	17,81	1068
9,40	5,47E-3	48,96	2937

Plotting the k_{cat}/K_M value versus pH, the following graph (**Figure 28**) was obtained:

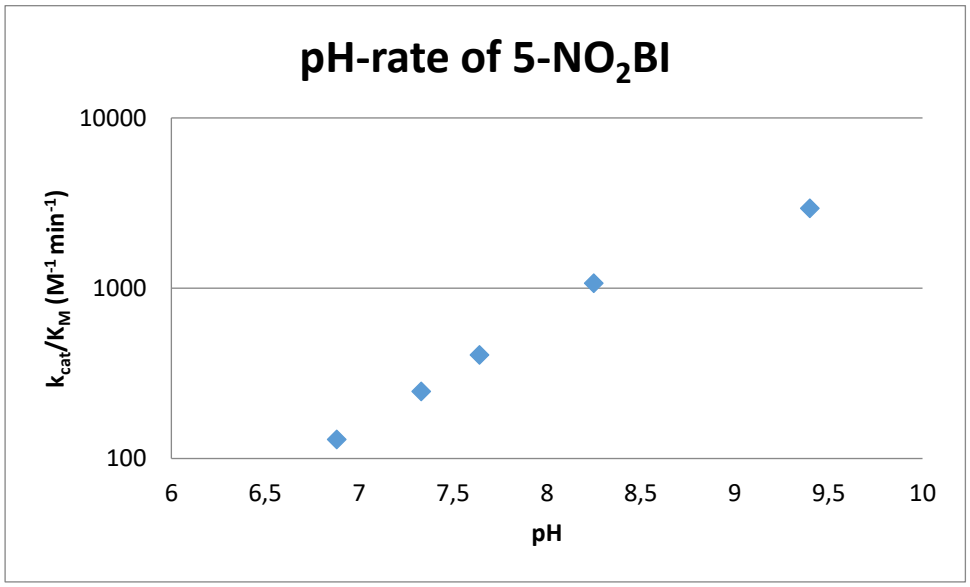

Figure 28. pH-rate of 5-NO2BI in the presence of Cytochrome c.

This graph shows that from pH=6,88 to pH=8,25 the prevailing reaction is that of back-ground since k_{cat}/K_M increases with the pH approximately in a linear manner. It must be considered that it exists an equilibrium between protonated and deprotonated carboxy groups in the enzyme that changes according to pH:

$$E_{COOH} \rightleftharpoons E_{COO^-} + H^+$$

As the pH increases, the carboxy group is more easily deprotonated, and the rate increases until the enzyme is saturated. Using the Kaleidagraph program, making an integration for a dependence on a deprotonation event, it results that an important deprotonation at an apparent p*Ka* value approximately of 8.6 occurs. This value is very similar to that of a carboxylate group on the heme of hemoprotein. These findings suggest the following questions: i) is the carboxylate on the eme involved like a base? or ii) is there anything that happens on the carboxylate that inhibits the enzymatic reaction when it is deprotonated?

Since it is not possible to remove the carboxy group from the enzyme, to try to answer to the previous questions it is possible to study the reaction through isotope effect or to study what happens when other hemoproteins are used (this will be discussed in subsequent pharagraphs).

In **Table 10** are collected the experimental conditions used in the case of 5-BrBI.

Table 10. Trials with 5-BrBI for pH-rate.

Reagents	TRIALS					
	16	**17**	**18**	**19**	**20**	**21**
H_2O	470 µL	470 µL	470 µL	470 µL	470 µL	470 µL
Buffer 500 mM pH=9,40	25 µL	/	/	/	/	/
Buffer 500 mM pH=8,70	/	25 µL	/	/	/	/
Buffer 500 mM pH=8,25	/	/	25 µL	/	/	/
Buffer 500 mM pH=7,64	/	/	/	25 µL	/	/
Buffer 500 mM pH=7,33	/	/	/	/	25 µL	/
Buffer 500 mM pH=6,88	/	/	/	/	/	25 µL
5-BrBI 53 mM	3 µL	3 µL	3 µL	3 µL	3 µL	3 µL
Cyt c 2,75 mM	3 µL	3 µL	3 µL	3 µL	3 µL	3 µL
Ascorbate 400 mM	5 µL	5 µL	5 µL	5 µL	5 µL	5 µL
Volume tot	506 µL	506 µL	506 µL	506 µL	506 µL	506 µL

For the trials 16, 17 and 18 a scan every 5 seconds was performed; whereas a scan every 20 seconds was performed for the trials 19, 20 and 21. The data obtained, already normalized, are reported in the following graphs (**Figure 29-30**):

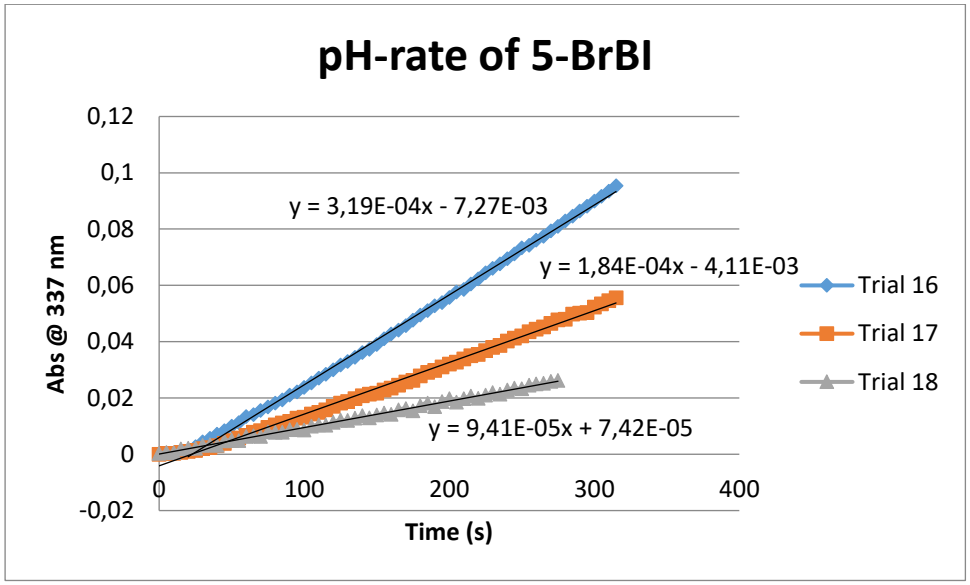

Figure 29. pH-rate of trials 16, 17 and 18.

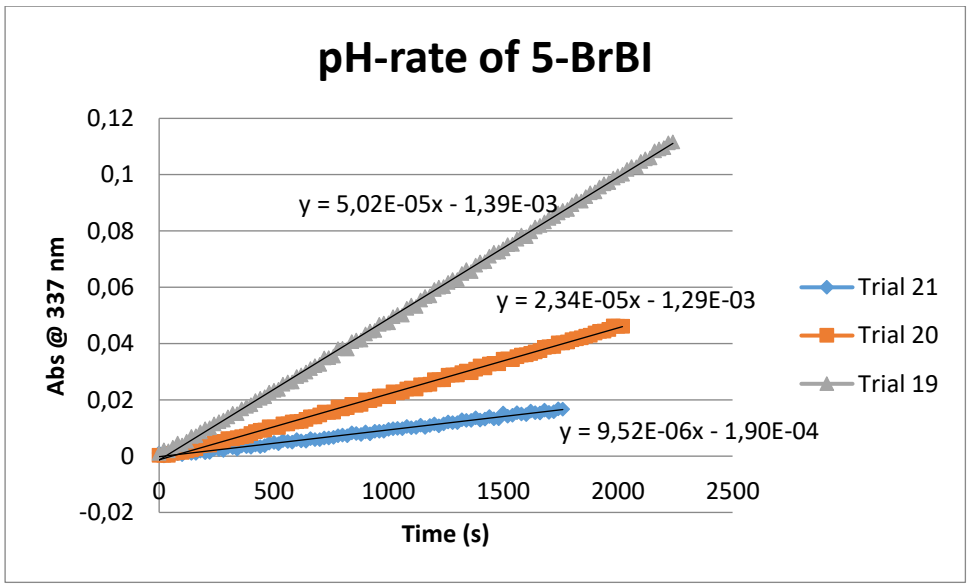

Figure 30. pH-rate of trials 19, 20 and 21.

The related k_{cat}/K_M are collected in **Table 11**.

Table 11. pH-rate for 5-BrBI.

pH	Abs (nm/s)	K_{cat}/K_M (M^{-1} s^{-1})	K_{cat}/K_M (M^{-1} min^{-1})
6,88	9,52E-6	0,33	19,71
7,33	2,34E-5	0,76	45,50
7,64	5,02E-5	1,60	95,82
8,25	9,41E-5	2,95	177,19
8,70	1,84E-4	5,76	345,47
9,40	3,19E-4	9,97	598,19

For the reaction carried out with 6-OMeBI the experimental conditions used are collected in **Table 12**.

Table 12. Trials with 6-OMeBI for pH-rate.

Reagents	TRIALS				
	22	**23**	**24**	**25**	**26**
H_2O	470 µL	470 µL	470 µL	470 µL	470 µL
Buffer 500 mM pH=9,40	25 µL	/	/	/	/
Buffer 500 mM pH=8,70	/	25 µL	/	/	/
Buffer 500 mM pH=8,25	/	/	25 µL	/	/
Buffer 500 mM pH=7,64	/	/	/	25 µL	/
Buffer 500 mM pH=6,88	/	/	/	/	25 µL
5-OMeBI 74 mM	3 µL	3 µL	3 µL	3 µL	3 µL
Cyt c 2,75 mM	3 µL	3 µL	3 µL	3 µL	3 µL
Ascorbate 400 mM	5 µL	5 µL	5 µL	5 µL	5 µL
Volume tot	506 µL	506 µL	506 µL	506 µL	506 µL

A scan was performed every 20 seconds for the trials 22 and 23, instead a scan was performed every 60 seconds for the trials 24, 25 and 26. The data obtained, already normalized, are reported in the following graphs (**Figure 31-32**):

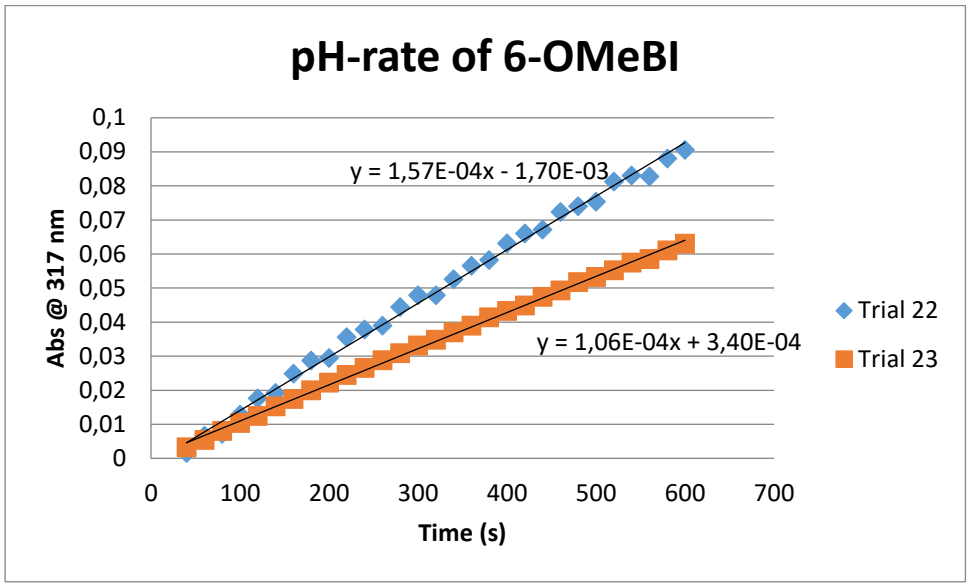

Figure 31. pH-rate of trials 22 and 23.

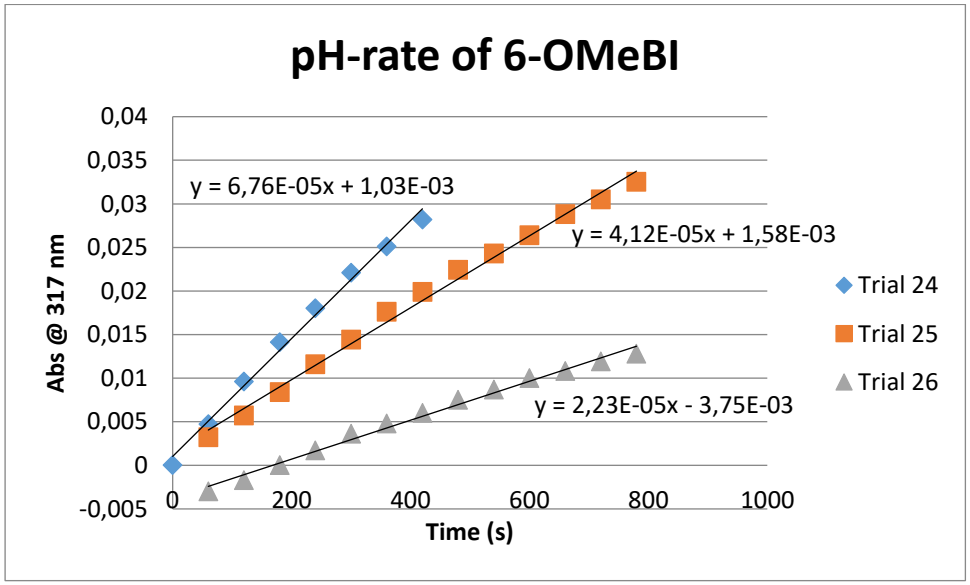

Figure 32. pH-rate of trials 24, 25 and 26.

The related k_{cat}/K_M are collected in **Table 13**.

Table 13. pH-rate for 6-OMeBI.

pH	Abs (nm/s)	K_{cat}/K_M (M^{-1} s^{-1})	K_{cat}/K_M (M^{-1} min^{-1})
6,88	2,23E-5	0,93	55
7,64	4,12E-5	0,91	54
8,25	6,76E-5	1,28	77
8,70	1,06E-4	1,96	118
9,40	1,57E-4	2,85	171

In **Figure 33** are plotted the pH-rates obtained with the different substrates in order to compare them.

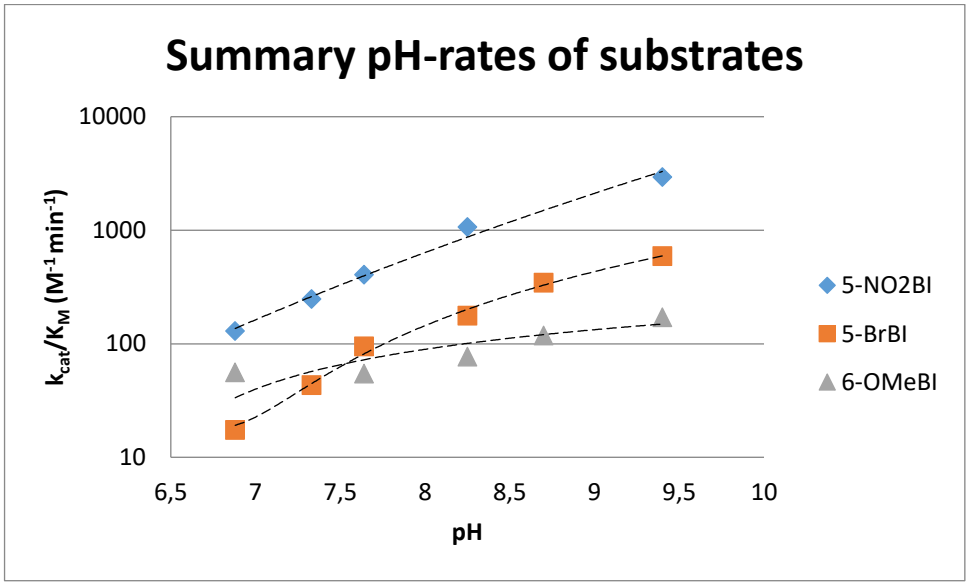

Figure 33. Summary of pH-rates of substrates **15b**, **15d** and **15e**.

Comparing the pH-rate curve for the substrate 5-NO_2BI with that obtained with 5-BrBI it can be noted that in the first case the enzyme is not saturated, while in the second case the enzyme starts to be saturate after a pH value close to 8.4. This event suggests that a deprotonation event with pK_a close to 8,4 (deduced from a mathematical fitting associated to enzyme and/or enzyme-substrate complex) is important for the Kemp elimination catalyzed by Cytochrome c. This value is very similar to that obtained for 5-NO_2BI (8,6, almost the same value considering the errors derived from various approximations): this

suggests that the p*Ka* value is not dependent on the substrate used and that the saturation is due to an important deprotonation occurring at the above pKa value, instead of a saturation due to a slow step. In the latest case, the substrates 5-NO_2BI and 5-BrBI would saturate to the same apparent k_{cat}/K_M value, as it occurs, for example, in the presence of a conformational change of the enzyme; but, as a matter of facys, this does nor occur. Since the p*Ka* value of a carboxy group belonging to the heme is 8,6, and since this value is similar to the kinetic p*Ka* deduced from mathematical fitting, that does not exclude (but, at the same time, this is not sufficient to confirm) that the process might depend on the presence of the carboxy group in anionic form of the heme group that can act as a base. However, it is known that the reduction potential of Cytochrome c is pH-dependent, with an inflection at pH close to 8,6 and thus the observation of a pH-inflection does not preclude such mechanism[32]. In contrast to what observed in the presence of 5-NO_2BI, 6-OMeBI does not show a log-linear dependence with a slope of 1 in the region below pH 7,5. Actually, the **Figure 33** above shows that the k_{cat}/K_M value obtained in trial 26 (at pH=6.88) is greater than that obtained in trial 25 and this seems anomalous: a lower k_{cat}/K_M value was expected since the acidic pH does not promote the Kemp reaction as effectively as an alkaline one. It is possible that this value is not reliable and thus it is necessary to repeat the trial 26. Unfortunately, this was not possible due to lack of time; further studies have been planned to join to a reliable determination of the k_{cat}/K_M value at pH=6.88 to clarify if the reaction with 6-OMeBI depends on the p*Ka* or not. Another possibility is that a different mechanism occur with this substrate below pH 7,5. As stated above, our data cannot solve this ambiguity at the moment.

3.2.1.2. Monitoring of the Kemp elimination of 5-BrBI in the presence of Cytc and ascorbate in the wavelength range 280-650 nm

To further monitor the Kemp reaction on the 5-BrBI, we decided to made UV/Vis analyses recording the spectrum of the system in the 280-650 nm wavelength range. Under the experimental conditions showed in **Table 14**, the solution was monitored setting up 20 cycles, each one of 180 seconds.

Table 14. Solution for the scan of Cyt c.

Reagent	Amount
H_2O	467 µL
Buffer 500 mM pH=8,25	25 µL
5-BrBI 53 mM	3 µL
CytC 2,75 mM	3 µL
Ascorbate 400 mM	5 µL

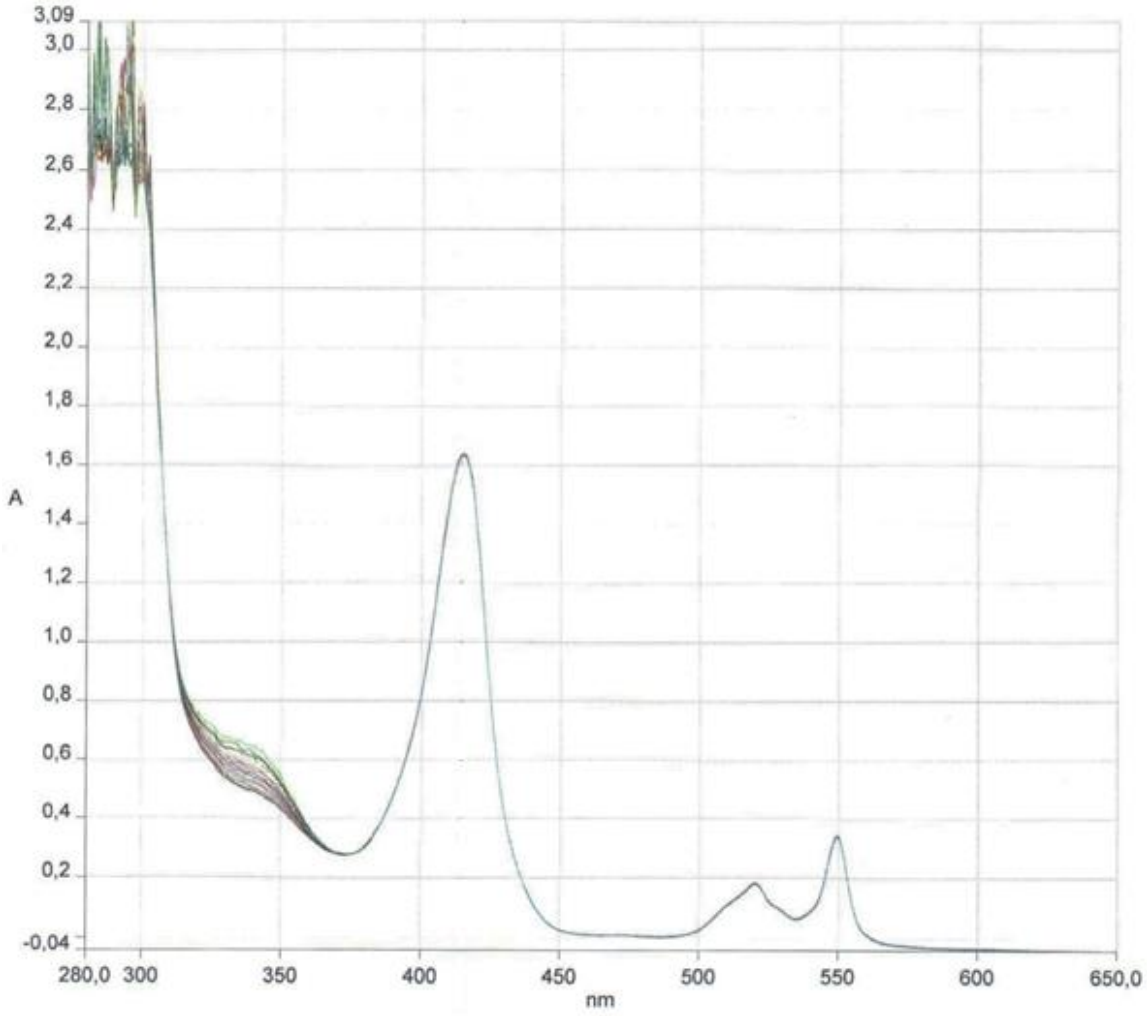

Figure 34. UV/Vis spectra of the system 5-BrBI, Cyt c, ascorbate at pH=8,25.

The spectrum (**Figure 34**) shows the three characteristic bands[33,34] of the Cytochrome c in its reduced form (due to the ascorbate) at about 420 nm, 520 nm and 550 nm: the three bands are unchanged even after 20 cycles, this means that the hemoprotein remains reduced and his behavior towards the substrate does not change. On the contrary, the intensity of the absorbance of the band at 337 nm, typical of 5-BrBI$_a$ (the product derived from the opening of the heterocyclic ring of 5-BrBI), increases with each cycle. This suggests that the protein remains active in the interval of time that we usually used for these reactions.

3.2.1.3. Brønsted plot

Summarizing, the analyzed substrates show different k_{cat}/K_M values in presence of Cytochrome c at pH=8,25, and each one value can be correlated with the characteristic pKa of the opening product, as shown in **Table 15**:

Table 15. Summary at pH=8,25 with Cyt c.

	pKa Product	K_{cat}/K_M (M^{-1} min^{-1})
6-OMeBI$_a$	7.0[10]	58
5-BrBI$_a$	5.9[10]	177
5-NO$_2$BI$_a$	4.1[10]	1068

In according to the Brønsted relationship, we can relate the pKa of the opening product with the logarithm of the kinetic constant:

$$log\left(\frac{k_{cat}}{K_M}\right) = \alpha \cdot pKa + C$$

Where α is the angular coefficient of the straight line and C is the value at the intersection with the reference axis.

Plotting the data **Figure 35** is obtained:

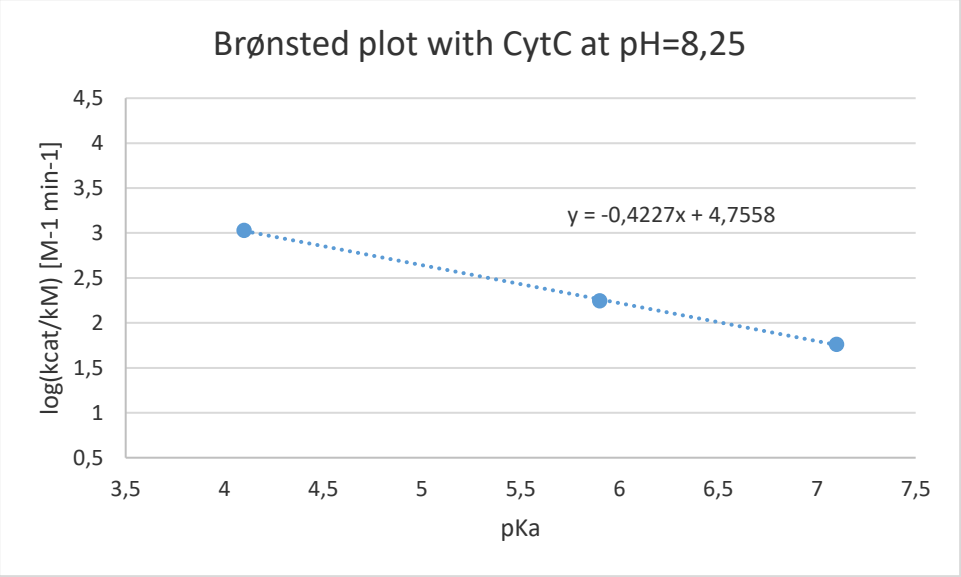

Figure 35. Brønsted plot with Cytochrome c at pH=8,25.

This relationship provides some informations on the mechanism of the Kemp elimination. By comparing the result obtained using different substrates, it can evince that the reaction outcome is influenced by the kind of substituent bound to the benzene ring of the benzisoxazole. In particular, the deprotonation rate decreases in the order: 5-NO_2BI > 5-BrBI > 6-OMeBI, that is on going from more to less electron-withdrawing substituents. One possible reason is that electron-withdrawing groups might facilitate the charge delocalization on the ring in the transition state. Furthermore, the negative value (-0,42) of the slope of the straight line, falling between $-1 < \alpha < 0$, is consistent with the occurrence of a base-catalysized reaction, where the deprotonation is the rate-limiting step of the Kemp reaction (the proton is in a "flight" state during the transition step). Nevertheless, this value of α is smaller than those observed in other systems that catalyze the Kemp elimination through a base-catalyzed mechanism, as shown in **Table 16**, which reports the values of the angular coefficient using different systems, including our reactions in the presence of Cytochrome c.

Table 16. Slope-values of Bronsted relationship for the Kemp elimination catalysed by acetate and proteins.

Acetate and proteins	Slope	Ref.
Cytc	-0,42	[a]
COO^- in H_2O	-0,60	8
COO^- in CH_3CN	-0,85	8
D38N tKSI	-0,96	10
HG3.17	-1,36	26

[a] data from current study.

The above data indicate that the slope value obtained in the case under examination for the Cytochrome c is lower than that of acetate in water. Similarly, the slope values reported with the other proteins such as D38N tKSI and HG3.17 are greater than those obtained for Cytochrome c and acetate, and indicate an important role played by the proton transfer. In the case of Cytochrome c, this role seems to be reduced, and this observation is consistent with a redox mechanism in which the α value represents the variation of the reduction potential of the substrate as a function of the substituent on the phenyl ring.

Unfortunately, the reduction potential of benzisoxazoles as a function of the substituent has never been studied, so we do not have a direct comparison. However, it is known that the redution potential of phenols correlates with the nature of the subtituent on the ring, with electron-withdrawing substituents that facilitate the reduction and electron-donating substituents that facilitate oxidation[35]. We are aware that is difficult to join to a unequivocable conclusion by comparing the slopes related to different systems and in different solvents; however, it is possible to state that the Cytochrome c reacts with a number of benzisoxazole substrates with a decreasing rate as the p*Ka* of the reaction product increases. Because of the need of ascorbate for the reaction of Cytochrome c, and because of the shallow slope in the Brønsted plot (small α), we favor a redox mechanism rather than a base-catalyzed one.

3.2.1.4. Isotope effect at basic pH

To further investigate on the nature of the mechanism of the Kemp elimination, the isotope effect was studied at basic pH at first, since the catalysis is favoured in this environment. We tried to saturate the enzyme, changing the substrate concentration in order to measure the isotope effect during the reaction, without to influence the binding of the substrate on the Cytochrome c. To measure the isotope effect, the reaction course was monitored by UV/Vis spectrophotometry both in the presence and in the absence of enzyme. In this manner it is possible to compare the two reactions: the first one is catalyzed by enzyme and basic environment; the second one is catalyzed by basic environment only. The reaction conditions are summarized in **Table 17**.

Table 17. Kemp reaction on 5-BrBI and D-5-BrBI. Trials with ± Cytc.

Reagents	TRIALS			
	27	**28**	**29**	**30**
H_2O	470 µL	470 µL	470 µL	470 µL
Buffer 500 mM pH=9,4	25 µL	25 µL	25 µL	25 µL
5-BrBI 70 mM	3 µL	/	3 µL	/
D-5-BrBI 70 mM	/	3 µL	/	3 µL
CytC 2,75 mM	3 µL	3 µL	/	/
Ascorbate 400 mM	5 µL	5 µL	5 µL	5 µL
Volume tot	506 µL	506 µL	506 µL	506 µL

The reaction course was monitored through UV/Vis spectrophotometry at λ_{max}=337nm, the characteristic wavelength of the opening products of the heterocyclic ring of 5-BrBI and D-5-BrBI[10]. A scan every 5 seconds was performed for the trials 27 and 28; whereas a scan every 20 seconds was performed for the trials 29 and 30.

The corresponding graphics (Abs vs. time) obtained are the following:

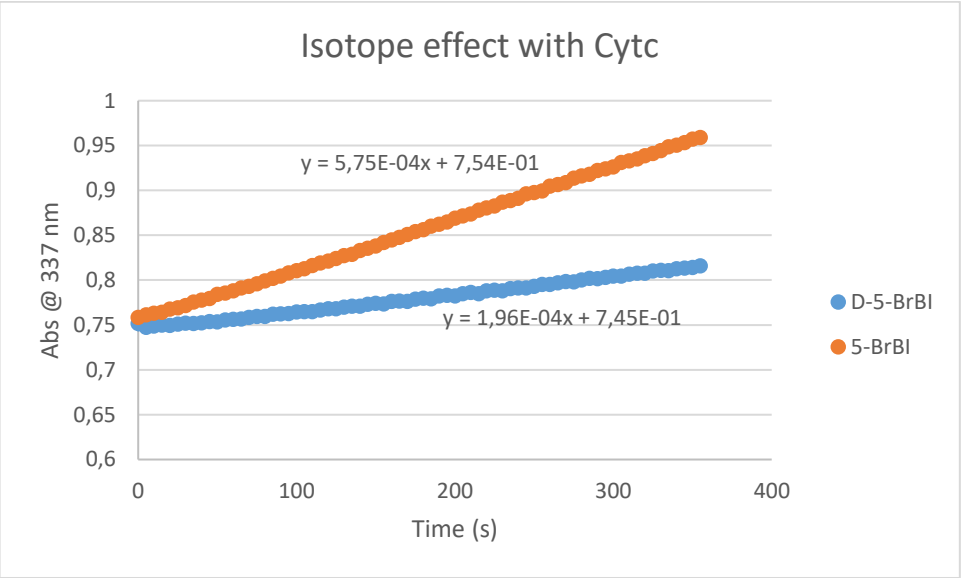

Figure 36. Kemp reaction on 5-BrBI and D-5-BrBI with Cytochrome c at pH=9.4.

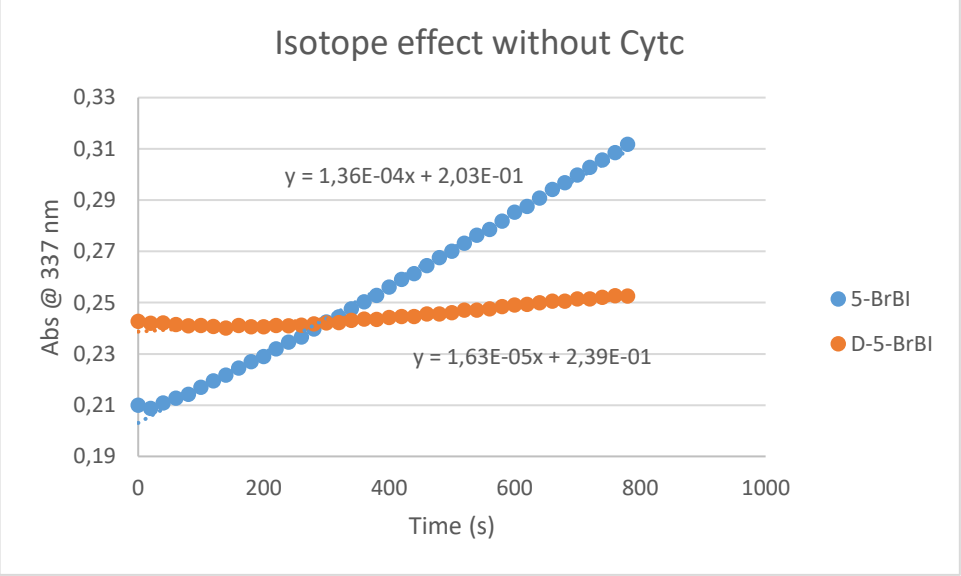

Figure 37. Kemp reaction on 5-BrBI and D-5-BrBI without Cytochrome c at pH=9.4.

Since the two substrates have the same concentration, the isotope effects are obtained through the ratio between the slope values obtained, with and without enzyme. The data obtained are the following (**Table 18**):

Table 18. Isotope effects ± Cytc.

	with CytC	without CytC
$m_{5\text{-BrBI}}$	5,75E-4	1,36E-4
$m_{D\text{-}5\text{-BrBI}}$	1,96E-4	1,63E-5
Isotope effect (EI)= ($m_{5\text{-BrBI}}$)/($m_{D\text{-}5\text{-BrBI}}$)	2,93	8,34

To calculate the concentration of the starting substrates (5-BrBI and D-5-BrBI) by spectrophotometric method, they were reacted with aq. 10 M NaOH (reaction conditions are summarized in **Table 19**), to obtain the corresponding opening products.

Table 19. Kemp reaction with NaOH 10 M.

Reagents	TRIALS	
	31	32
H_2O	498 µL	498 µL
5-BrBI 70 mM	3 µL	/
D-5-BrBI 70 mM	/	3 µL
NaOH 10 M	5 µL	5 µL
Volume tot	506 µL	506 µL

Both the solutions were diluted in ratio 1:5 (without this dilution the absorbance would be out of scale) and were monitored by UV/Vis spectrophotometry in the 300-400 nm wavelength range. The absorbances of 5-BrBI and the relative deuterated substrate at λ_{max}=337nm are equal to 0,379 and 0,243, respectively. Using the Lambert-Beer's law, the concentrations of the relative substrates are:

$$[5-BrBI] = \frac{Abs}{\varepsilon\, l} \times f \times \frac{V_{tot}}{V_{eff}} = \frac{0{,}379}{6100\ M^{-1}cm^{-1}\ \times 1\ cm} \times 5 \times \frac{506\ \mu L}{3\ \mu L} = 52{,}3\ mM$$

$$[D-5-BrBI] = \frac{Abs}{\varepsilon\, l} \times f \times \frac{V_{tot}}{V_{eff}} = \frac{0{,}243}{6100\ M^{-1}cm^{-1}\ \times 1\ cm} \times 5 \times \frac{506\ \mu L}{3\ \mu L} = 33{,}6\ mM$$

Since the concentrations obtained are different, the isotope effects are not valid: we must recalculate them.

$$\frac{V_{5-BrBI}}{[5-BrBI]} = \frac{5{,}75\mathrm{E}-4}{52{,}3} = 1{,}1E-5$$

$$\frac{V_{D-5-BrBI}}{[D-5-BrBI]} = \frac{2{,}03\mathrm{E}-4}{33{,}6} = 6{,}0E-6$$

$$EI_{with\ CytC} = \frac{\frac{V_{5-BrBI}}{[5-BrBI]}}{\frac{V_{D-5-BrBI}}{[D-5-BrBI]}} = \frac{1{,}1E-5}{6{,}0E-6} = 1{,}8$$

$$EI_{without\ CytC} = \frac{\frac{V_{5-BrBI}}{[5-BrBI]}}{\frac{V_{D-5-BrBI}}{[D-5-BrBI]}} = \frac{\frac{1{,}36\mathrm{E}-4}{52{,}3}}{\frac{2{,}37\mathrm{E}-5}{33{,}6}} = \frac{2{,}60E-6}{7{,}23E-7} = 3{,}6$$

3.2.1.5. Isotope effect at acidic pH

To evidence if the isotope effect is referred to k_{cat} or K_M, we tried to saturate the enzyme varying the concentration of 5-BrBI and D-5-BrBI. The reactions were carried out under the conditions reported in **Table 20**, where "master mix" is a solution containing water, Cythocrome c, buffer and ascorbate in relative ratio reported in **Table 20**.

Table 20. Preparation of "master mix".

Reagent	Amount
H_2O	3199 µL
Ascorbate 400 mM	35 µL
CytC 2,75 mM	21 µL
Buffer 500 mM pH=6,88	175 µL

Adding to this solution the substrates, deuterated or not, and a further amount of EtOH (**Table 21**) to favor the substrates solubility in the whole system, it has been possible to monitor the reactions by UV/Vis spectrophotometry:

Table 21. Kemp reaction varying [5-BrBI] and [D-5-BrBI].

Reagent	TRIALS					
	33	**34**	**35**	**36**	**37**	**38**
Master mix	490 µL	490 µL	490 µL	490 µL	490 µL	490 µL
5-BrBI 53 mM	2 µL	4 µL	6 µL	8 µL	/	/
D-5-BrBI 34 mM	/	/	/	/	10 µL	3 µL
EtOH	8 µL	6 µL	4 µL	2 µL	/	7 µL
Volume tot	500 µL	500 µL	500 µL	500 µL	500 µL	500 µL

A scan every 30 seconds was performed for the trials 33, 34, 35 and 36; whereas a scan every 20 seconds was performed for the trials 37 and 38. The data obtained are the following:

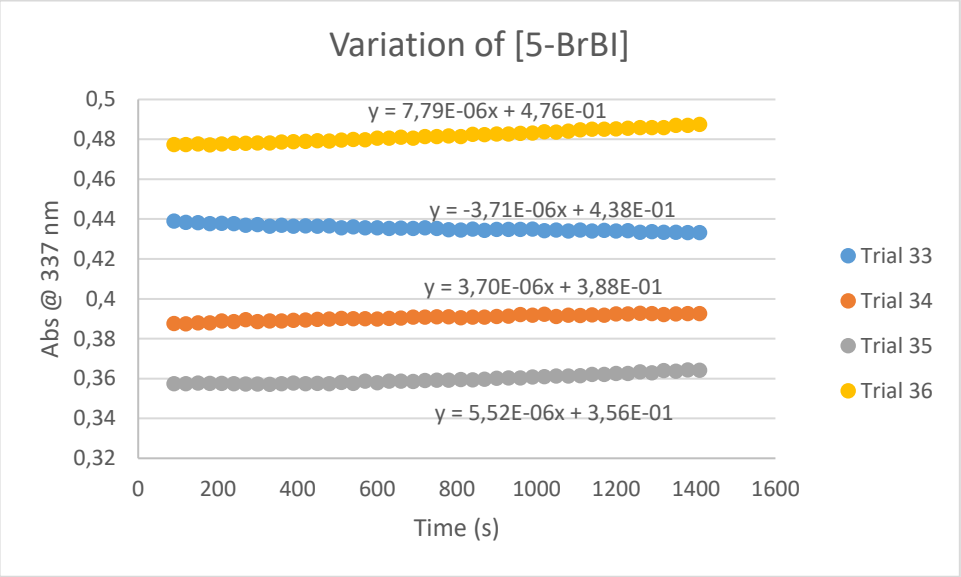

Figure 38. Kemp elimination varying [5-BrBI] at pH=6.88.

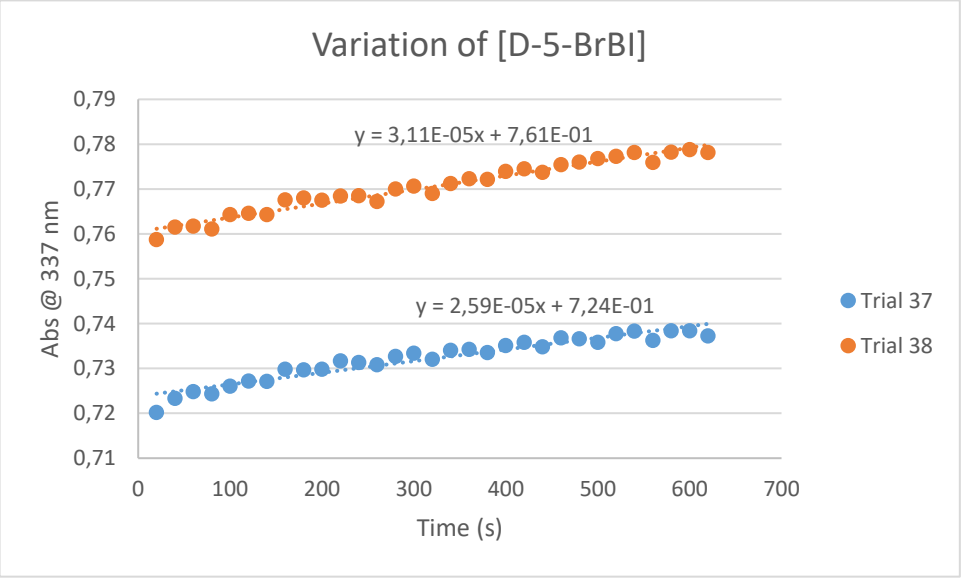

Figure 39. Kemp elimination varying [D-5-BrBI] at pH=6.88.

As it can be shown from the graphs above, it wasn't possible to saturate the enzyme varying the concentration of substrate. Actually, the absorbance increases linearly with time, albeit in a slight extent, except for the trial 33 where the slope is negative: this might be explained hypothesizing a conformational change of the protein or the occurrence of a not-identified event that, in the presence of little amount of substrate might prevail.

After these experiments, the isotope effect was calculated in a similar way to the previous one, comparing the results obtained from substrates with similar effective concentrations:

$$[5-BrBI]_{Trial\ 33} = \frac{53mM \times 2\mu L}{500\ \mu L} = 212\ \mu L$$

$$[5-BrBI]_{Trial\ 34} = \frac{53mM \times 4\mu L}{500\ \mu L} = 424\ \mu L$$

$$[5-BrBI]_{Trial\ 35} = \frac{53mM \times 6\mu L}{500\ \mu L} = 636\ \mu L$$

$$[5-BrBI]_{Trial\ 36} = \frac{53mM \times 8\mu L}{500\ \mu L} = 848\ \mu L$$

$$[D-5-BrBI]_{Trial\ 37} = \frac{34mM \times 10\mu L}{500\ \mu L} = 680\ \mu L$$

$$[D-5-BrBI]_{Trial\ 38} = \frac{34mM \times 3\mu L}{500\ \mu L} = 204\ \mu L$$

Thus, comparing the trial 35 with the trial 37, the isotope effect is:

$$EI = \frac{\frac{V_{5-BrBI}}{[5-BrBI]}}{\frac{V_{D-5-BrBI}}{[D-5-BrBI]}} = \frac{\frac{5{,}52E-6}{52{,}3}}{\frac{2{,}59E-5}{33{,}6}} = \frac{1{,}05E-7}{7{,}71E-7} = 0{,}1$$

From the above experiments it emerges that the isotope effect seems to be pH-dependent: EI=0,1 at pH=6,88 (inverse kinetic isotope effect); whereas EI=1,8 at pH=9,4 (normal kinetic isotope effect). This change, from normal isotope effect to inverse isotope effect, may be due to a different affinity of the two substrates towards the Cytochrome c or to different rate-limiting steps. Unfortunately, we were not able to saturate the enzyme, thus the isotope effect refers to both the kinetic constants (k_{cat} and K_M). Furthermore, inverse isotopic effect of 0,1 is unusual: in literature it has been reported is known that inverse primary kinetic isotope effects are usually 0,6-0,9[36,37]. Further studies have been planned to join to a reliable isotope effect at pH=6,88 to clarify if the reaction occurs through a different mechanism from the traditional one or not.

3.2.2. Kemp reaction on benzisoxazoles (15b,d,e) carried out in the presence of myoglobin

After the experiments on the Kemp reaction on the synthesized benzisoxazoles in the presence of Cytochrome c, we planned to extend the study on the enzymatic catalysis of this reaction in the prersence of two other hemoproteins, *i.e.* myoglobin and hemoglobin. To understand whether the myoglobin also catalyzes the Kemp reaction thanks to the combined effect of hemoprotein and ascorbate, three trials have been conducted using 5-BrBI as substrate under the conditions reported in **Table 22**.

Table 22. Kemp reaction on 5-BrBI. Trials with ±Myo, ±asc.

Reagents	TRIALS		
	39	**40**	**41**
H_2O	452 µL	467 µL	457 µL
Buffer 500 mM pH=7,64	25 µL	25 µL	25 µL
5-BrBI 53 mM	3 µL	3 µL	3 µL
Myoglobin 0,667 mM	15 µL	/	15 µL
Ascorbate 400 mM	5 µL	5 µL	/
Volume tot	500 µL	500 µL	500 µL

The reaction course has been monitored by UV/Vis spectrophotometry (one scan every 20 seconds), at the characteristic wavelength of the opening product of the heterocyclic ring (λ_{max}=337 nm), operating at 20°C.

The corresponding graphics (Abs vs. time) obtained are the following (**Figure 40-42**):

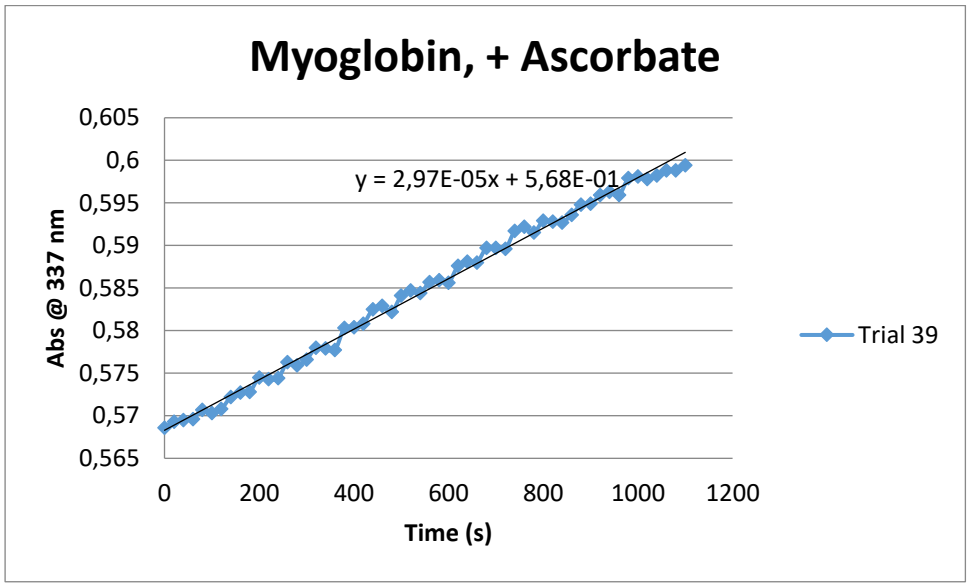

Figure 40. Trial 39 with myoglobin and ascorbate.

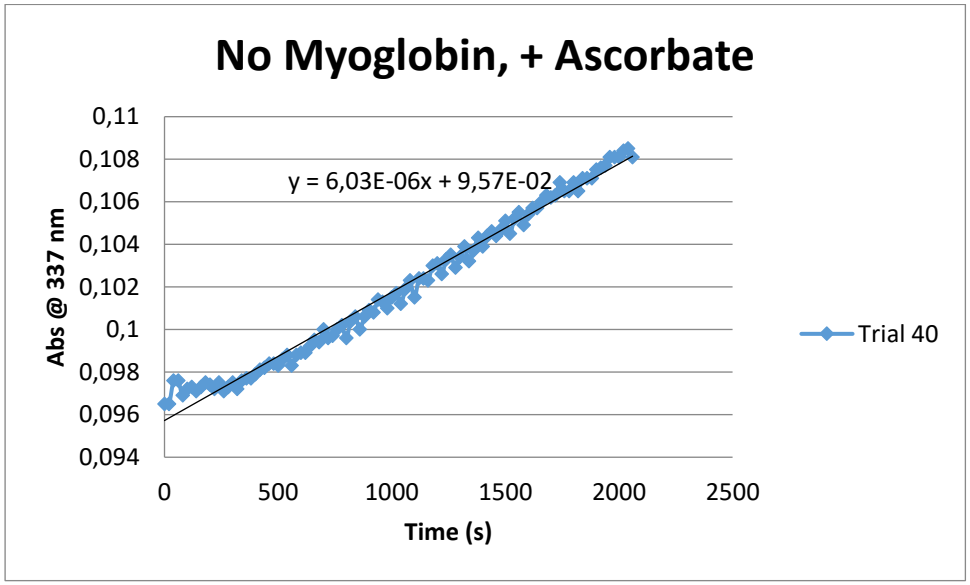

Figure 41. Trial 40 with ascorbate.

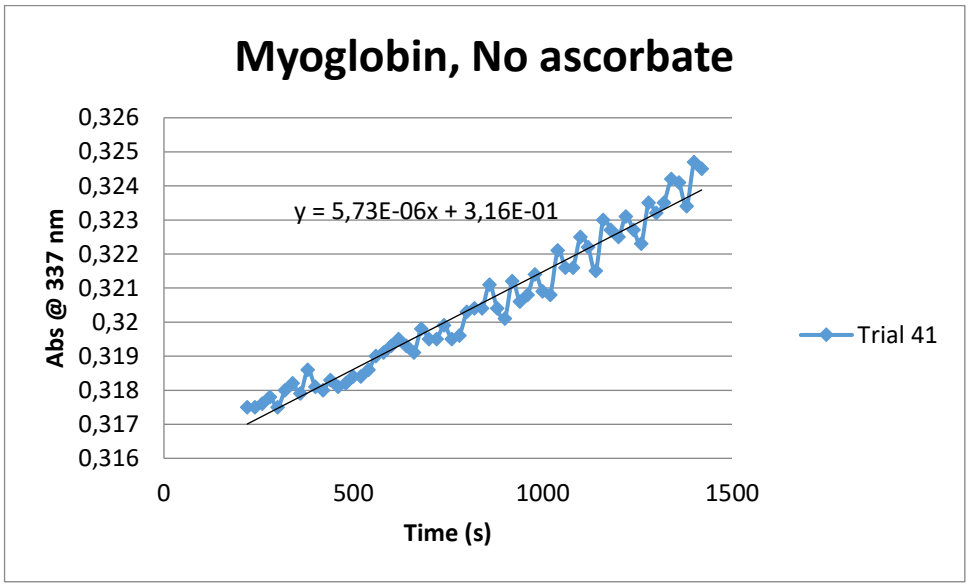

Figure 42. Trial 41 with myoglobin.

The data obtained, already normalized, are reported in **Figure 43**:

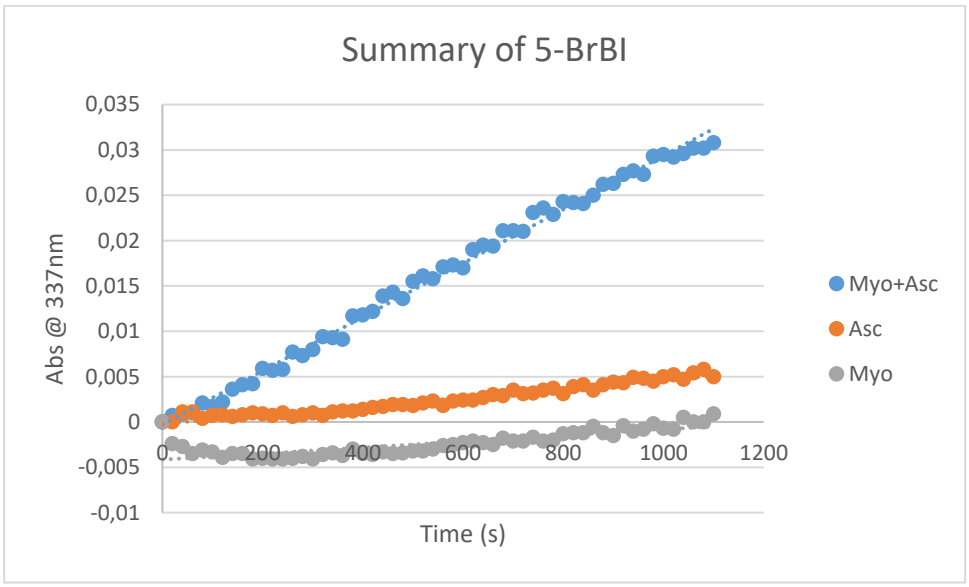

Figure 43. Summary of the data obtained with 5-BrBI in the presence of myoglobin.

As for the Cytochrome c, the slope of the trial 39 (with presence of both, myoglobin and ascorbate) is greater with respect to that of the other two cases: the combined action of hemoprotein and ascorbate catalyzes efficiently the Kemp reaction on the 5-BrBI substrate.

The k_{cat}/K_M in the case of trial 39 is:

$$\frac{k_{cat}}{K_M} = \frac{m_1 - m_2}{\varepsilon_{5-BrBI_a}[E][S]} = \frac{2{,}97 \times 10^{-5} - 6{,}03 \times 10^{-6}}{6100 \cdot 2 \cdot 10^{-5} \cdot 3{,}18 \cdot 10^{-4}} = 36{,}59\ M^{-1}min^{-1} = 0{,}610\ M^{-1}s^{-1}$$

In this study we decided do not made similar trials using the other benzisoxazoles because likely, as shown for the Cytochrome c, they are opened catalitically according to the Kemp reaction in a similar way to that of the 5-BrBI.

However, even in this case, to compare the behavior of the three benzisoxazoles (6-OMeBI, 5-BrBI and 5-NO_2BI) in the presence of myoglobin at pH=8,25, we carried out the Kemp reaction monitoring it by UV/Vis spectrophotometry as a function of time (reaction conditions are summarized in **Table 23**). The data were recorded at the wavelength characteristic of the different opened products[10]. On the basis of the previous data obtained with Cytochrome c, we decided to use three different acquisition times, depending on the substrate (*i.e.* every 2 seconds for 5-NO_2BI, every 5 seconds for 5-BrBI and every 10 seconds for 6-OMeBI).

Table 23. Kemp reaction on different substrates in the presence of myoglobin and ascorbate.

Reagents	TRIALS		
	42	**43**	**44**
H_2O	450,8 µL	451,4 µL	452 µL
Buffer 500 mM pH=8,25	25 µL	25 µL	25 µL
5-BrBI 53 mM	4,2 µL	/	/
5-NO_2BI 61 mM	/	3,6 µL	
6-OMeBI 74 mM	/	/	3 µL
Myoglobin 0,667 mM	15 µL	15 µL	15 µL
Ascorbate 400 mM	5 µL	5 µL	5 µL
Volume tot	500 µL	500 µL	500 µL

The data obtained are reported in **Figures 44-46**:

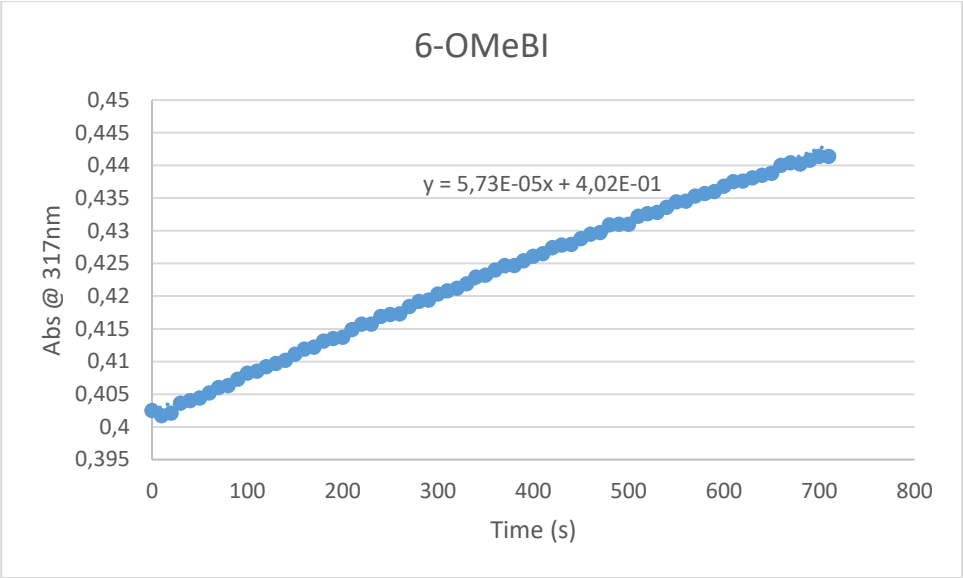

Figure 44. Plot of Abs vs time for 6-OMeBI at pH=8,25.

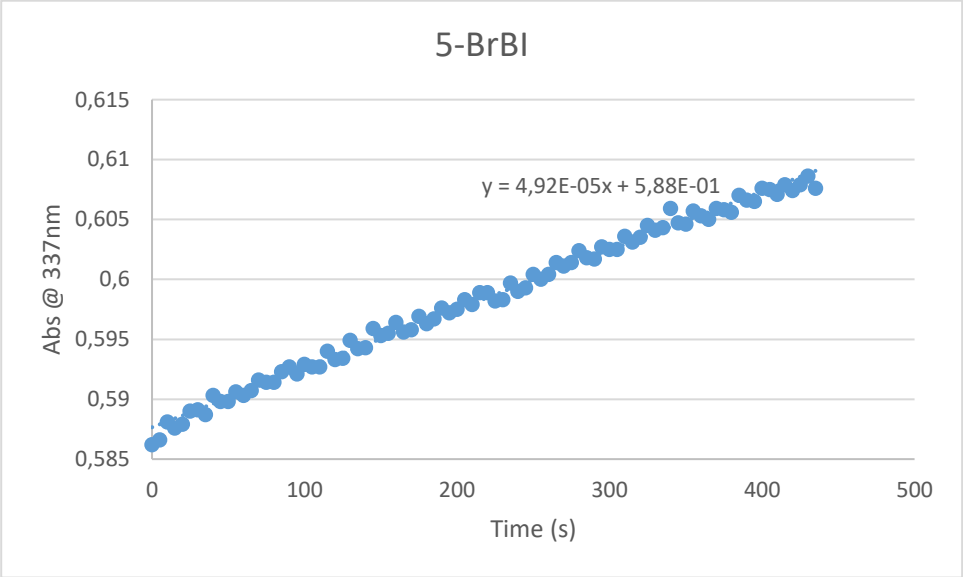

Figure 45. Plot of Abs vs time for 5-BrBI at pH=8,25.

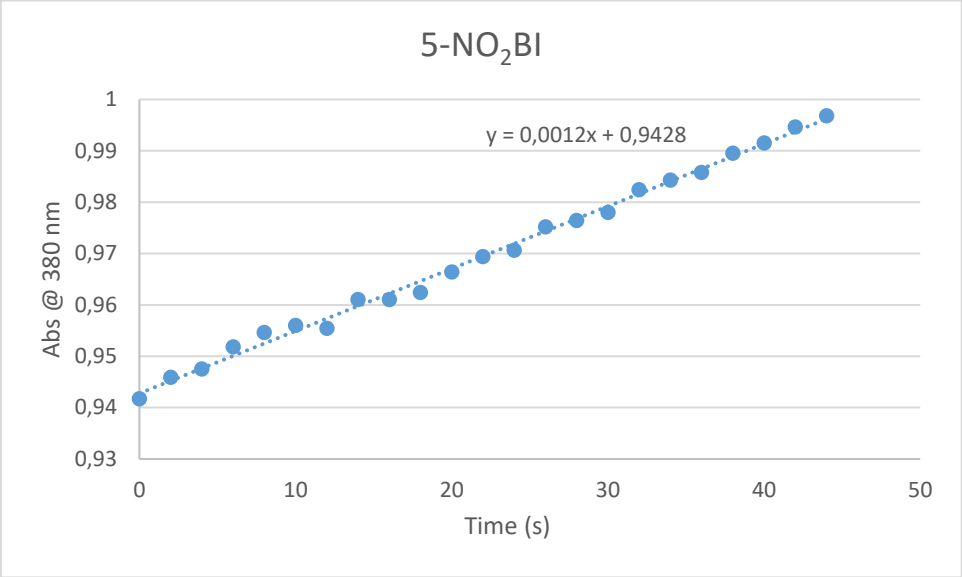

Figure 46. Plot of Abs vs time for 5-NO_2BI at pH=8,25.

So the k_{cat}/K_M value obtained for the three substrates are:

$$\left(\frac{k_{cat}}{K_M}\right)_{6-OMeBI_a} = \frac{m_{6-OMeBI}}{\varepsilon_{6-OMeBI_a}[E][S]} = \frac{5{,}73 \times 10^{-5}}{7500 \cdot 1{,}98 \cdot 10^{-5} \cdot 4{,}47 \cdot 10^{-3}} = 51{,}79\ M^{-1}min^{-1}$$
$$= 0{,}86\ M^{-1}s^{-1}$$

$$\left(\frac{k_{cat}}{K_M}\right)_{5-BrBI_a} = \frac{m_{5-BrBI}}{\varepsilon_{5-BrBI_a}[E][S]} = \frac{4{,}92 \times 10^{-5}}{6100 \cdot 1{,}98 \cdot 10^{-5} \cdot 4{,}49 \cdot 10^{-3}} = 54{,}43\ M^{-1}min^{-1}$$
$$= 0{,}91\ M^{-1}s^{-1}$$

$$\left(\frac{k_{cat}}{K_M}\right)_{5-NO2BI_a} = \frac{m_{5-NO2BI}}{\varepsilon_{5-NO2BI_a}[E][S]} = \frac{0{,}0012}{18400 \cdot 1{,}98 \cdot 10^{-5} \cdot 4{,}42 \cdot 10^{-3}} = 473{,}21\ M^{-1}min^{-1}$$
$$= 7{,}89\ M^{-1}s^{-1}$$

As for the case of Cytochrome c, 5-NO_2BI showed the fastest reaction rate, instead the ring-opening for the other two substrates has a paragonable rate, although it seems that in case of 5-BrBI the rate is a little faster than in the case of 6-OMeBI.

3.2.2.1. pH-rate for the Kemp reaction on 5-BrBI in the presence of myoglobin and ascorbate

The reactions were carried out under the conditions reported in **Table 24**, where "master mix" is a solution containing water, myoglobin and ascorbate in relative ratio reported in **Table 24**.

Table 24. Preparation of the "master mix".

Reagent	Amount
H_2O	4520 µL
Ascorbate 400 mM	50 µL
Myoglobin 0,667 mM	150 µL

Adding to this solution 5-BrBI and buffers at different pH values (9,4; 8,70; 8,25; 7,64; 7,33; 6,88) it has been possible to model a pH-rate for 5-BrBI (**Table 25**).

Table 25. pH rate of 5-BrBI.

Reagent	TRIALS					
	45	**46**	**47**	**48**	**49**	**50**
Master mix	472 µL	472 µL	472 µL	472 µL	472 µL	472 µL
Buffer 500 mM pH=9,40	25 µL	/	/	/	/	/
Buffer 500 mM pH= 8,70	/	25 µL	/	/	/	/
Buffer 500 mM pH=8,25	/	/	25 µL	/	/	/
Buffer 500 mM pH=7,64	/	/	/	25 µL	/	/
Buffer 500 mM pH=7,33	/	/	/	/	25 µL	/
Buffer 500 mM pH=6,88	/	/	/	/	/	25 µL
5-BrBI 53 mM	3 µL	3 µL	3 µL	3 µL	3 µL	3 µL
Volume tot	500 µL	500 µL	500 µL	500 µL	500 µL	500 µL

The scans were performed every 5 seconds for the trials 46 and 47; every 20 seconds for trial 6, and every 30 seconds for the trials 48, 49 and 50. The data obtained from UV/Vis spectrophotometry, already normalized, are plotted in **Figures 47-49**:

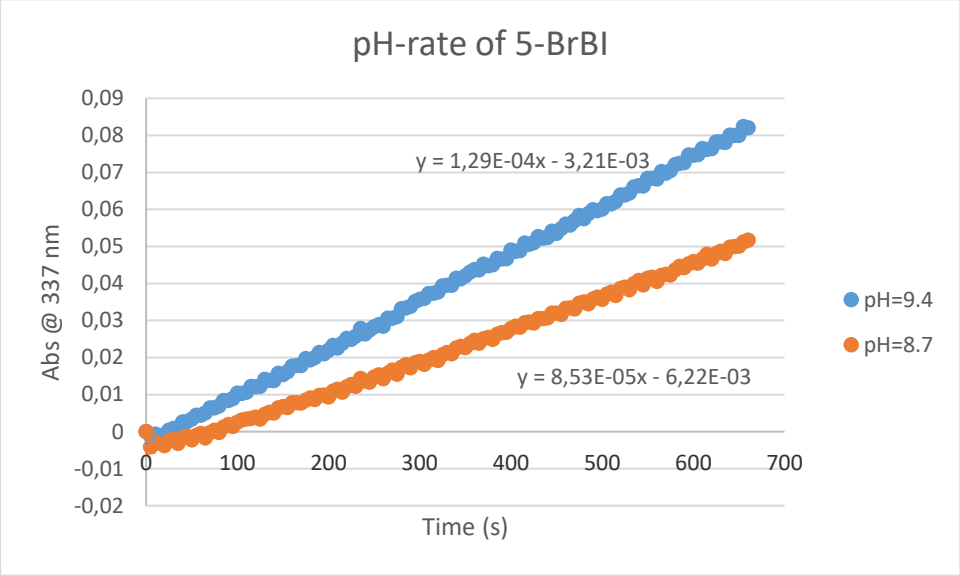

Figure 47. Plot of Abs vs time at different pH values for the system 5-BrBI/myoglobin/ascorbate.

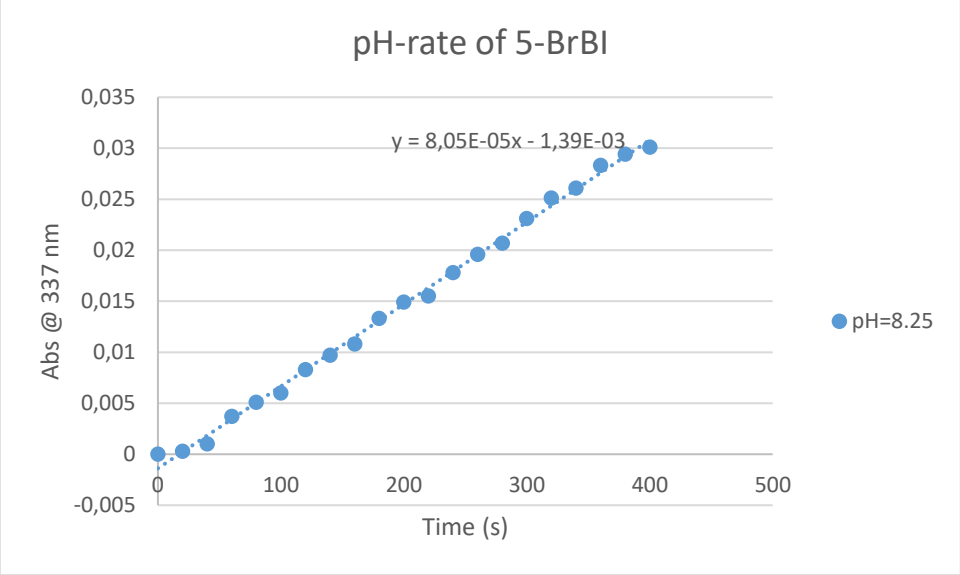

Figure 48. Plot of Abs vs time at pH = 8.25 for the system 5-BrBI/myoglobin/ascorbate.

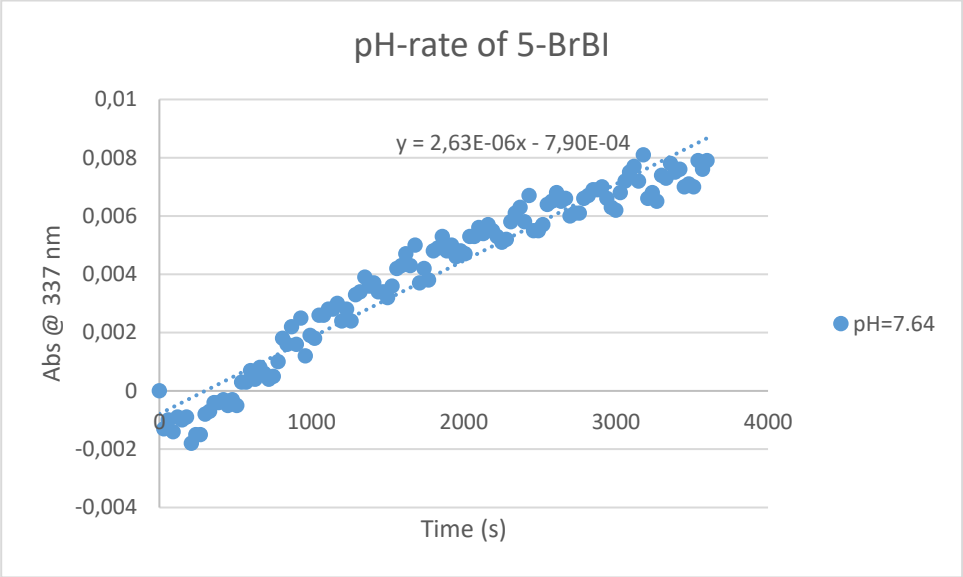

Figure 49. Plot of Abs vs time at pH = 7.64 for the system 5-BrBI/myoglobin/ascorbate.

As can be shown from the graphs above, the values obtained for trial 48 (pH=7,64) are rather oscilling, so the slope of the straight line is poorly reliable. It is worth noting the long acquisition time (about 4000 seconds) that this reaction needs: at the other pH values the acquisition time was in the range 500-700 seconds. Furthermore, after about 3000 seconds it seems that the rate decreases. This behavior might be due to any kind of inhibition possibly because of the binding of oxygen to myoglobin, or to an inhibition of the reaction by the product at the slightly acidic pH values. To further investigate this aspect, a scan of the solution was performed to analyze an eventual inibition effect (see two pages after).

There were some problems for the trials 49 and 50. In the first one (see **Figure 50**) the slope was negative: being the reaction very slow, if something occurs (for example the protein changes his spectrum) producing an absorbance variation at 337 nm, this may hide the small absorance variations due to the Kemp reaction.

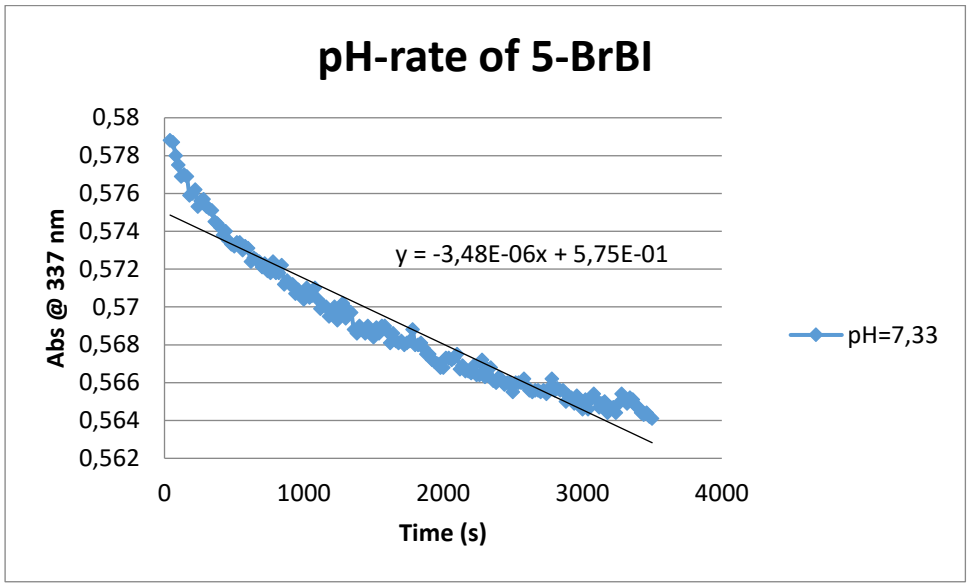

Figure 50. Plot of Abs vs time at pH = 7.33 for the system 5-BrBI/myoglobin/ascorbate.

In the second case (trial 50, pH = 6.88) the reaction does not occur.

After these experiments, the k_{cat}/K_M values were calculated in a similar way to the previous ones (**Table 26**):

Table 26. Summary of k_{cat}/K_M at different pH values for the system 5-BrBI/myoglobin/ascorbate.

pH	Abs (nm/s)	K_{cat}/K_M (M^{-1} s^{-1})	K_{cat}/K_M (M^{-1} min^{-1})
7,64	2,97E-5	0,78	46,75
8,25	8,05E-5	2,08	124,99
8,70	8,56E-5	2,21	132,53
9,40	1,29E-4	3,32	199,47

The obtained data have been reported in the following graph (**Figure 51**) and compared with those obtained for the reaction of 5-BrBI in the presence of Cytochrome c:

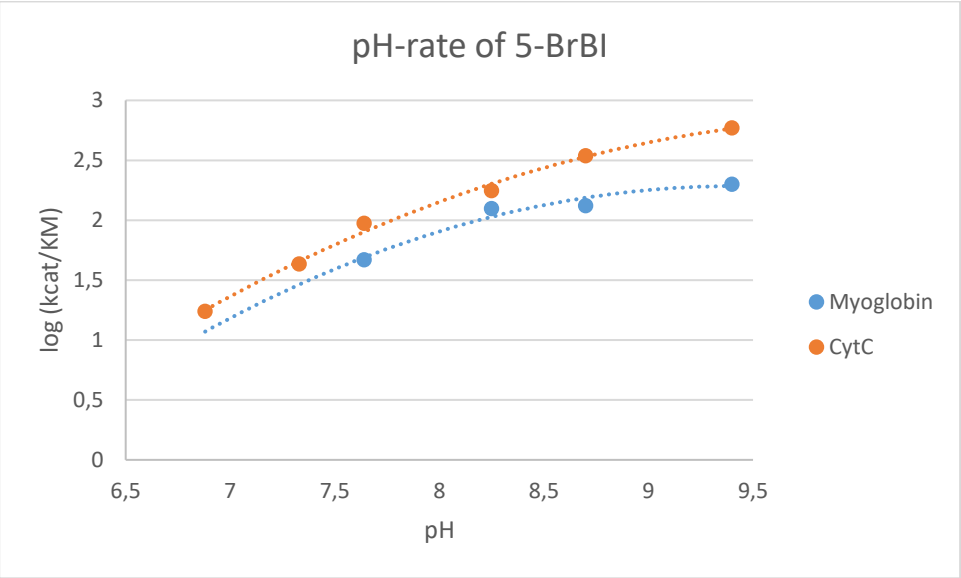

Figure 51. Plots of log(k_{cat}/K_M) vs. pH for the Kemp reaction of 5-BrBI with cytochrome and myoglobin.

From **Figure 51** it can argue that Cytochrome c catalyzes the Kemp reaction faster than myoglobin at all the pH values tested. Furthermore, the curves show the same trend thus suggesting the same mechanism of action in the presence of the two hemoproteins.

3.2.2.2. Monitoring of the Kemp elimination with 5-BrBI in the wavelength range 280-650 nm

As for the Cytochrome c, a scan was perfomed (shown in **Table 27**) in presence of myoglobin, monitoring the sample in a range between 280-650 nm, setting up 40 cycles, each one of 30 minutes. The choice of this acquisition time was established in order to collect accurate data.

Table 27. Content of the sample used to monitor the Kemp elimination on 5-BrBI in the presence of myoglobin and ascorbate in the wavelength range 280-650 nm.

Reagent	Amount
H_2O	452 µL
Buffer 500mM pH=8,25	25 µL
5-BrBI 53 mM	3 µL
Myoglobin 0,66 mM	15 µL
Ascorbate 400 mM	5 µL

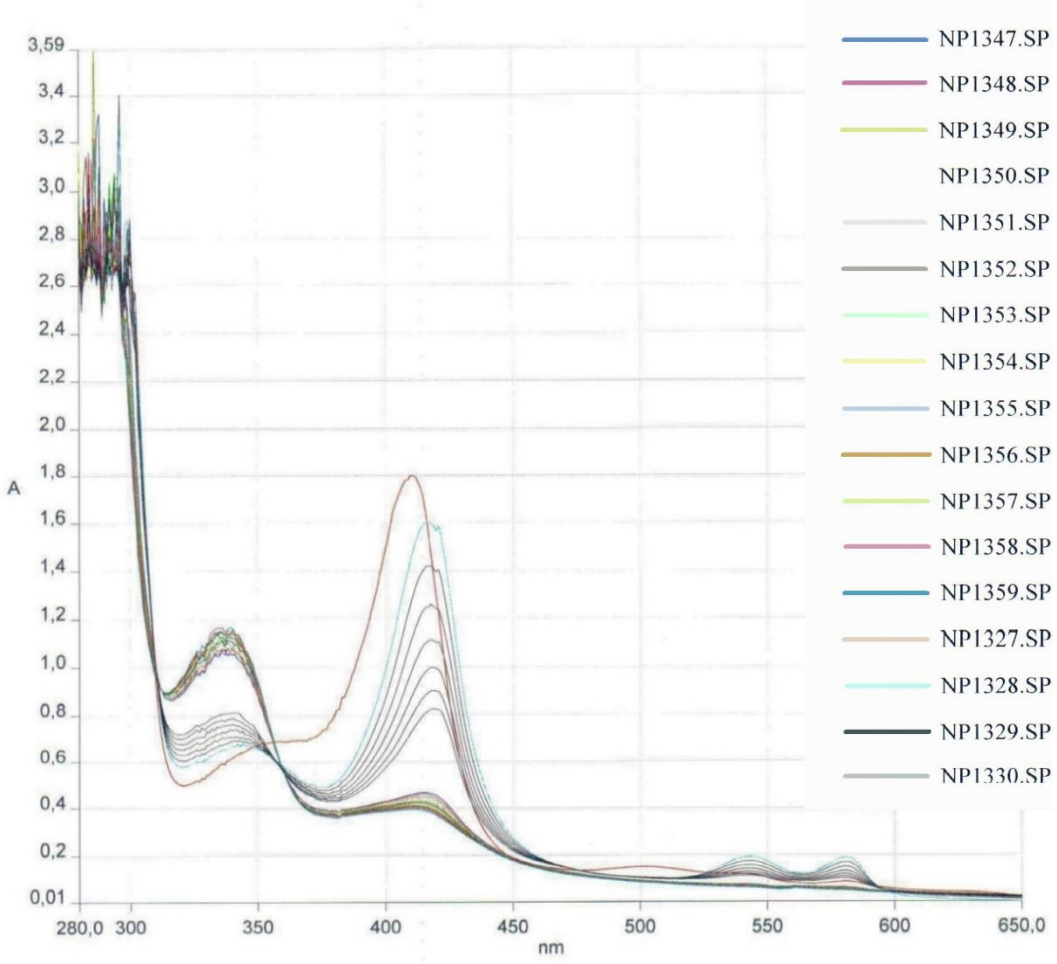

Figure 52. UV/Vis spectra of the system 5-BrBI, myoglobin, ascorbate at pH=8,25.

The spectra are showed in **Figure 52**, where the most significant cycles have been highlighted. The spectrum related to the first cycle (NP1327.NP) shows the characteristic bands of the not-oxygenated myoglobin[38] at about 410 nm and 500 nm. As the reaction proceeds, the band at 410 nm moves at 420 nm and its absorbance decreases, while the one at 500 nm disappears and two bands emerge at 545 and 580 nm, typical bands of oxygenated myoglobin[33]. Furthermore, it is possible to note two isosbestic points at about 360 and 475 nm for the first six scans: for the first one wavelenght, after six scans, the isosbestic point moves to right slightly; whereas for the second one, after six scans, the isosbestic point disappears. It is possible to note an isosbestic point at 590 nm that persists for the all the scansion. It is possible that not only an oxygenated form of myoglobin exists so that it could inhibit the Kemp reaction, but also that various species, in equilibrium one each other, are formed within the solution, with λ_{max} at about 360, 475 and 590 nm. Finally, it is important to note that, for almost all the previous kinetic experiments, the reaction time did not exceed 10 minutes; in this case, where the reaction time is longer (20 hours), it seems that myoglobin changes structure, thus deactivating itself over time.

If the problem is actually the oxygen, the same behavior should be highlighted even in absence of the substrate. So we established to perform a scan of a solution identical to the previous one (shown in **Table 28**) but without the substrate, using the same acquisition time and wavelength range.

Table 28. Solution to monitor the behavior of myoglobin in the wavelength range 280-650 nm in absence of the benzisoxazole.

Reagent	Amount
H_2O	455 µL
Buffer 500 mM pH=8,25	25 µL
Myoglobin 0,66 mM	15 µL
Ascorbate 400 mM	5 µL

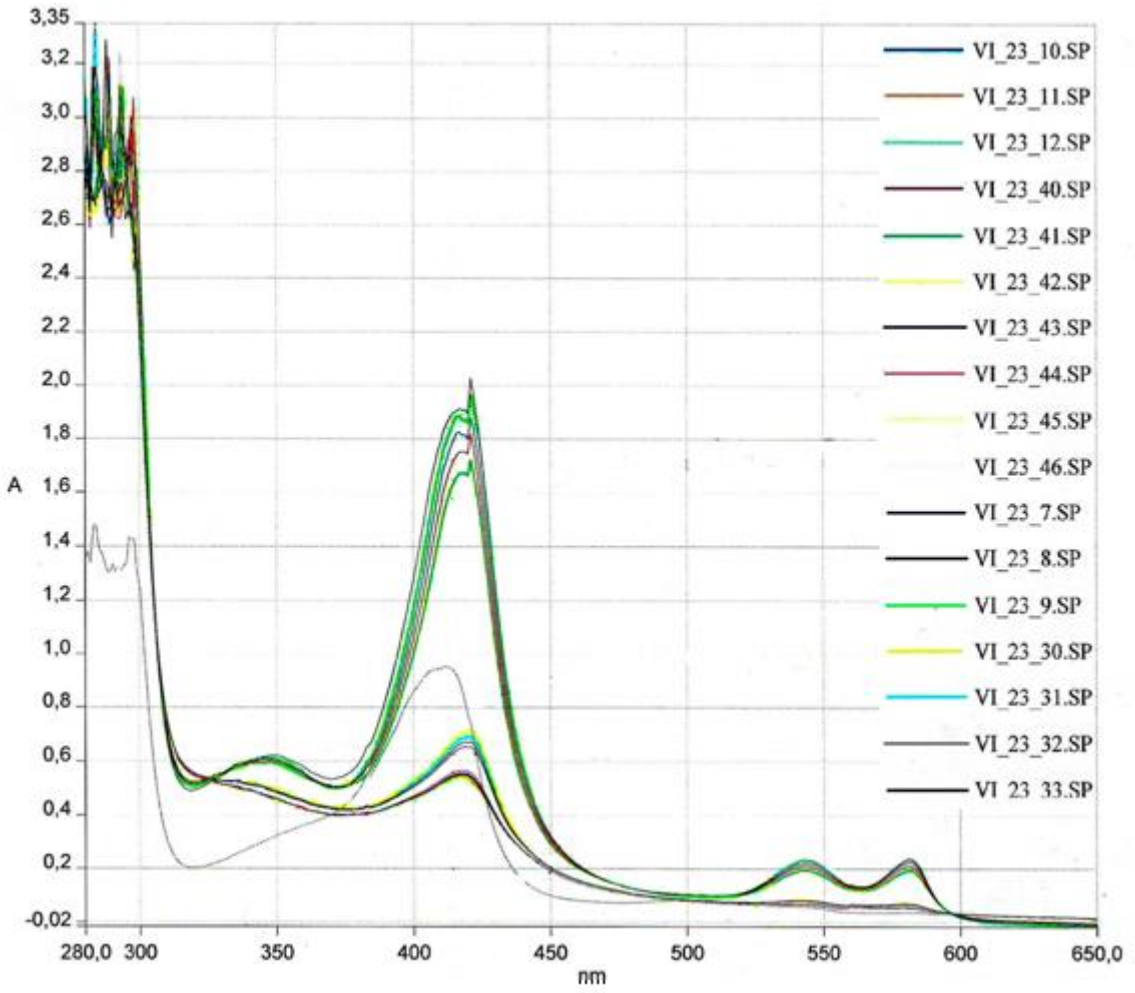

Figure 53. UV/Vis spectra of the system myoglobin/ascorbate at pH=8,25.

The spectra (among them the most significant were highlighted), show a behavior similar to the previous (**Figure 53**), even without the substrate, although with little changes. Similary to the previous behavior, initially there is the not-oxygenated myoglobin (410 and 500 nm), where Fe has an oxidation state +3, which turns into oxygenated myoglobin (545 and 580 nm), due to the action of ascorbate which reduces the iron to an oxidation state +2, and the band at 410 nm moves at 420 nm, decreasing in absorbance over time. Moreover, even in this case it persists an isosbestic point at 590 nm: this might be an indication of the existence of some possible equilibrium forms not influenced by the substrate. It is possible to underline an apparent peak at 425 nm, unlike the previous spectrum where it was not very pronounced, which decreases in absorbance together with

the peak at 420 nm: what could happen is that the water or the air or both[39,40] present in the solution reacts with the ascorbate to give hydrogen peroxide which in turn reacts with the myoglobin to form the ferrylmyoglobin[33]. This particular form of myoglobin (whose characteristic λ is at 425 nm), characterized by the Fe ion in an oxidation state +4 and linked to the oxygen through a double bond (Fe=O), could be responsible for the de-activation of the hemoprotein over time[41], thus inhibiting the Kemp reaction. Finally, it is possible to underline an isosbestic point at 325 nm common to all the cycles: this point was not evident in the previous spectra but probably it was not visible because it was covered by the band of the opening product at 337 nm. Furthermore, comparing the two spectra, with and without substrate, we can say that probably the isosbestical points at 360 and 475 nm (present in the previous spectrum) are related to some equilibrium forms related to the substrate-enzyme complex since they are absent in the spectra recorded without substrate.

3.2.2.3. Effect of hydrogen peroxide

To confirm the presence of ferrylmyoglobin and her inhibition effect against the Kemp reaction, some experiments have been carried out in presence of different concentrations of hydrogen peroxide (**Table 29**).

Table 29. Effect of peroxide oxygen.

Reagents	TRIALS				
	51	**52**	**53**	**54**	**55**
H_2O	460 µL	453 µL	453 µL	453 µL	458 µL
Buffer 500 mM pH=8,25	25 µL	25 µL	25 µL	25 µL	25 µL
Ascorbate 400 mM	/	5 µL	5 µL	5 µL	/
5-BrBI 53 mM	/	3 µL	3 µL	3 µL	/
Myoglobin 0,66 mM	15 µL	15 µL	15 µL	15 µL	15 µL
H_2O_2 1 mM	/	2 µL	/	/	2 µL
H_2O_2 0,5 mM	/	/	2 µL	/	/
H_2O_2 0,1 mM	/	/	/	2 µL	/
Volume tot	500 µL	500 µL	500 µL	500 µL	500 µL

All the reactions have been monitored by UV/Vis spectrophotometry in a range 280-650 nm within 15-20 minutes and after 24 hours. Three cycles, each one of 5 minutes, and a cycle after 24 hours were set up for the trials 51 and 55; instead for the trials 52,53, and 54 an initial cycle, without hydrogen peroxide and substrate, was set up, then, after the addition of hydrogen peroxide, three cycles, each one of 5 minutes, were set up. Subsequently, a scan was performed for trials 52,53 and 54, as a function of time (one scan every 5 min), using λ_{max}=337nm, the characteristic wavelength of the opening product of the heterocyclic ring[10] (5-$BrBI_a$). Finally, a last scan was recorded for all samples after 24 hours.

Scan of trial 51:

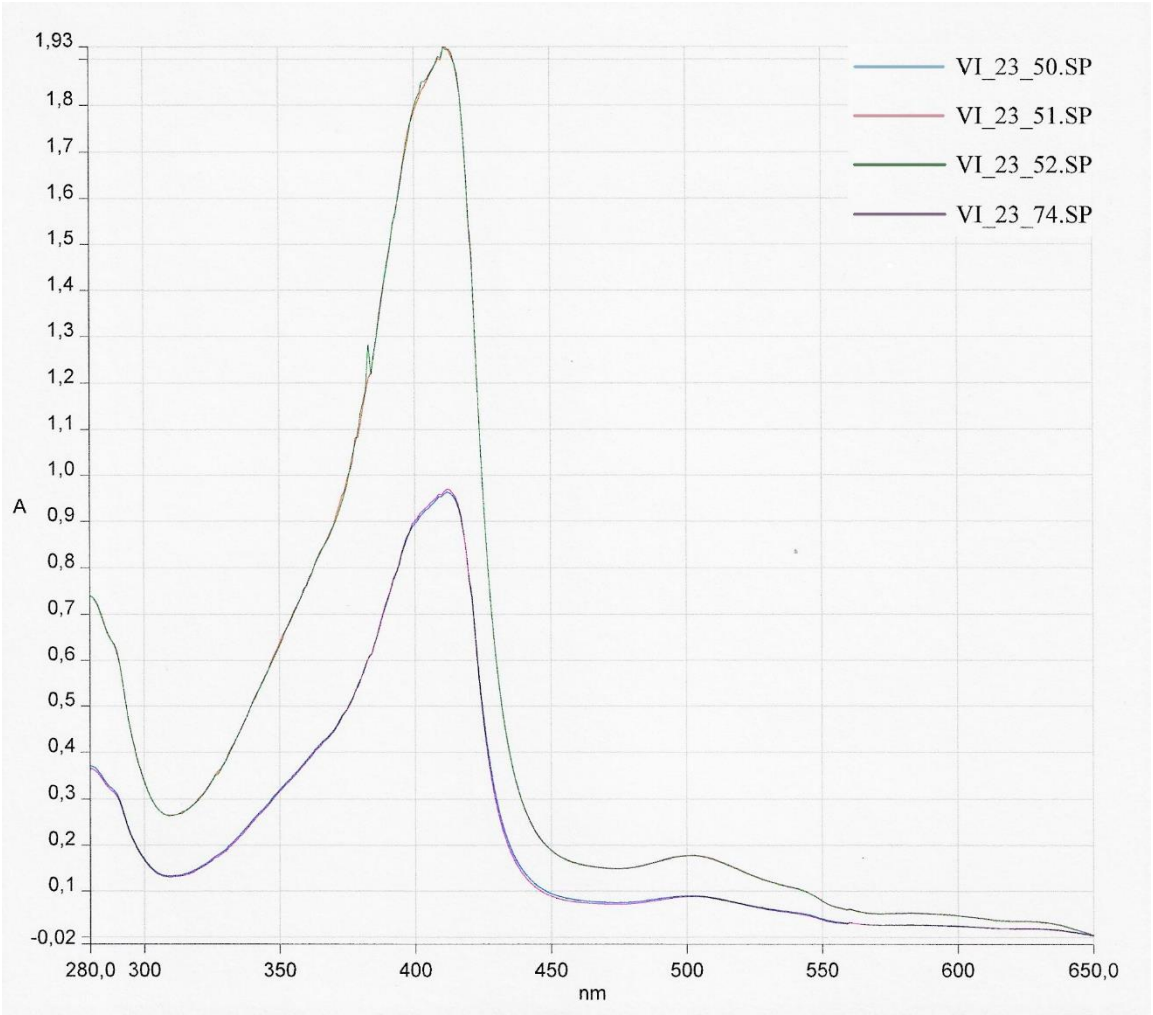

Figure 54. UV/Vis spectra of myoglobin at pH=8,25.

The spectrum (**Figure 54**) shows that the band at 410 nm increases after 15 minutes (red line), then decreases to the point of departure after 24 hours. Since there are no evident changes and it is no present the ascorbate in solution, so the change highlighted in the previous scans (**Figure 53**) relating to myoglobin at 410 and 420 nm are related to ascorbate and the possible formation of hydrogen peroxide.

Scan of trial 52:

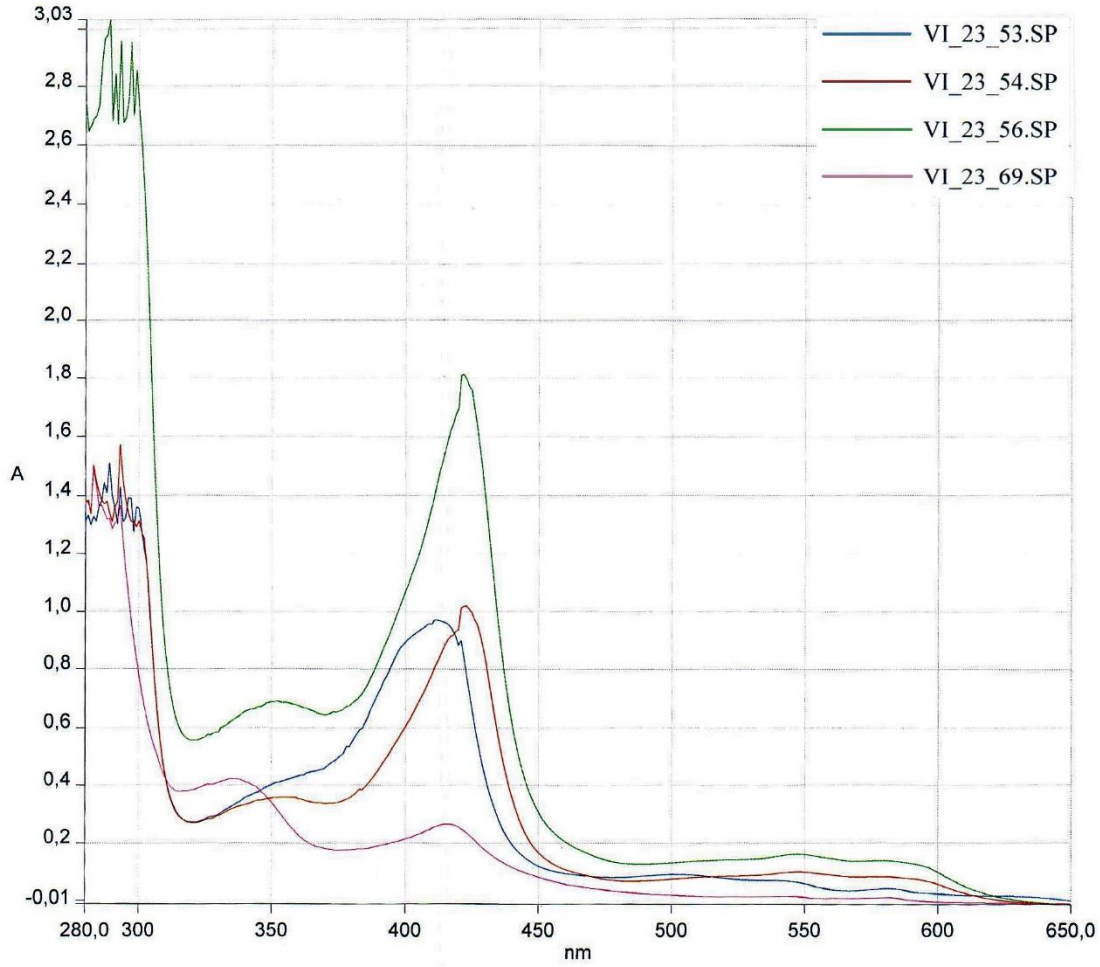

Figure 55. UV/Vis spectra of the system myoglobin/ascorbate/H_2O_2 1 M at pH=8,25.

This spectrum (**Figure 55**) shows that initially (VI_23_53.SP) there are the tipical bands of not-oxydated myoglobin at 410 and 500 nm, with a small hump at 425 nm, characteristic of ferrylmyoglobin. After addition of H_2O_2 1M and setting up three cycles, each one of 5 minutes, it is possible to underline that at first the band at 410 nm decreases and the band at 425 nm increases, then, after 15 minutes (VI_23_56.SP) this difference becomes more evident, with a slight increase of oxidized myoglobin (bands at about 545 and 580 nm). Adding the substrate and reacting for 24 hours (VI_23_69.SP), it is possible to note not only the increase, although less marked than in the presence of Cytochrome c, of the characteristic band of the opening product at 337 nm, but also the appearance of a band

at 420 nm with a very low absorbance. So it seems not only that there are 3 forms of myoglobin (oxidized, reduced and ferrylmyoglobin), but also that the formation of ferryl-myoglobin, due to the presence of hydrogen peroxide, inhibits the Kemp reaction. Particularly, once Fe (IV) is formed, it does not participate in the Kemp reaction, the concentration of active enzyme tends to zero over time and the reaction is catalyzed only by effect of the background.

Scan of trial 53:

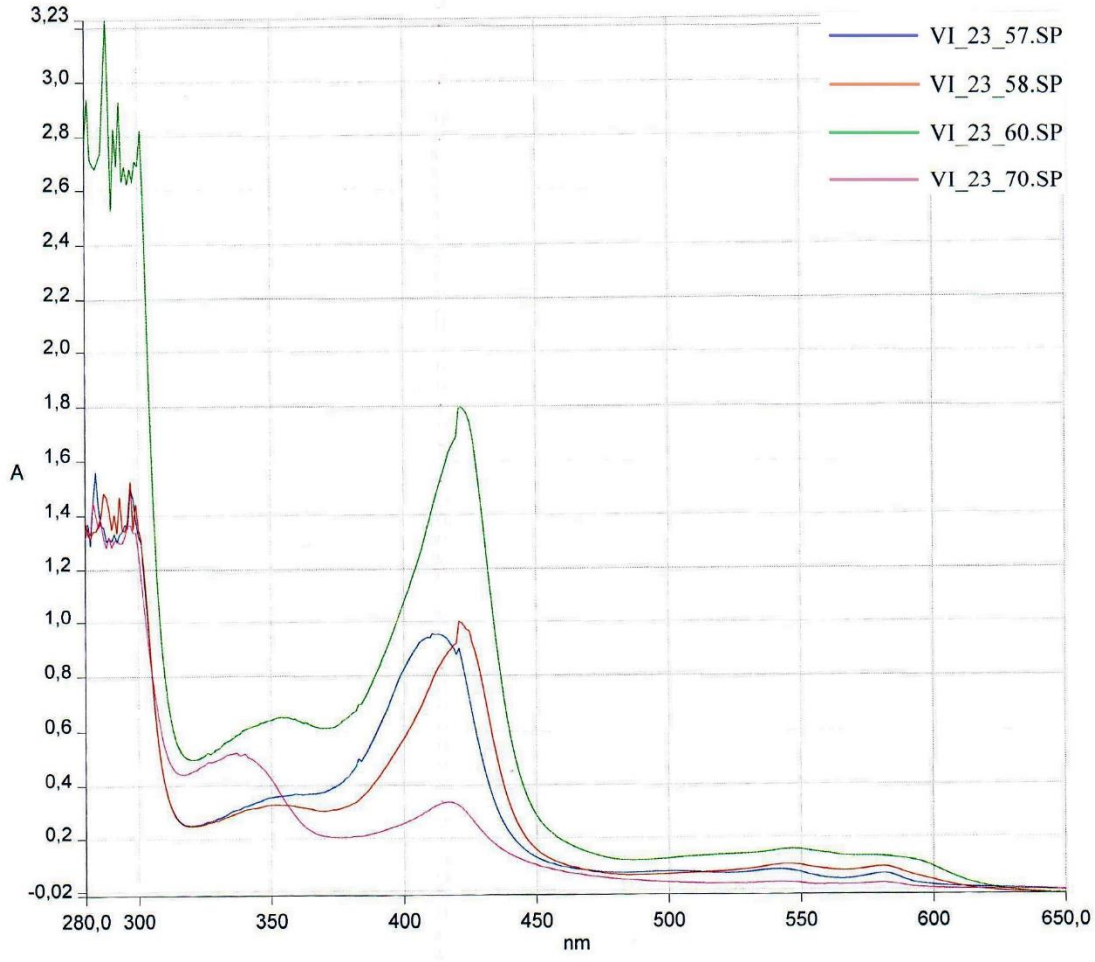

Figure 56. UV/Vis spectra of the system myoglobin/ascorbate/H_2O_2 0,5 M at pH=8,25.

The spectrum (**Figure 56**), similarly to the previous one, shows the presence of the three forms of myoglobin within 24 hours, although slightly less evident. Indeed the characteristic band of the opening product, at 337 nm, is increased in absorbance to a greater extent than the previous trial: it seems that the reaction is influenced by the concentration of hydrogen peroxide, since with a more diluted concentration (0.5 M) the reaction is less inhibited.

Scan of trial 54:

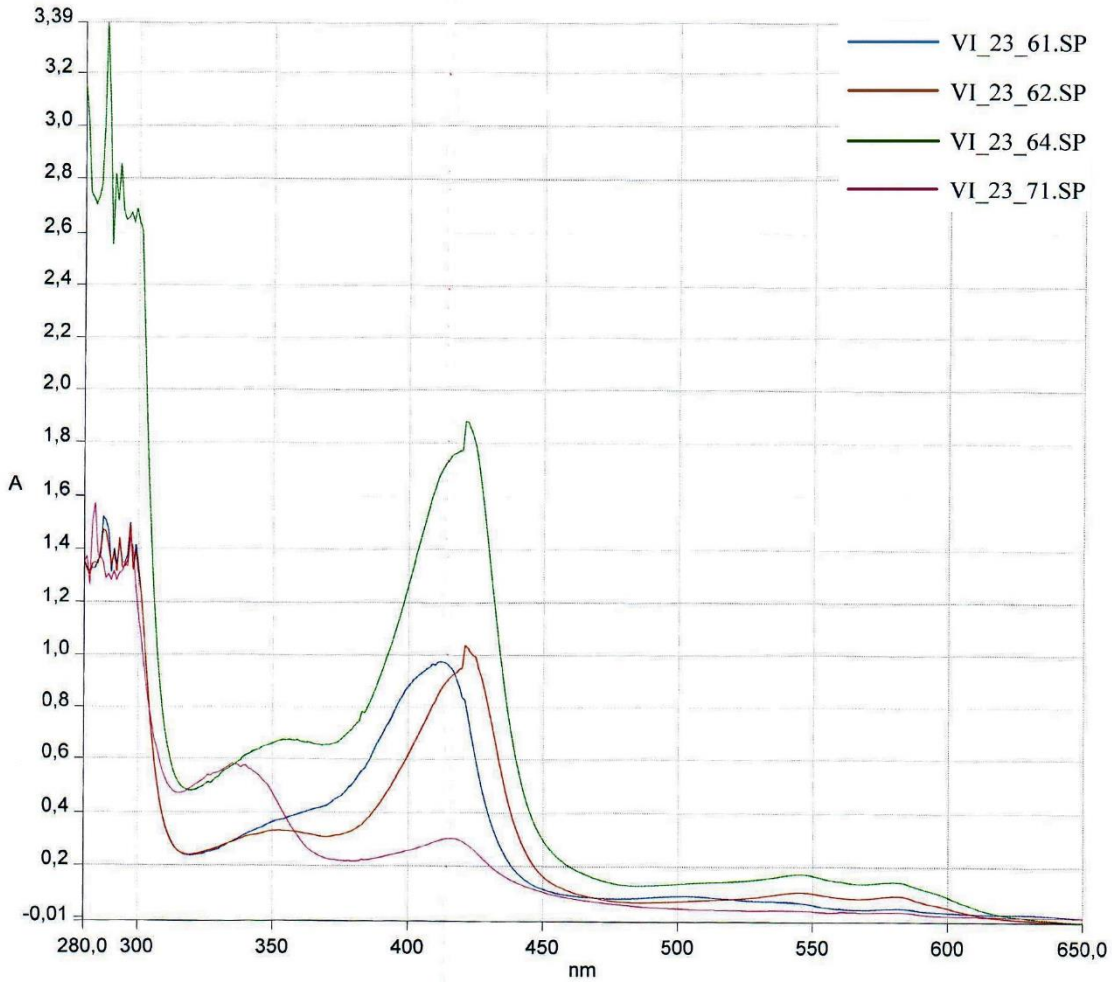

Figure 57. UV/Vis spectra of the system myoglobin/ascorbate/H_2O_2 0,1 M at pH=8,25.

The spectrum (**Figure 57**), similarly to the two previous ones, shows both the presence of the three forms of myoglobin both the formation of the opening product at 337 nm within 25 hours. Particularly, the formation of the opening product occurs in a more marked way compared to the other two trials, using a solution of hydrogen peroxide still less concentrated than the other two solutions (0.1 M), so confirming the inhibition of the Kemp reaction by the same hydrogen peroxide.

Scan of trial 55:

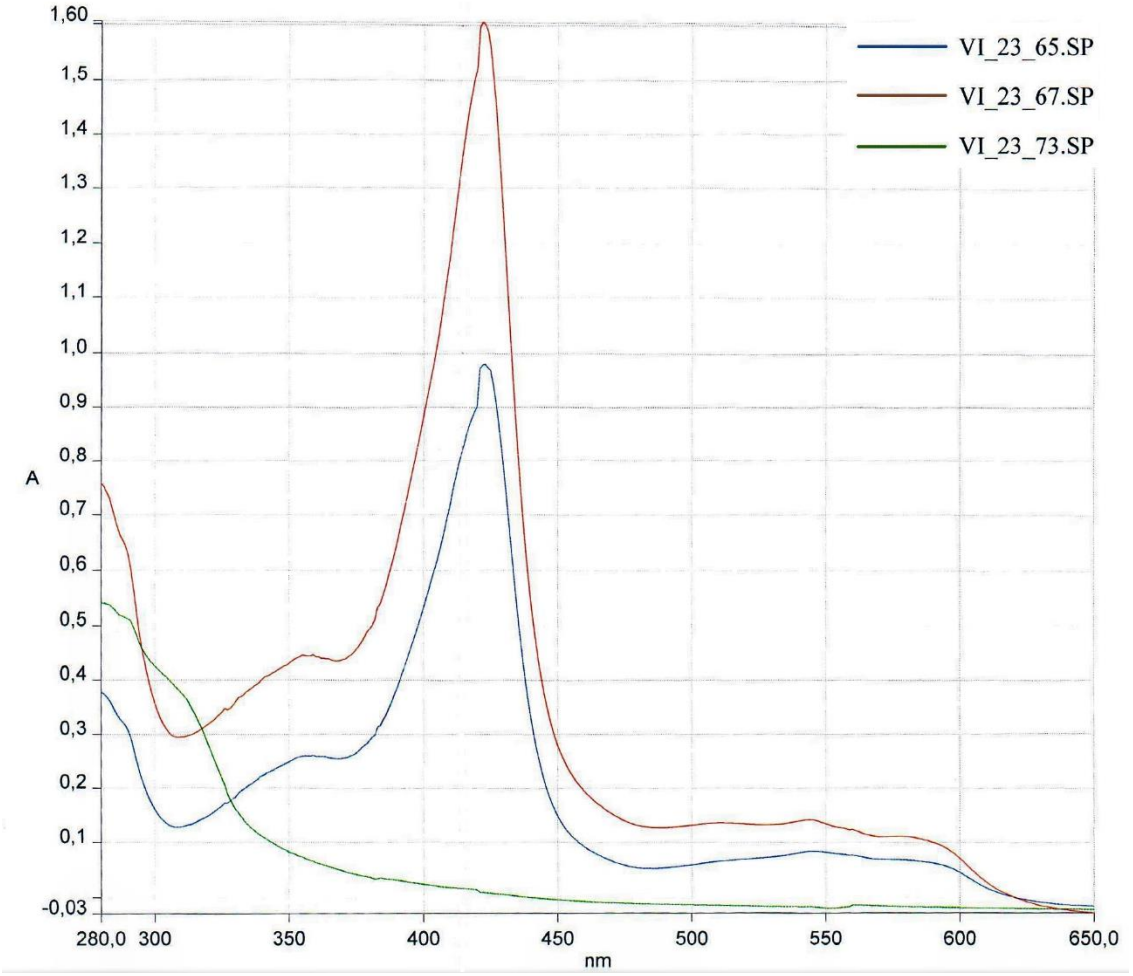

Figure 58. UV/Vis spectra of the system myoglobin/H_2O_2 1 M at pH=8,25.

The spectrum of the trial 55 (**Figure 58**), unlike the spectrum of the trial 51 (**Figure 54**) where it is no present the hydrogen peroxide, shows an increase of the band at 425 nm within 15 minutes (VI_23_73.SP), with subsequent denaturation of the enzyme after 24 hours (VI_23_73.SP). The denaturation of enzyme is not only confirmed by UV/Vis spectrophotometry (the characteristic bands of myoglobin disappeared), but also by the fact that the color of the solution in the cuvette, initially straw-yellow, has become transparent with time. So the hydrogen peroxide has a negative effect both on the Kemp reaction, since the formation of ferrylmyoglobin inhibits the reaction, and on the stability of the hemoprotein itself, since it denatures after 24 hours.

The plots of Absorbance vs. time in the cases tests 52,53 and 54 are represented in **Figures 59**, **60** and **61** respectively.

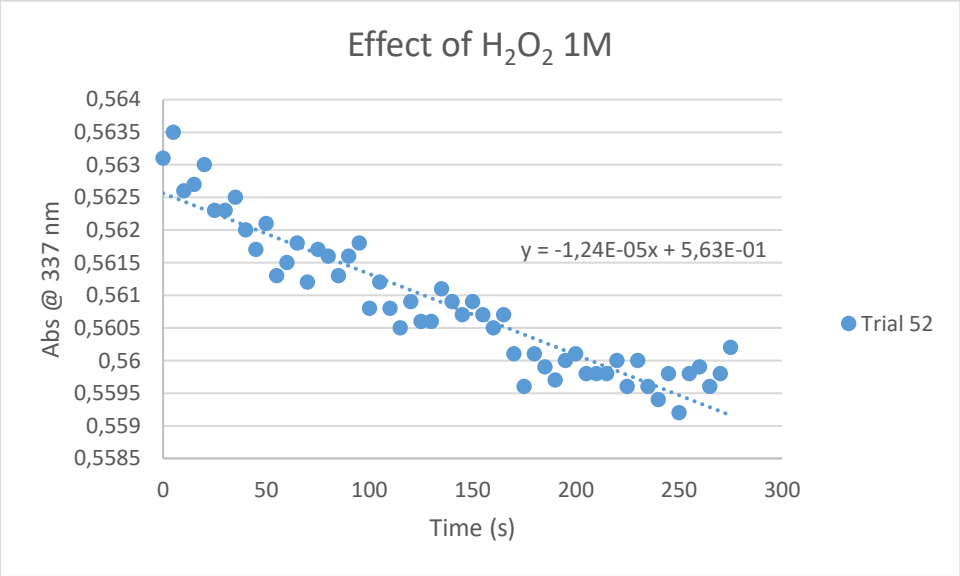

Figure 59. Plot Abs vs time of trial 52 after 24 h.

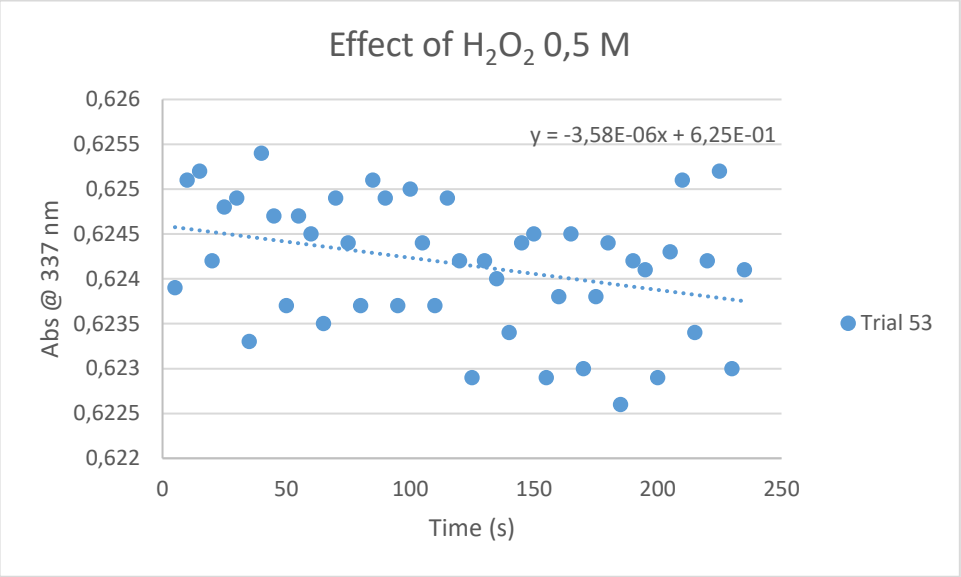

Figure 60. Plot Abs vs time of trial 53 after 24 h.

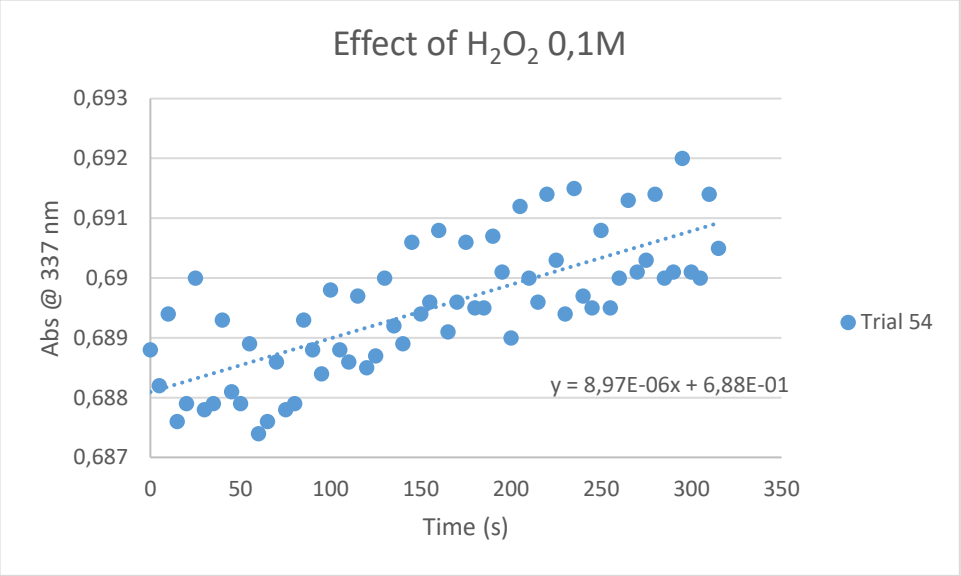

Figure 61. Plot Abs vs time of trial 54 after 24 h.

Although the data oscillate a lot in every trials under examination, it is possible to infer a negative slope for the first two trials and a positive slope for the last one: the variation of the concentration of the hydrogen peroxide influences greatly the Kemp reaction. Particularly the higher is the concentration of hydrogen peroxide, the more the reaction is slow, since the concentration of the active enzyme decreases.

3.2.3. Experiments with hemoglobin

To understand whether the hemoglobin also catalyzes the Kemp reaction thanks to the combined effect of hemoprotein and ascorbate, four trials have been conducted for the substrate 5-NO_2BI (**Table 30**):

Table 30. Kemp reaction on 5-NO_2BI. Trials with ±hemo, ±asc.

Reagents	TRIALS			
	56	**57**	**58**	**59**
H_2O	470 µL	470 µL	470 µL	470 µL
Buffer 500 mM pH=8,25	25 µL	25 µL	25 µL	25 µL
5-NO_2BI 61 mM	3 µL	3 µL	3 µL	3 µL
Hemoglobin 0,30 mM	/	/	3 µL	3 µL
Ascorbate 400 mM	/	5 µL	/	5 µL
Volume tot	498 µL	503 µL	501 µL	506 µL

The trials have been monitored by UV/Vis spectrophotometry (one scan every 50 seconds), using the characteristic wavelength of the opening product of the heterocyclic ring (λ_{max}=380 nm)[10].

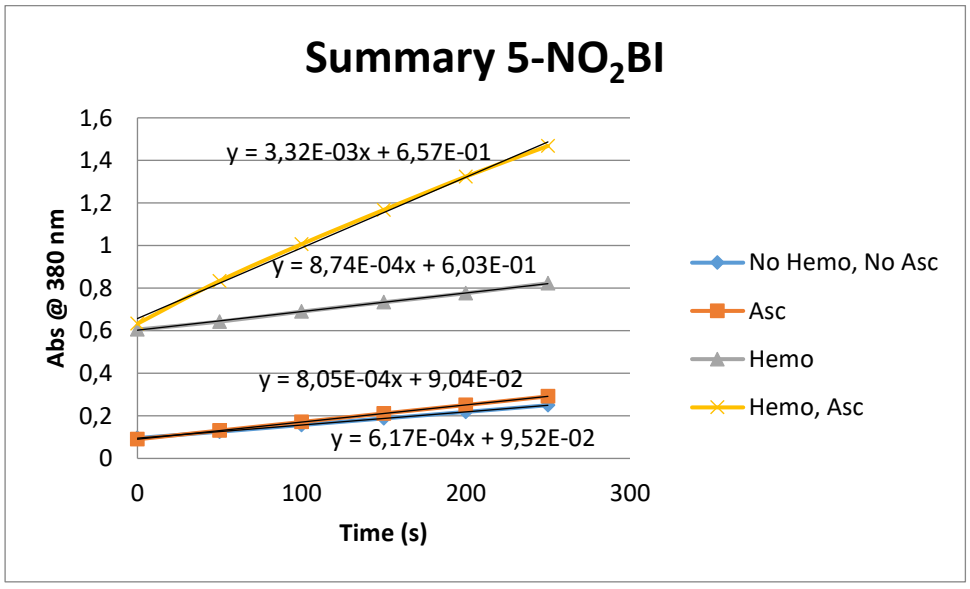

Figure 62. Plots Abs vs. time for solutions corresponding to conditions of trials in **Table 30**.

As can be shown from the above graph, the straight line with the greatest slope is that deriving from the presence of both hemoglobin and ascorbate. So it can be said that also for the case of hemoglobin, the combined action of hemoprotein and of the reducing agent has a more efficient catalytic effect than the other cases.

The k_{cat}/K_M value was:

$$\frac{k_{cat}}{K_M} = \frac{m}{\varepsilon_{6-OMeBI_a}[E][S]} = \frac{0{,}00323}{18400 \cdot 1{,}8 \cdot 10^{-7} \cdot 3{,}66 \cdot 10^{-4}} = 273{,}88\ M^{-1}s^{-1} = 16433\ M^{-1}min^{-1}$$

We must not be deceived by the high k_{cat}/K_M value: the hemoglobin is composed of 4 subunits, so to obtain the effective value of k_{cat}/K_M of the single monomer the previous value must be divided by 4. Consequently, assuming that the reaction takes place on a subunit:

$$\left(\frac{k_{cat}}{K_M}\right)_{eff} = \frac{273{,}88}{4} = 68{,}47\ M^{-1}s^{-1} = 4108\ M^{-1}min^{-1}$$

This value is comparable (as order of magnitude) to that of Cytochrome c ($k_{cat}/K_M \cong 40\ M^{-1}\ s^{-1}$).

Even in this case, a comparison of the behavior at pH=8,25 of the substituted benzisoxazoles 6-OMeBI, 5-BrBI, and 5-NO_2BI and also of the unsubstituted benzisoxazole (λ=323 nm)[10] in the presence of hemoglobin was made. The Kemp reaction has been monitored by UV/Vis spectrophotometry, as a function of time (**Table 31**), at the characteristic wavelength of the different opening products of the heterocyclic rings. Taking in considertion the data related to Cytochrome c, we decided to use three different acquisition times, depending on the substrate (every 2 seconds for 5-NO_2BI, every 30 seconds for the other ones). In **Table 31** are indicated the experimental conditions used.

Table 31. Trials with different substrates.

Reagents	TRIALS			
	60	**61**	**62**	**63**
H_2O	464 µL	464 µL	464 µL	464 µL
Buffer 500 mM pH=8,25	25 µL	25 µL	25 µL	25 µL
5-BrBI 53 mM	3 µL	/	/	/
5-NO_2BI 61 mM	/	3 µL	/	/
6-OMeBI 74 mM	/	/	3 µL	/
BI 61 mM	/	/	/	3 µL
Hemoglobin 0,30 mM	3 µL	3 µL	3 µL	3 µL
Ascorbate 400 mM	5 µL	5 µL	5 µL	5 µL
Volume tot	500 µL	500 µL	500 µL	500 µL

The data obtained are shown in the following **Figures 63** and **64**.

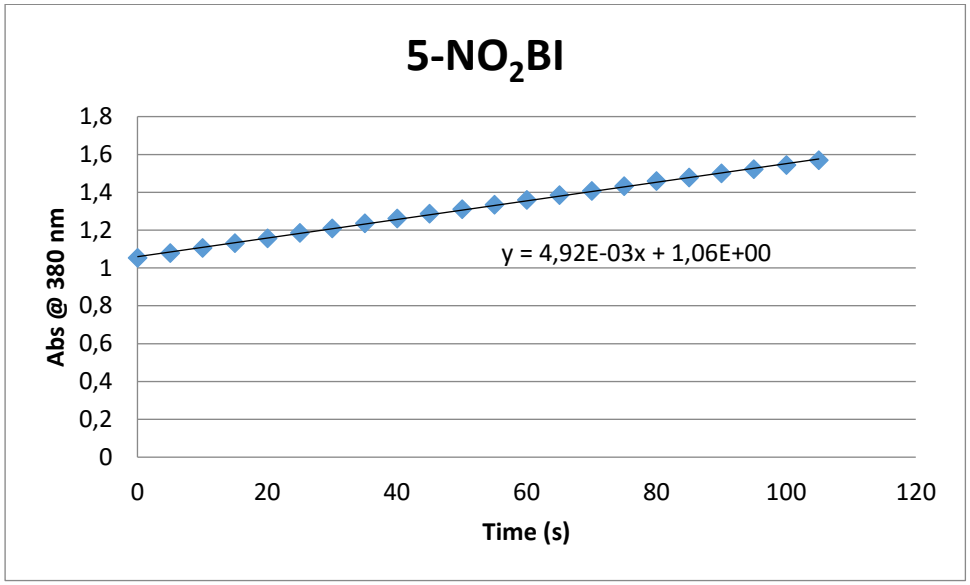

Figure 63. Plot Abs vs time of the Kemp elimination on 5-NO_2-BI in the presence of hemoglobin.

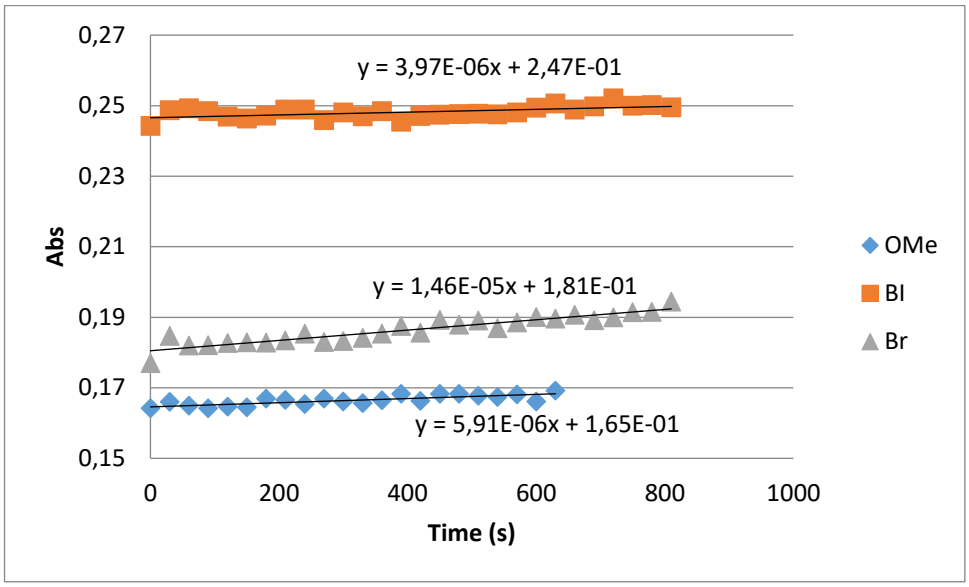

Figure 64. Plot Abs vs time of the Kemp elimination on 6-OMeBI, BI and 5-BrBI in the presence of hemoglobin.

The k_{cat}/K_M values are:

$$\left(\frac{k_{cat}}{K_M}\right)_{6-OMeBI_a} = \frac{m_{6-OMeBI}}{\varepsilon_{6-OMeBI_a}[E][S]} = \frac{5{,}91 \times 10^{-6}}{7500 \cdot 1{,}8 \cdot 10^{-6} \cdot 4{,}44 \cdot 10^{-4}} = 59{,}16\ M^{-1}min^{-1}$$
$$= 0{,}99\ M^{-1}s^{-1}$$

$$\left(\frac{k_{cat}}{K_M}\right)_{BI_a} = \frac{m_{BI}}{\varepsilon_{5-BI_a}[E][S]} = \frac{3{,}97 \times 10^{-6}}{5080 \cdot 1{,}8 \cdot 10^{-6} \cdot 3{,}66 \cdot 10^{-4}} = 71{,}17\ M^{-1}min^{-1}$$
$$= 1{,}19\ M^{-1}s^{-1}$$

$$\left(\frac{k_{cat}}{K_M}\right)_{5-BrBI_a} = \frac{m_{5-BrBI}}{\varepsilon_{5-BrBI_a}[E][S]} = \frac{1{,}46 \times 10^{-5}}{6100 \cdot 1{,}8 \cdot 10^{-6} \cdot 3{,}18 \cdot 10^{-4}} = 250{,}88\ M^{-1}min^{-1}$$
$$= 4{,}18\ M^{-1}s^{-1}$$

$$\left(\frac{k_{cat}}{K_M}\right)_{5-NO2BI_a} = \frac{m_{5-NO2BI}}{\varepsilon_{5-NO2BI_a}[E][S]} = \frac{0{,}00492}{18400 \cdot 1{,}8 \cdot 10^{-6} \cdot 3{,}66 \cdot 10^{-4}}$$
$$= 24352{,}58\ M^{-1}min^{-1} = 405{,}88\ M^{-1}s^{-1}$$

As for the case of Cytochrome c, but keeping in mind that the k_{cat}/K_M values refer to the whole enzyme, consisting of 4 subunits, the substrate that reacts fastest is 5-NO_2BI, whereas the slowest is 6-OMeBI.

Varying the concentration of the substrate 5-NO_2BI, as shown in **Table 32**, in presence of hemoglobin [0,0018 M] at pH=8,25, it is possible, calculating the rate of the reaction as function of concentration of enzyme (values reported in **Table 32**), to deduce an effect (or a not effect) of saturation of enzyme.

Table 32. Variation of [5-NO_2BI].

[5-NO_2BI]	ΔAbs/s	[a]M/s	v/[E]
0,366	0,0000667	2,99076E-08	1,66153E-05
0,0366	0,0000294	1,75543E-09	9,75242E-07
0,0732	0,0000111	6,10326E-09	3,3907E-06
0,1098	0,000029	8,4837E-09	4,71316E-06
0,00366	-0,00000882	8,14674E-10	4,52597E-07
0,0018	-0,00000139	2,40458E-10	1,33588E-07
0,0009	-0,00000625	4,22131E-10	2,34517E-07
0,18	0,000134	9,20884E-09	5,11602E-06
0,3	0,0000682	2,37792E-08	1,32107E-05

[a]the data are obtained considering the rate of reaction without enzyme.

Plotting the v/[E] values vs. the concentration of the substrate, the curve shown in **Figure 65** was obtained:

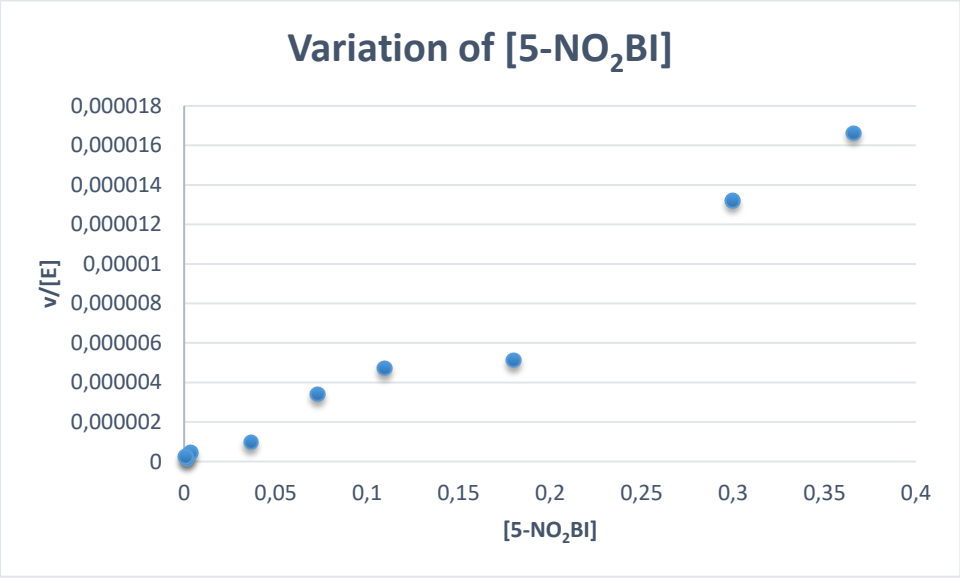

Figure 65. Plot v/[E] vs [S] at pH=8,25.

The graph (**Figure 65**) shows that as the substrate concentration increases, the reaction rate linearly increases, without evidence of the saturation of enzyme at the analyzed concentrations of 5-NO_2BI. This is consistent with the finding obtained above for the others considered hemoproteins, since the Kemp elimination, that is faster when the carbocyclic ring of the benzisoxazole bear a NO_2 group as substituent, and it is plausible that it is weakly bound to the protein.

3.2.3.1. pH rate of 5-BrBI

As for the Cytochrome c and myoglobin, the influence of pH on the Kemp reaction on 5-BrBI, in presence of hemoglobin, was analyzed (**Table 33**), using buffers at different pH value (9,4; 8,70; 8,33; 7,64).

Table 33 collects information about the trials made.

Table 33. pH rate of 5-BrBI.

Reagents	TRIALS			
	64	**65**	**66**	**67**
H_2O	464 µL	464 µL	464 µL	464 µL
Buffer 500 mM pH=9,40	25 µL	/	/	/
Buffer 500 mM pH= 8,70	/	25 µL	/	/
Buffer 500 mM pH=8,25	/	/	25 µL	/
Buffer 500 mM pH=7,64	/	/	/	25 µL
Ascorbate 400 mM	5 µL	5 µL	5 µL	5 µL
Hemoglobin 0,30 mM	3 µL	3 µL	3 µL	3 µL
5-BrBI 53 mM	3 µL	3 µL	3 µL	3 µL
Volume tot	500 µL	500 µL	500 µL	500 µL

A UV/Vis spectrophotometric scan was performed every 5 seconds for the trials 64, 65 and 66; whereas a scan every 20 seconds was performed for the trial 67. The data obtained, already normalized, are shown in **Figure 66**:

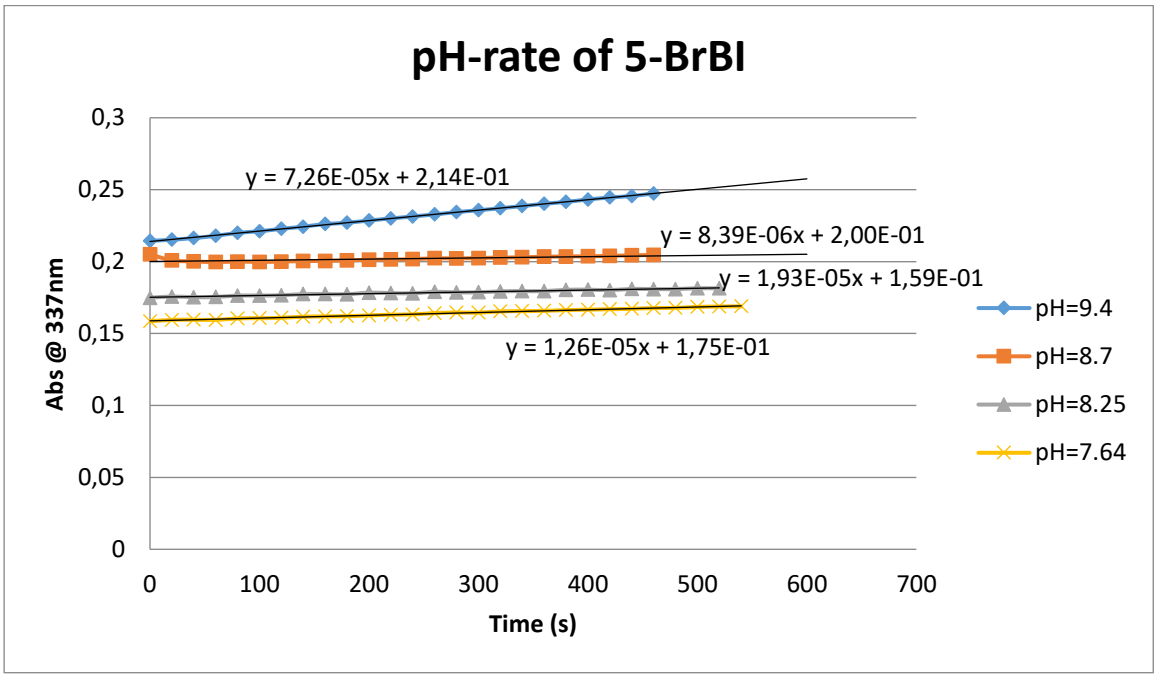

Figure 66. Plot of Abs vs time at different pH values for the system 5-BrBI/hemooglobin/ascorbate.

The k_{cat}/K_M values were calculated in a similar way to the previous ones and are collected in **Table 34**.

Table 34. Summary of k_{cat}/K_M at different pH values.

pH	Abs (nm/s)	K_{cat}/K_M (M^{-1} s^{-1})	K_{cat}/K_M (M^{-1} min^{-1})
9,4	7,26E-05	20,79252	1247,551
8,70	3,97E-05	11,22682	673,609
8,33	1,61E-05	4,611014	276,6608
7,64	1,06E-05	3,035823	182,1494

The obtained data have been reported in the following graph (**Figure 67**) and compared with those of 5-BrBI in the presence of Cytochrome c and myoglobin. Furthermore, to compare the values, the k_{cat}/k_M values was divided for 4, being hemoglobin a tetramer.

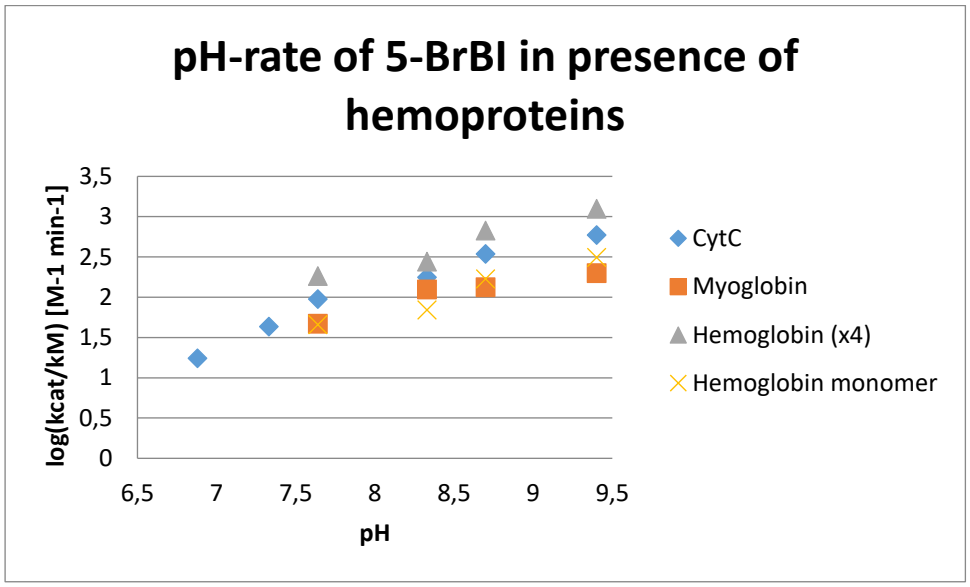

Figure 67. pH-rates of hemoproteins analyzed.

As showed in the graph above (**Figure 67**), all the analyzed hemoproteins are influenced by pH: the more the pH becomes more acidic, the more the k_{cat}/K_M decreases. The three hemoproteins have a catalytic rate very similar, highlighting that the heme group, common to all the three hemoproteins, is the real catalyst of the Kemp reaction, the remaning part of the protein doesn't seem to affect the reaction particularly. Finally, it is possible to show that the behaviors as function of pH are very similar, revealing a common mechanism of action towards 5-BrBI as substrate.

3.2.3.2. Monitoring of the Kemp elimination with 5-BrBI in the wavelength range 280- 650 nm

As for the Cytochrome c and myoglobin, a scan was perfomed (shown in **Table 35**) in presence of hemoglobin, monitoring the sample prepared as described in **Table 35**, in a range between 280-650 nm, setting up 20 cycles, each one of 180 seconds.

Tabella 35. Content of the sample used to monitor the Kemp elimination on 5-BrBI in the presence of hemoglobin and ascorbate in the wavelength range 280-650 nm.

Reagent	Amount
H_2O	460 µL
Buffer 500 mM pH=8,25	25 µL
5-BrBI 53 mM	3 µL
Hemoglobin 0,30 mM	3 µL
Ascorbate 400 mM	5 µL

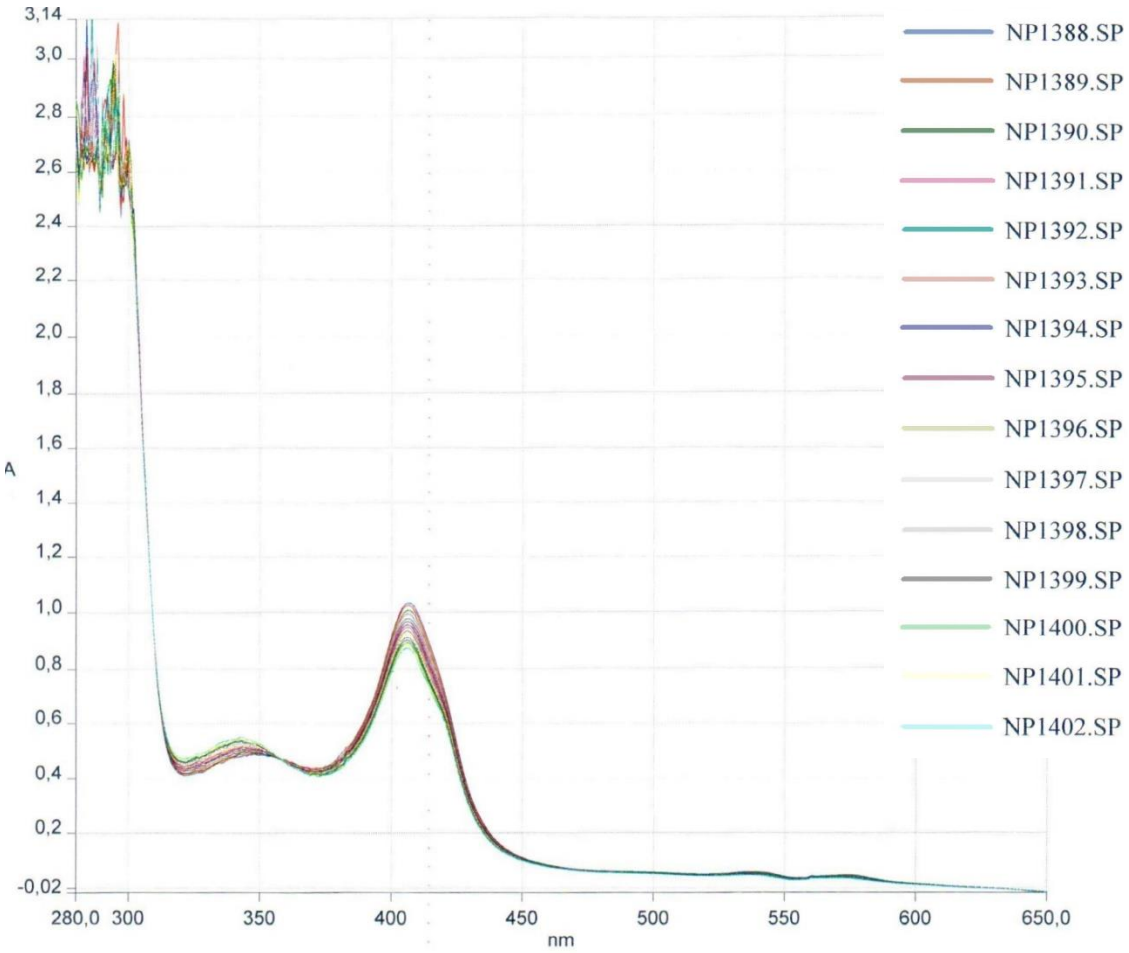

Figure 68. UV/Vis spectra of the system 5-BrBI/ hemoglobin/ascorbate at pH=8,25.

The spectra (**Figure 68**) show three characteristic bands of hemoglobin[42] at 410 nm, 540 nm and 560 nm which, unlike the Cytochrome c, vary: the absorbance decreases during 20 cycles. It might be due to a deactivation of the hemoprotein by the oxygen, which is reversibly coordinated to the heme group[43], unlike the Cytochrome c which do not bind oxygen being it dedicated to the transport of electrons[30]. This event is also confirmed by the increase in absorbance of the characteristic band of the opening product at 337 nm, which is less marked than in the case of use of Cytochrome c: the free site of the enzyme is occupied by oxygen and it is therefore less available for the Kemp reaction on the substrate.

3.2.3.3. Effect of peroxide hydrogen

From the literature it is known[34] that the ascorbate plays a key role in production of hydrogen peroxide[33], through free radical species and, consequently, it can influence the catalysis, acting on the substrate. Thus, we established to analyze the behavior of the Kemp reaction in the presence of hydrogen peroxide, using various concentrations of the latter, and to compare the data obtained with the interaction between the enzyme and the substrate in the presence of the ascorbate (**Table 36**).

Table 36. Effect of peroxide hydrogen.

Reagents	TRIALS			
	68	**69**	**70**	**71**
H_2O	464 µL	470 µL	470 µL	470 µL
Buffer 500 mM pH=8,25	25 µL	25 µL	25 µL	25 µL
Ascorbate 400 mM	5 µL	/	/	/
5-NO_2BI 61 mM	3 µL	3 µL	3 µL	3 µL
Hemoglobin 0,30 mM	3 µL	/	/	/
H_2O_2 4 mM	/	2 µL	/	/
H_2O_2 1 mM	/	/	2 µL	/
H_2O_2 0,4 mM	/	/	/	2 µL
Volume tot	500 µL	500 µL	500 µL	500 µL

The reactions have been monitored by UV/Vis spectrophotometry (one scan every 5 seconds), using the characteristic wavelength of the opening product of the heterocyclic ring (λ_{max}=380 nm)[10].

The data obtained are shown in **Figure 69**:

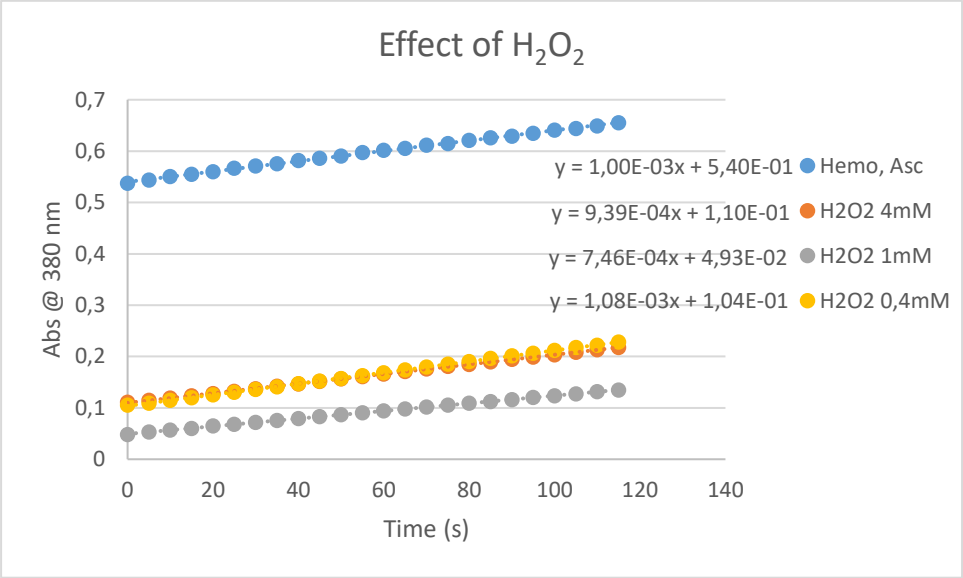

Figure 69. Plot Abs vs time of trials 68-71.

From the graphs in the **Figure 69** it is possible to deduce that the presence of hydrogen peroxide does not produce a considerably increase of the rate of the Kemp reaction: the three rates have the same order of magnitude; furthermore the solution containing the lower concentration of hydrogen peroxide has a slope very similar to that containing the enzyme and the reducing agent. Thus, a comparison of the data obtained by enzymatic catalysis of hemoglobin plus ascorbate with the data in presence of H_2O_2 suggests that hydrogen peroxide does not influence considerably the Kemp reaction rate.

4. Conclusion

Through a multistep synthesis, all the desired substrates were obtained which, completely spectroscopically characterized, have been the subject of kinetic analysis for the study of the Kemp reaction.

The optimization of the first synthetic passage allowed to obtain the aldehyde intermediate **11b** by chromatographic purification, thus by-passing the distillation method.

The optimization of each synthetic step allowed to follow the same synthetic strategy to obtain the deuterated benzisoxazole **15c**, using commercially available deuterated reagents. Furthermore, the deuterated aldehyde **11c**, completely characterized spectroscopically, will be the object of research to understand the Riemer-Tiemann mechanism.

Subsequently, the base-catalysis decomposition was analyzed, in the presence of three different enzymes, using UV/Vis spectroscopy. Cytochrome c, myoglobin and hemoglobin catalyze the reaction of Kemp, after reduction of Fe (III) present in the heme group of all three enzymes, by the ascorbate. Unlike Cytochrome c, which is faster to catalyze the Kemp reaction, myoglobin and hemoglobin are deactivated over time: myoglobin is deactivated due to the production of hydrogen peroxide by ascorbate; instead the hemoglobin is deactivated due to oxygen. Furthermore, the catalysis is influenced both by the substrate and by the pH for all the hemoproteins, which operate through a common mechanism, independent of the substrate, which primarily involves the heme group of the enzyme.

The observations reported in this eleaborate, ie that the reactions are dependent on the presence of a reducing agent (ascorbate) and that the slope in the Brønsted plots is lower than that of reactions catalyzed by a base, suggest that these hemoproteins catalyze the Kemp reaction through an oxidation-reducing mechanism that requires the presence of Fe (II) in the heme group.

Finally, we have not succeeded in further confirming the reaction mechanism through the isotope effect, unfortunately, but further studies will be carried out in the future.

5. Experimental section

5.1. General:

The solvents and reagents used, where not otherwise specified, are commercial products supplied by Aldrich or Fluka.

Dichloromethane (CH_2Cl_2) was anhydrified by distillation before use, purifying it on CaH_2.

Thin layer chromatography (TLC) was performed using silica gel containing fluorescent indicator at 254 nm, supported on aluminum foil, supplied by Fluka (DC-Alufolien-Kieselgel).

The ^{1}H-NMR e ^{13}C-NMR spectra were recorded using the following instruments:

- Inova 300 (300 MHz for ^{1}H-NMR and 75.4 MHz for ^{13}C-NMR), using $CDCl_3$ as solvent.
- Mercury 400 (399.9 MHz for ^{1}H-NMR and 100.6 MHz for ^{13}C-NMR), using $CDCl_3$ as solvent.
- Inova 600 (599,7 MHz for ^{1}H-NMR and 150.8 MHz for ^{13}C-NMR), using $CDCl_3$ as solvent.

The chemical shifts are measured in δ (ppm) and the values of the coupling costant are given in Hz.

The reference line is that of solvents δ=7.26 ppm relative to ^{1}H-NMR in $CDCl_3$ and δ=77.2 ppm relate to ^{13}C-NMR in $CDCl_3$.

Melting points were recorded with a Buchi 535 device.

The ESI-MS spectra were recorded with a Water 2Q 4000 device in *Electron Spray Ionisation* (ESI).

The infrared spectra were recorded with a PerkinElmer 1000 FT-IR spetrophotometer in the ATR (*Attenuated Total Reflectance*) technique for solid phase.

The buffers at different pH were prepared from a solution of 1,3-bis(tris(hydroxymethyl)methylamino)propane (BTP) 1 M stock and HCl 4 M.

The kinetic trials were performed with a Perkin Elmer Lambda 12 spectrophotometer UV/vis, using plastic cuvettes. The measurements executed in this elaborate have been replicated several times and showed a good reproducibility (≤ 6%).

Cytochrome c was provided to us by MP *Biomedicals*.

Myoglobin comes from the equine skeleton muscle and it was supplied to us by Sigma.

Hemoglobin comes from bovine blood and it was supplied to us by Sigma.

5.2. Synthesis of substituted benzisoxazoles

5.2.1. Reimer-Tiemann reaction

5.2.1.1. Synthesis of 5-bromo-2-hydroxybenzaldehyde:

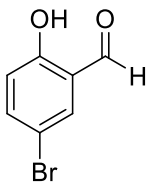

11b

Into a round-bottom flask, equipped with a reflux condenser, a heating bath and a magnetic stirrer, is placed 5,19 g of 4-bromophenol (30 mmol) and 18 ml of a solution of NaOH 10M (0,18 mol) were introduced. The reaction mixture was heated at 65°C and is added dropwise 4,8 ml of $CHCl_3$ (60 mmol). The mixture is heated at reflux in chloroform for 2 h. After cooling to room temperature, the mixture is acidified to pH=4-5 with $HCl_{(conc)}$, then the aqueous solution is extracted with $CHCl_3$ (3x20 ml) and the combined organic layers were dried over anhydrous $MgSO_4$. The crude product was purified by two columns chromatography on silica gel made two fold: the first one the eluent was a 2:1 mixture *n*-hexane:diethyl ether and the second one *n*-hexane:dichloromethane (1:1). The desired product **11b** was obtained in 17% yield (1 g, 5 mmol) as yellow solid.

^{1}H-NMR (300 MHz, $CDCl_3$): δ= 10.94 (s, 1H, OH), 9.85 (s, 1H, CHO), 7.68 (d, *J*=2.5 Hz, 1H, ArH), 7.61 (dd, *J*=8.6, 2.4 Hz, 1H, ArH), 6.92 (d, *J*=8.9 Hz, 1H, ArH) ppm.

^{13}C-NMR (75 MHz, $CDCl_3$): δ= 195.4, 160.5, 139.7, 135.6, 121.7, 119.8, 111.3 ppm.

ESI-MS (ESI$^-$), m/z: 202 $[M - H^+]^-$.

P.f.: 102-103°C.

5.2.1.2. Synthesis of 5-bromo-2-hydroxybenzaldehyde-d (1-d):

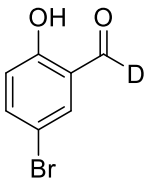

11c

Into a three-neck round-bottom flask, equipped with a reflux condenser, a heating bath and a magnetic stirrer, under inert atmosphere of Argon, is placed 1,87 g of 4-bromophenol (10,8 mmol) and 6,5 ml of a solution of NaOD 40% (D_2O) were introduced. The reaction mixture was heated at 65°C and $CDCl_3$ (1,7 ml, 21,6 mmol) was added dropwise. The mixture was heated at reflux in chloroform for 2 h. After cooling to room temperature, under inert atmosphere of Argon, the mixture was acidified to pH=4-5 with $HCl_{(conc)}$, then the aqueous solution was extracted with $CHCl_3$ (3x20 ml) and the combined organic layers were dried over anhydrous Na_2SO_4. The crude product was purified by two consecutive columns chromatography on silica gel: the first one with petroleum ether:diethyl ether (2:1) as eluent and the second one with *n*-hexane:dichloromethane (3:1) to yield 398 mg of the desired product **11c** (2 mmol, yield 19%) as yellow solid.

^{1}H-NMR (400 MHz, $CDCl_3$): δ= 10.96 (s, 1H, OH), 7.68 (d, *J*=2.8 Hz, 1H, ArH), 7.59 (dd, *J*=9.2, 2.3 Hz, 1H, ArH), 6.91 (d, *J*=8.9 Hz, 1H, ArH) ppm.

^{13}C-NMR (75 MHz, $CDCl_3$): δ= 195.4, 195.1, 194.8, 160.6, 139.7, 135.6, 121.6, 119.8, 111.3 ppm.

ATR: *v*=3220.3, 2145.8, 1651.5 cm^{-1}.

ESI-MS (ESI^-), m/z: 202 $[M - H^+]^-$.

P.f.= 102-103 °C.

5.2.2. Synthesis of oximes

5.2.2.1. Synthesis of 5-bromo-2-hydroxybenzaldehyde oxime:

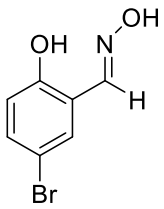

12

Into a round-bottom flask, equipped with a reflux condenser, a heating bath and a magnetic stirrer, were placed 120 mg of **11b** (0,60 mmol), 65 mg of hydroxylamine hydrochloride (0,93 mmol) and 5 ml of EtOH. The reaction mixture is heated at 65°C overnight. After cooling in an ice bath, is added cold water (20 ml). The suspension is filtered and washed with cold water: the filtrate is concentrated *in vacuo* to give 103 mg of the desired product **12** (0,48 mmol, 80% yield) as white solid.

^{1}H-NMR (300 MHz, $CDCl_3$): δ= 9.71 (s, 1H, OH), 8.16 (s, 1H, CHN), 7.37 (dd, *J*=8.55, 1.9 Hz, 1H, ArH), 7.30 (d, *J*=2.3 Hz, 1H, ArH), 7.22 (s, 1H, NOH), 6.88 (d, *J*=8.55 Hz, 1H, ArH) ppm.

^{13}C-NMR (75 MHz, $CDCl_3$): δ= 156.4, 151.9, 134.0, 132.8, 118.7, 117.9, 111.3 ppm.

ESI-MS (ESI^-), m/z: 217 $[M - H^+]^-$.

P.f.: 119-122°C.

5.2.2.2. Synthesis of of 5-bromo-2-hydroxybenzaldehyde oxime-d (1-d):

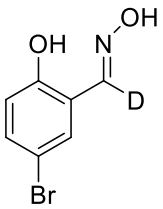

13

Into a three-neck round-bottom flask, equipped with a reflux condenser, a heating bath and a magnetic stirrer, under inert atmosphere of Argon, were placed 300 mg of **11c** (1,5 mmol), 158 mg of hydroxylamine hydrochloride (2,3 mmol) and 13 ml of EtOH. The reaction mixture was heated at 65°C overnight. After cooling in an ice bath, cold water (30 ml) was added. The suspension was filtered and washed with cold water: the filtrate was concentrated *in vacuo* to give 263 mg of the desired product **13** (1,2 mmol, 80% yield) as white solid.

^{1}H-NMR (400 MHz, $CDCl_3$): δ= 9.72 (s, 1H, OH), 7.37 (dd, *J*=9.1, 2.2 Hz, 1H, ArH), 7.30 (d, *J*=2.4 Hz, 1H, ArH), 7.23 (s, 1H, NOH), 6.88 (d, *J*=8.7 Hz, 1H, ArH) ppm.

^{13}C-NMR (75 MHz, $CDCl_3$): δ= 156.3, 151.6, (t, CD), 133.9, 132.8, 118.6, 117.9, 11.3.

ESI-MS (ESI^-), m/z: 218 $[M - H^+]^-$.

P.f.: 122-126°C.

5.2.2.3. Synthesis of 2-hydroxy-4-methoxybenzaldehyde oxime:

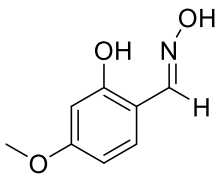

14

Into a round-bottom flask, equipped a magnetic stirrer, were placed 500 mg of **11d** (3,28 mmol), 272 mg of hydroxylamine hydrochloride (3,94 mmol), 11 ml of EtOH and 22 ml of water, in an ice bath. After adding dropwise 0,65 ml of a 50% aqueous solution of NaOH, the mixture was keept for 1h at room temperature. The mixture was acidified to pH=5 with HCl 1M, then the aqueous solution was extracted with CH_2Cl_2 (3x20 ml) and a saturated solution of NaCl (2x20 ml) and the organic phase was dried over Na_2SO_4. The crude product was filtered and concentrated *in vacuo* to give 541 mg of the desired product **14** (3,23 mmol, 98% yield) as pink solid.

^{1}H-NMR (300 MHz, $CDCl_3$): δ= 9.89 (s, 1H, COH), 8.16 (s, 1H, CHN), 7.07 (d, *J*=8.6 Hz, 1H, ArH), 6.93 (s, 1H, ArH), 6.46-6.53 (m, 2H, ArH, NOH, overlapped signals), 3.81 (s, 3H, OCH_3) ppm.

^{13}C-NMR (75 MHz, $CDCl_3$): δ=162.3, 159.0, 152.8, 131.8, 109.7, 106.9, 101.4, 55.4 ppm.

ESI-MS (ESI^-), m/z: 167 $[M - H^+]^-$.

P.f.: 135-143°C.

5.2.3. Cyclization reaction

5.2.3.1. Synthesis of 5-bromobenzo[d]isoxazole:

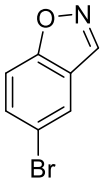

15b

Into a three-neck round-bottom flask, equipped with a magnetic stirrer, under inert atmosphere of Argon, were placed 393 mg of triphenylphosphine (1,5 mmol), 339 mg of 2,3-dichloro-5,6-dicyano-1,4-benzoquinone (1,5 mmol) and 5 ml of dry CH_2Cl_2. After adding of **12** (1 mmol), the mixture was magnetically stirred for 5 minutes. The crude product was purified by column chromatography on silica gel with *n*-hexane:dichloromethane (3:1) as eluent, to yield 142 mg of the desired product **15b** (0,72 mmol, 72% yield) as white solid.

^{1}H-NMR (600 MHz, $CDCl_3$): δ= 8.67 (s, 1H, CHN), 7.89 (d, *J*=1.6 Hz, 1H, ArH), 7.67 (dd, *J*=8.9, 1.9 Hz, 1H, ArH), 7.53 (d, *J*=9.1 Hz, 1H, ArH) ppm.

^{13}C-NMR (75 MHz, $CDCl_3$): δ= 161.1, 145.4, 133.1, 124.4, 123.1, 116.6, 111.2 ppm.

ESI-MS (ESI^-), m/z: 199 $[M - H^+]^-$.

P.f.: 83-86°C.

5.2.3.2. Synthesis of 5-bromobenzo[d]isoxazole-3-d:

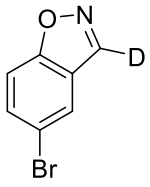

15c

Into a three-neck round-bottom flask, equipped with a magnetic stirrer, under inert atmosphere of Argon, were placed 78 mg of triphenylphosphine (0,30 mmol), 68 mg of 2,3-dichloro-5,6-dicyano-1,4-benzoquinone (0,30 mmol) and 1 ml of dry CH_2Cl_2. After adding of **13** (0,20 mmol), the mixture was magnetically stirred for 5 minutes. The crude product was purified by column chromatography on silica gel with *n*-hexane:dichloromethane (3:1) as eluent, to yield 36 mg of the desired product **15c** (0,18 mmol, 90% yield) as white solid.

^{1}H-NMR (600 MHz, $CDCl_3$): δ= 7.89 (d, *J*=1.8 Hz, 1H, ArH), 7.67 (dd, *J*=8.7, 1.8 Hz, 1H, ArH), 7.52 (d, *J*=8.9 Hz, 1H, ArH) ppm.

^{13}C-NMR (75 MHz, $CDCl_3$): δ= 161.2, 145.2 (t, CD), 133.1, 124.4, 123.1, 116.6, 111.2.

ESI-MS (ESI^-), m/z: 199 $[M - H^+]^-$.

P.f.: 82-85°C.

5.2.3.3. Synthesis of 6-methoxybenzo[d]isoxazole:

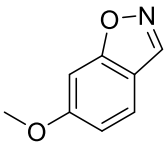

15d

Into a three-neck round-bottom flask, equipped with a magnetic stirrer, under inert atmosphere of Argon, were placed 393 mg of triphenylphosphine (1,5 mmol), 339 mg of 2,3-dichloro-5,6-dicyano-1,4-benzoquinone (1,5 mmol) and 5ml of dry CH_2Cl_2. After adding of **14** (1 mmol), the mixture was magnetically stirred for 5 minutes. The crude product is purified by column chromatography on silica gel with *n*-hexane:dichloromethane (3:1) as eluent, to yield 109 mg of the desired product **15d** (0,73 mmol, 73% yield) as green oil.

^{1}H-NMR (600 MHz, $CDCl_3$): δ= 8.58 (s, 1H, CHN), 7.56 (d, *J*=9.0 Hz, 1H, ArH), 7.04 (s, 1H, ArH), 6.93 (dd, *J*=8.7, 2.1 Hz, 1H, ArH), 3.89 (s, 3H, OCH_3) ppm.

^{13}C-NMR (75 MHz, $CDCl_3$): δ= 164.1, 162.3, 145.8, 122.0, 114.7, 114.6, 92.3, 55.7.

ESI-MS (ESI^-), m/z: 149 $[M - H^+]^-$.

5.2.4. Nitration reaction

5.2.4.1. Synthesis of 5-nitrobenzo[d]isoxazole:

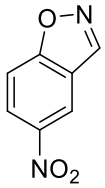

15e

Into a round-bottom flask immersed in an ice bath, equipped with a magnetic stirrer, 500 mg of 1,2-benzisoxazole **15** (4,2 mmol) and 2,15 ml of H_2SO_4 were placed. After adding dropwise a solution of 96% H_2SO_4 (0,1 ml) and >90% HNO_3 (0,275 ml), the reaction mixture was carried out for 30 minutes. The reaction mixture was poured into an ice/water mixture, then the suspension is filtered and crystallized from EtOH. The crude product was concentrated *in vacuo* to give 364 mg of the desired product **15e** (2,21 mmol, 53% yield) as white solid.

^{1}H-NMR (600 MHz, $CDCl_3$): δ= 8.9 (s, 1H, CHN), 8.73 (d, *J*=2.4 Hz, 1H, ArH), 8.51 (dd, *J*=9.1, 2.1 Hz, 1H, ArH), 7.76 (d, *J*=9.1, 1H, ArH) ppm.

^{13}C-NMR (75 MHz, $CDCl_3$): δ= 164.3, 147.0, 144.7, 125.6, 121.8, 119.2, 110.5.

ESI-MS (ESI^-), m/z: 164 $[M - H^+]^-$.

P.f.: 122-126°C.

6. Bibliography

[1] Lehninger A.L. *Biochimica Zanichelli* **2003**, 196-210.
[2] Fruschicheva M.P.; Mills M.J.; Schopf P.; Singh M.K.; Prasad R.B.; Warshel A. *Curr. Opin. Chem. Biol.* **2014**, *21*, 56-62.
[3] Korendovych I.V.; DeGrado W.F. *Curr. Opin. Struct. Biol.* **2014**, *27*, 113-121.
[4] Privett H.K.; Kiss G.; Lee T.M. *P. Natl. Acad. Sci*. **2012**, *109*, 3790-3795.
[5] Rothlisberger D.; Khersonsky O.; Wollacott A.M. *Nature* **2008**, *453*, 190-194.
[6] Casey M.L.; Kemp D.S.; Paul K.G.; Cox D.D. *J. Org. Chem.* **1973**, *38*, 2294-3201.
[7] Dale T.J.; Sather A.C.; Rebek J. *Tetrahedron Lett.* **2009**, 6173-6175.
[8] Hollfelder F.; Kirby A.J.; Tawfik D.S. *J. Org. Chem.* **2001**, *66*, 5866-5874.
[9] Iranpoor N.; Firouzabadi H.; Nowrouzi N. *Tetrahedron Lett.* **2006**, *47*, 8247-8250.
[10] Lamba V.; Sanchez E.; Fanning L.R.; Howe K.; Alvarez M.A.; Herschlag D.; Forconi M. *Biochemistry* **2017**, *56*, 582-591.
[11] Kemp D.S.; Cox D.D.; Paul K.G. *J. Am. Chem. Soc.* **1975**, *97*, 7312-7318.
[12] Kennan A.J.; Whitlock H.W. *J. Am. Chem. Soc.* **1996**, *118*, 3027-3028.
[13] Kalgutkar A.S.; Nguyen H.T.; Vaz A.D.N.; Doan A.; Dalvie D.K.; Mcleod D.G.; Murray J.C. *Drug. Chem. Toxicol.* **2003**, *31*, 1240-1250.
[14] Sanchez E.; Lu S.; Reed C.; Schmidt J.; Forconi M. *J. Phys. Org. Chem.* **2016**, *29*, 185-189.
[15] Merski M.; Shoichet B.K. *PNAS* **2012**, *109*, 16179-16183.
[16] Hollfelder F.; Kirby A.J.; Tawfik D.S.; Kikuchi K.; Hilvert D. *J. Am. Chem. Soc.* **2000**, *122*, 1022-1029.
[17] Roat-Malone R.M. *Bioinorganic chemistry Wiley* **2007**, 343-453.
[18] Miao Y.; Metzener R.; Asano Y. *Chem. Bio. Chem* **2017**, *18*, 451-454.
[19] Li A.; Wang B.; Llie A.; Dubey K.D.; Bange G.; Korendovych I.V.; Shaik S.; Reetz M.T. *Proc. Natl. Acad. Sci.* **2011**, *108*, 6823.
[20] Kiss G.; Houk K.N.; Moretti R.; Baker D. *Angew. Chem. Int. Ed.* **2013**, *52*, 5700-5725.
[21] Muller R.; Debler E.W.; Steinmann M.; Seeback F.P.; Wilson I.A.; Hilvert D. *J. Am. Chem. Soc.* **2007**, *129*, 460-461.
[22] Hollfelder F.; Kirby A.J.; Tawfik D.S. *Nature* **1996**, *383*, 60-63.
[23] Thorn S.N.; Daniels R.G.; Auditor M.T.; Hilvert D. *Nature* **1995**, *373*, 228-230.
[24] Privett H.K.; Kiss G.; Lee T.M.; Blomberg R.; Chica R.A.; Thomas M.L.; Hilvert D. Houk K.N.; Mayo S.L. *PNAS* **2012**, *109*, 3790-3795.
[25] Rothlisberg D.; Khersonsky O.; Wollacott A.M.; Jiang L.; DeChancie J.; Betker J.; Houk K.N.; Baker D. *Nature* **2008**, *453*, 190-194.
[26] Blomberg R.; Kries H.; Pinkas D.M.; Mittl P.R.E.; Grutter M.G.; Privett H.K.; Mayo S.L.; Hilvert D. *Nature* **2013**, *503*, 418-421.
[27] Boukharsa Y.; Meddah B.; Ibrahimi A.; Benomar A.; Cherrah Y. *Med. Chem. Res.* **2016**, *25*, 494-500.
[28] Tetrahedron 2012, 53, 127-131.
[29] Andreu R.; Ronda J.C. *Synth. Commun.* **2008**, *38*, 2316-2329.
[30] Vibhute Y.B.; Lonkar S.M.; Sayyed M.A.; Baseer M.A. *Mendeleev Commun.* **2007**, *17*, 51.
[31] Mao J.; Hauser K.; Gunner M.R. *Biochemistry* **2003**, *42*, 9829-9840.
[32] Margalit R.; Schejter A. *Eur. J. Biochem.* **1973**, *32*, 492-499.
[33] Wallace C.J.A.; Clark-Lewis I. *J. Biol. Chem.* **1992**, *267*, 3852-3861.
[34] Quian X.; Mester T.; Morgado L.; Arakawa T.; Sharma M.L.; Inoue K.; Joseph C.; Maroney M.J.; Lovley D.R. *Biochim. Biophys. Acta* **2011**, *1807*, 404-412.
[35] Li C.; Hoffman M. Z. *J. Phys. Chem.* **1999**, *103*, 6653-6656.
[36] Thornton R. E. *Phys. Org. Chem.* **1996**, *17*, 349-372.
[37] Chen Y.; Tsai Y.; Hirsch L.; Bassani M. D. *J. Am. Chem. Soc.* **2017**, *139*, 16359-16364.
[38] Richards M.P. *Therapeutics* **2013**, *18*, 2342-2351.
[39] Tsukahara K.; Wada Y.; Kimura M. *Bull. Chem. Soc.* **1991**, *64*, 908-915.

[40] Tovmasyan A.; Weitner T.; Sheng H.; Lu M.; Rajic Z.; Warner D.S.; Reboucas J.S.; Benov L. *Inorg. Chem.* **2013**, *52*, 5677-5691.
[41] Wazawa T.; Matsuoka A.; Tajima G.; Sugawara Y.; Nakamura K. *Biophys J.* **1992**, *63*, 544-550.
[42] Dessy A.; Piras A.M.; Schirò G.; Levantino M.; Cupane A.; Chiellini F. *Eur. J. Pharmacol. Sci.* **2011**, *43*, 57-64.
[43] Schlereth D.D.; Mantele W. *Biochemistry* **1992**, *31*, 7494-7502.